

THE EFFECTS OF THE PRESSURE ARCH
UPON MULTIPLE SEAM MINING

by

Stephen David Hudock

Thesis submitted to the Faculty of the
Virginia Polytechnic Institute and State University
in partial fulfillment of the requirements for the degree of

MASTER OF SCIENCE

in

Mining Engineering

APPROVED:

C. Haycocks, Chairman

M. Karmis

G. Faulkner

J. R. Lucas, Department Head

August, 1983
Blacksburg, Virginia

ACKNOWLEDGEMENTS

I wish to express my deepest gratitude to my advisor and thesis chairman, Dr. Christopher Haycocks, for his guidance throughout my graduate years, particularly in the area of my thesis work.

I would also like to thank the other members of my thesis committee, Dr. Michael Karmis, Dr. Gavin Faulkner, and Dr. J. Richard Lucas, for the advice and information that I received from them.

I would also like to thank my family for their support through my graduate years. I also thank the staff and graduate students of the Department of Mining and Minerals Engineering.

TABLE OF CONTENTS

	<u>Page</u>
ACKNOWLEDGEMENTS	ii
LIST OF FIGURES	v
LIST OF TABLES	viii
I. INTRODUCTION	1
II. LITERATURE REVIEW	3
2.1 Arching Theory	3
2.2 Arch Shape and Size	18
2.3 Finite Element Method	24
III. CASE STUDIES	33
3.1 White Pine Copper Mine	33
3.2 Cadley Hill Colliery	37
3.3 Monongalia County, West Virginia	39
IV. FINITE ELEMENT MODEL DEVELOPMENT	43
4.1 The Finite Element Computer Program	43
4.2 The Mesh-Plot Program	47
4.3 The Stress-Plot Program	49
4.4 The General Purpose Contouring Program	49
V. PHOTOELASTIC MODEL DEVELOPMENT	54
VI. CASE STUDY CORRELATION	59
VII. FINITE ELEMENT RESULTS	63
VIII. SUMMARY	69

	<u>Page</u>
IX. CONCLUSIONS AND RECOMMENDATIONS	71
9.1 Conclusions	71
9.2 Recommendations	72
REFERENCES	74
BIBLIOGRAPHY	76
APPENDICES	78
Appendix A - Sigma (Y) Values	78
Appendix B - Sigma (X) Values	116
Appendix C - Listing of Computer Programs . . .	153
Appendix C-1 - Finite Element Program . . .	154
Appendix C-2 - Mesh-Plot Program	178
Appendix C-3 - Stress-Plot Program	184
Appendix C-4 - GPCP Input	188
VITA	197
ABSTRACT	

LIST OF FIGURES

<u>Figure</u>		<u>Page</u>
1.	Arch Formed in Stratified Rock (after Fayol, 1885)	5
2.	Pressure Arch Theory Terminology (after Dinsdale, 1937)	7
3.	Minor Pressure Arches Across Excavation (after Dinsdale, 1937)	9
4.	Major Pressure Arch Formed From Merger of Minor Arches (after Dinsdale, 1937)	10
5.	Hypothetical Shape of Dome with Intradosal Voussoir Systems (after Denkhaus, 1964)	16
6.	Superposition of Arch Stresses (after Stemple, 1956)	20
7.	Extent of Major Pressure Arch	22
8.	Comparison of Pressure Arch Size, Theory Experience (after Barrientos and Parker, 1969)	23
9.	Numbering of Nodes to Reduce Band Width (after Desai and Abel, 1972)	29
10.	Inaccuracy of Solution as a Function of Aspect Ratio (after Desai and Abel, 1972)	30
11.	Effect of External Boundary Location on Accuracy of Finite Element Method Solution (after Kulhawy, 1974)	32

<u>Figure</u>	<u>Page</u>
12. Critical Width versus Depth (after Barrientos and Parker, 1974)	34
13. Extent of Pressure Arch Formed As Result of Mining at White Pine (after Barrientos and Parker, 1974)	36
14. Two Components of Lateral Stress (after Barrientos and Parker, 1974)	38
15. Cross-section of the Main Coal and Woodfield Workings	40
16. Cross-section of Sewickley and Pittsburgh Seams Showing Line of Damage Above Gob of the Lower Seam	42
17. Example of Mesh-Plot Output	48
18. Sign Convention for Plotting of Stress Vectors (after Coates, 1969)	50
19. Example of Stress Vector Diagram	51
20. Example of GPCP Output	53
21. Example No. 1 of Isochromatic Fringe Pattern	57
22. Example No. 2 of Isochromatic Fringe Pattern	58
23. Contour of Vertical Stresses, Hendrix Mine Case Study	61

<u>Figure</u>		<u>Page</u>
24.	Contour of Horizontal Stresses, Hendrix Mine Case Study	62
25.	Stress Trajectories of a Finite Element Model	66
26.	Stress Trajectories of a Photoelastic Model	67
27.	Example Grid of Location of Values from Tables in Appendices A and B	79

LIST OF TABLES

<u>Table</u>	<u>Page</u>
1.	Material Properties Used in the Analysis 46
A-1.	Sigma (Y), Opening 100' by 5', 500' Sandstone Overburden 80
A-2.	Sigma (Y), Opening 200' by 5', 500' Sandstone Overburden 81
A-3.	Sigma (Y), Opening 300' by 5', 500' Sandstone Overburden 82
A-4.	Sigma (Y), Opening 400' by 5', 500' Sandstone Overburden 83
A-5.	Sigma (Y), Opening 500' by 5', 500' Sandstone Overburden 84
A-6.	Sigma (Y), Opening 600' by 5', 500' Sandstone Overburden 85
A-7.	Sigma (Y), Opening 100' by 5', 750' Sandstone Overburden 86
A-8.	Sigma (Y), Opening 200' by 5', 750' Sandstone Overburden 87
A-9.	Sigma (Y), Opening 300' by 5', 750' Sandstone Overburden 88
A-10.	Sigma (Y), Opening 400' by 5', 750' Sandstone Overburden 89

<u>Table</u>	<u>Page</u>
A-11. Sigma (Y), Opening 500' by 5', 750' Sandstone Overburden	90
A-12. Sigma (Y), Opening 600' by 5', 750' Sandstone Overburden	91
A-13. Sigma (Y), Opening 100' by 5', 1000' Sandstone Overburden	92
A-14. Sigma (Y), Opening 200' by 5', 1000' Sandstone Overburden	93
A-15. Sigma (Y), Opening 300' by 5', 1000' Sandstone Overburden	94
A-16. Sigma (Y), Opening 400' by 5', 1000' Sandstone Overburden	95
A-17. Sigma (Y), Opening 500' by 5', 1000' Sandstone Overburden	96
A-18. Sigma (Y), Opening 600' by 5', 1000' Sandstone Overburden	97
A-19. Sigma (Y), Opening 100' by 5', 500' Shale Overburden	98
A-20. Sigma (Y), Opening 200' by 5', 500' Shale Overburden	99
A-21. Sigma (Y), Opening 300' by 5', 500' Shale Overburden	100
A-22. Sigma (Y), Opening 400' by 5', 500' Shale Overburden	101

<u>Table</u>	<u>Page</u>
A-23. Sigma (Y), Opening 500' by 5', 500' Shale Overburden	102
A-24. Sigma (Y), Opening 600' by 5', 500' Shale Overburden	103
A-25. Sigma (Y), Opening 100' by 5', 750' Shale Overburden	104
A-26. Sigma (Y), Opening 200' by 5', 750' Shale Overburden	105
A-27. Sigma (Y), Opening 300' by 5', 750' Shale Overburden	106
A-28. Sigma (Y), Opening 400' by 5', 750' Shale Overburden	107
A-29. Sigma (Y), Opening 500' by 5', 750' Shale Overburden	108
A-30. Sigma (Y), Opening 600' by 5', 750' Shale Overburden	109
A-31. Sigma (Y), Opening 100' by 5', 1000' Shale Overburden	110
A-32. Sigma (Y), Opening 200' by 5', 1000' Shale Overburden	111
A-33. Sigma (Y), Opening 300' by 5', 1000' Shale Overburden	112
A-34. Sigma (Y), Opening 400' by 5', 1000' Shale Overburden	113

<u>Table</u>	<u>Page</u>
A-35. Sigma (Y), Opening 500' by 5', 1000' Shale Overburden	114
A-36. Sigma (Y), Opening 600' by 5', 1000' Shale Overburden	115
B-1. Sigma (X), Opening 100' by 5', 500' Sandstone Overburden	117
B-2. Sigma (X), Opening 200' by 5', 500' Sandstone Overburden	118
B-3. Sigma (X), Opening 300' by 5', 500' Sandstone Overburden	119
B-4. Sigma (X), Opening 400' by 5', 500' Sandstone Overburden	120
B-5. Sigma (X), Opening 500' by 5', 500' Sandstone Overburden	121
B-6. Sigma (X), Opening 600' by 5', 500' Sandstone Overburden	122
B-7. Sigma (X), Opening 100' by 5', 750' Sandstone Overburden	123
B-8. Sigma (X), Opening 200' by 5', 750' Sandstone Overburden	124
B-9. Sigma (X), Opening 300' by 5', 750' Sandstone Overburden	125
B-10. Sigma (X), Opening 400' by 5', 750' Sandstone Overburden	126

<u>Table</u>	<u>Page</u>
B-11. Sigma (X), Opening 500' by 5', 750' Sandstone Overburden	127
B-12. Sigma (X), Opening 600' by 5', 750' Sandstone Overburden	128
B-13. Sigma (X), Opening 100' by 5', 1000' Sandstone Overburden	129
B-14. Sigma (X), Opening 200' by 5', 1000' Sandstone Overburden	130
B-15. Sigma (X), Opening 300' by 5', 1000' Sandstone Overburden	131
B-16. Sigma (X), Opening 400' by 5', 1000' Sandstone Overburden	132
B-17. Sigma (X), Opening 500' by 5', 1000' Sandstone Overburden	133
B-18. Sigma (X), Opening 600' by 5', 1000' Sandstone Overburden	134
B-19. Sigma (X), Opening 100' by 5', 500' Shale Overburden	135
B-20. Sigma (X), Opening 200' by 5', 500' Shale Overburden	136
B-21. Sigma (X), Opening 300' by 5', 500' Shale Overburden	137
B-22. Sigma (X), Opening 400' by 5', 500' Shale Overburden	138

<u>Table</u>	<u>Page</u>
B-23. Sigma (X), Opening 500' by 5', 500' Shale Overburden	139
B-24. Sigma (X), Opening 600' by 5', 500' Shale Overburden	140
B-25. Sigma (X), Opening 100' by 5', 750' Shale Overburden	141
B-26. Sigma (X), Opening 200' by 5', 750' Shale Overburden	142
B-27. Sigma (X), Opening 300' by 5', 750' Shale Overburden	143
B-28. Sigma (X), Opening 400' by 5', 750' Shale Overburden	144
B-29. Sigma (X), Opening 500' by 5', 750' Shale Overburden	145
B-30. Sigma (X), Opening 600' by 5', 750' Shale Overburden	146
B-31. Sigma (X), Opening 100' by 5', 1000' Shale Overburden	147
B-32. Sigma (X), Opening 200' by 5', 1000' Shale Overburden	148
B-33. Sigma (X), Opening 300' by 5', 1000' Shale Overburden	149
B-34. Sigma (X), Opening 400' by 5', 1000' Shale Overburden	150

<u>Table</u>		<u>Page</u>
B-35.	Sigma (X), Opening 500' by 5', 1000' Shale Overburden	151
B-36.	Sigma (X), Opening 600' by 5', 1000' Shale Overburden	152

I. - INTRODUCTION

The coalfields of the United States, and particularly those of the Appalachian region of the eastern United States, consist of many contiguously placed, mineable coal seams. Both historically and presently, the determination of the mining sequence of these contiguously placed coal seams has been based largely on the ownership of the coal seam, the availability of the coal seam, and the general economic situation at the time in question. If, however, the mining of any particular coal seam occurs without regard to any subsequent ground control problems which may arise, serious and hitherto unaccounted problems may affect any future mining operations in seams above or below that which was previously mined. This lack of concern for future operations may often be detrimental to the recovery, cost and safety of the mining operation of adjacent seams.

The ground control mechanisms which should be considered in an area of multiple seam or multiple horizon mining can be divided into four distinct areas. These areas are the arching of stresses around mine openings, the effects of subsidence from a previously mined lower seam upon an overlying seam, the transfer of pillar loads from one seam to another, and massive interseam failure (Haycocks and Karmis, 1981).

The concept of arching attempts to explain the interaction of stresses that results from mine openings rather than those which develop due to the pillars. The most common arching theory is the pressure arch theory which states that a high pressure zone arches over the opening in an elliptical shape, while the area inside this high pressure arch is de-stressed with respect to the normal cover load.

In multiple seam mining, the high arching stresses as well as the de-stressed area within the arch may affect the mining conditions in an adjacent overlying seam. The effects of arching upon multiple seam mining under sub-critical subsidence conditions are reported in this study.

The stresses around underground mine openings of various widths and depths of cover are modelled by use of the finite element computer program. The finite element program yields the horizontal and vertical stresses as well as the principal stresses and their inclinations across the model. The finite element method was verified by using photoelastic modelling which exhibited similar configurations of the pressure arch. The finite element method was then used to model an actual case study and produced results very close to the observed data. A series of design tables is included to give an approximation of the stresses that may be encountered in a variety of mining conditions.

II. - LITERATURE REVIEW

2.1 - Arching Theory

The concept that the rock above an underground mine opening would form an arch in order to support itself is one that is common to both the hard rock and coal mining industries. This arching must be considered in the design of any multiple horizon mining operation.

The concept of arching was first discussed by Fayol (1885) in his study of the effects of underground coal mining upon the surface. Fayol, who was one of the early investigators of mining subsidence, concluded that "the movement of strata is limited by a kind of dome which has for its base the area worked out, and that the amount of movement is less as it is further from the center of the excavation." Fayol postulated that when the areal extent of excavation was vast the height of the dome was not greater than 200 times the extracted seam height. When the area of excavation is of limited extent Fayol concluded that the height of the dome is between two and four times the width of the excavated area. More specifically, the height of the dome is twice the width of the excavation when the seam height is less than two meters (6.5 feet) and increases as the height of the extracted seam becomes greater. Fayol's

conclusions were based on model studies that dealt with a stratified medium. He felt that the roof consisted of a series of independent beams with fixed ends which fail due to the inward shearing of the beam ends. This action gives rise to the dome shape as shown in Figure 1. This dome theory that Fayol presented has become the basis of two-dimensional pressure arch theory.

One of the earliest proponents of arching, or pressure arch theory, was B. S. Randolph (1915). Randolph stated that when the coal is first mined, the first stress on the overlying strata is very similar to that on a uniformly loaded horizontal beam. Since the overlying strata tend to have a low tensile strength, an arch-shaped line of stress carries the weight of the overlying strata to the solid material on either side of the excavation. This line of stress would be in equilibrium and support all the material above it. Along and on both sides of this line of stress there is a zone of material upon which more or less pressure is exerted, its width depending on the total strength and elasticity of the material. This pressure tends to hold the material in place. Randolph felt that the position and type of forces acting on the arch would affect the shape of the line of stress or arch. If a hydrostatic pressure situation existed, the arch would be in the shape of a semi-circle. If there was a larger load toward the center of the

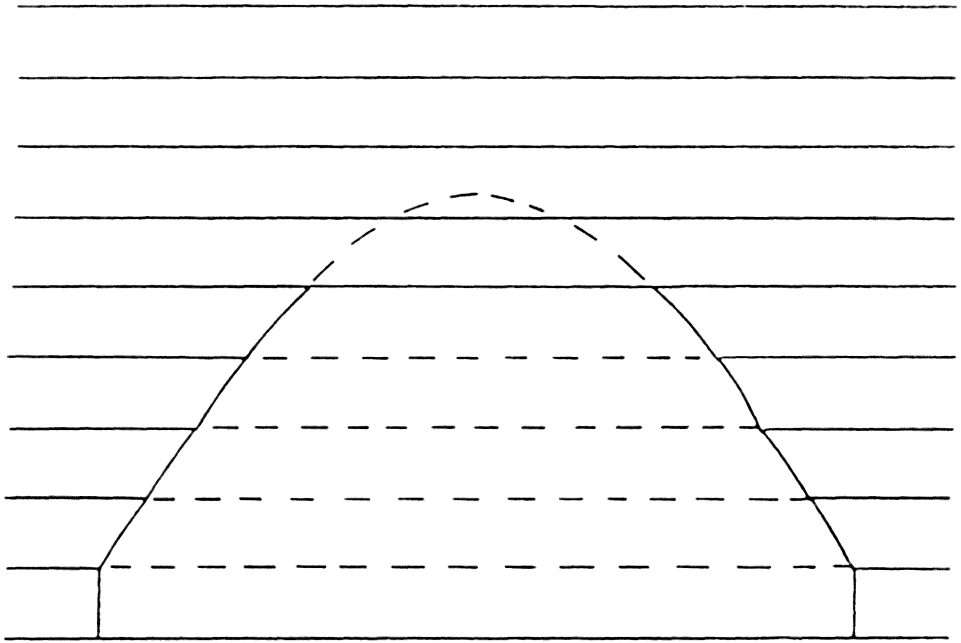


Figure 1. Arch Formed in Stratified Rock (after Fayol, 1885).

excavation, the arch would be in the shape of a parabola. Also, if the overlying strata is comprised of different materials, the position of the line of stress will be altered and the shape of the arch changed in order to maintain a state of equilibrium.

In 1937 J. R. Dinsdale presented a major work on the pressure arch theory. First, several terms must be defined before they are used to explain Dinsdale's paper. Before any excavation is made the ground at any depth is subjected to a pressure equal to the weight of the column of the ground above. This pressure is called the "superincumbent" or "undisturbed" pressure. When an excavation is opened, a pressure ring forms around the opening and the weight of the ground above, part of the superincumbent pressure, is deflected to the solid rock at the sides of the excavation. Since the sides of the excavation form the abutments of the pressure arch, the pressure on them is called the "abutment pressure". Inside this pressure ring there is a core of decompressed and fractured ground which is called the "intradosal" ground. Around the outside of this core of decompressed or de-stressed ground there is a zone of firm, compressed ground called the "extradosal" ground. These terms are illustrated in Figure 2.

According to Dinsdale, the height of the intradosal ground above the excavation is very dependent upon the

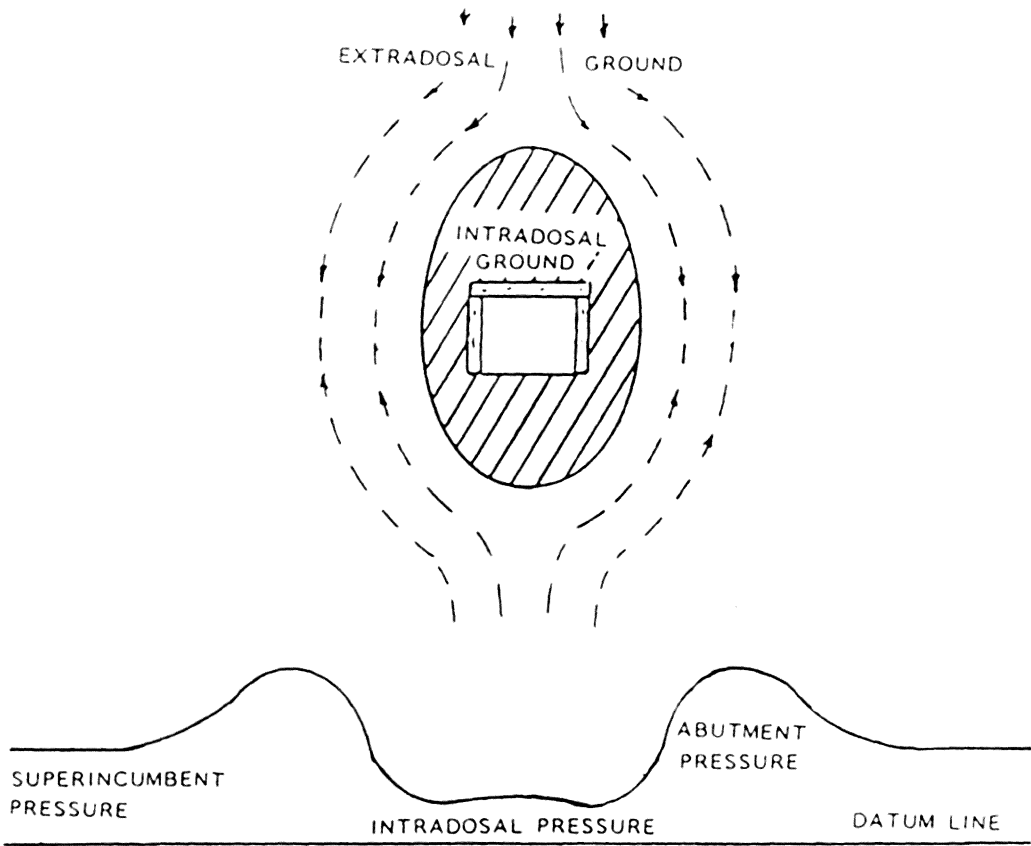


Figure 2. Pressure Arch Theory Terminology (after Dinsdale, 1937).

resistance of the material forming the arch to crushing and the intensity of pressure to which the arch is subjected. The stability of the pressure arch is maintained until failure takes place at either of the abutments or along the arch itself. Failure continues until a new pressure arch forms and equilibrium is restored.

Where pillars are left in place in the excavation, each pillar forms an abutment for the minor pressure arches which span the openings between the pillars as shown in Figure 3. If one of these pillars fails a sudden merging of adjacent minor pressure arches takes place. This merging results in the formation of a major pressure arch with a coinciding increase in the pressure on the abutments of the major arch. This occurrence is illustrated in Figure 4.

Dinsdale also noted that when the excavations are continually widening, as in the case of longwall mining, the pressure arch renews itself as the span of the arch increases. Eventually, the pressure arch is incapable of spanning the opening and obtaining support along the solid sides of the excavation. When this occurs, the arch and the extradosal ground it supports will collapse and result in the subsidence of the surface.

Denkhaus (1964) surveyed strata movement theories, including arching theory. Among these theories are the rigid dome theory, the presence of a fracture dome in elastic rock and its modifications and beam theory.

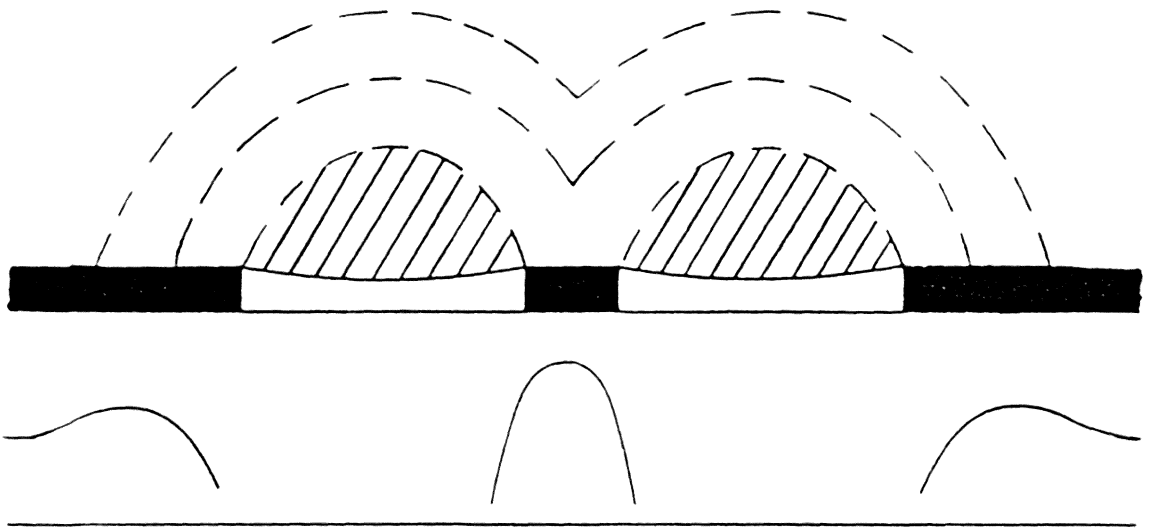


Figure 3. Minor Pressure Arches Across Excavation
(after Dinsdale, 1937).

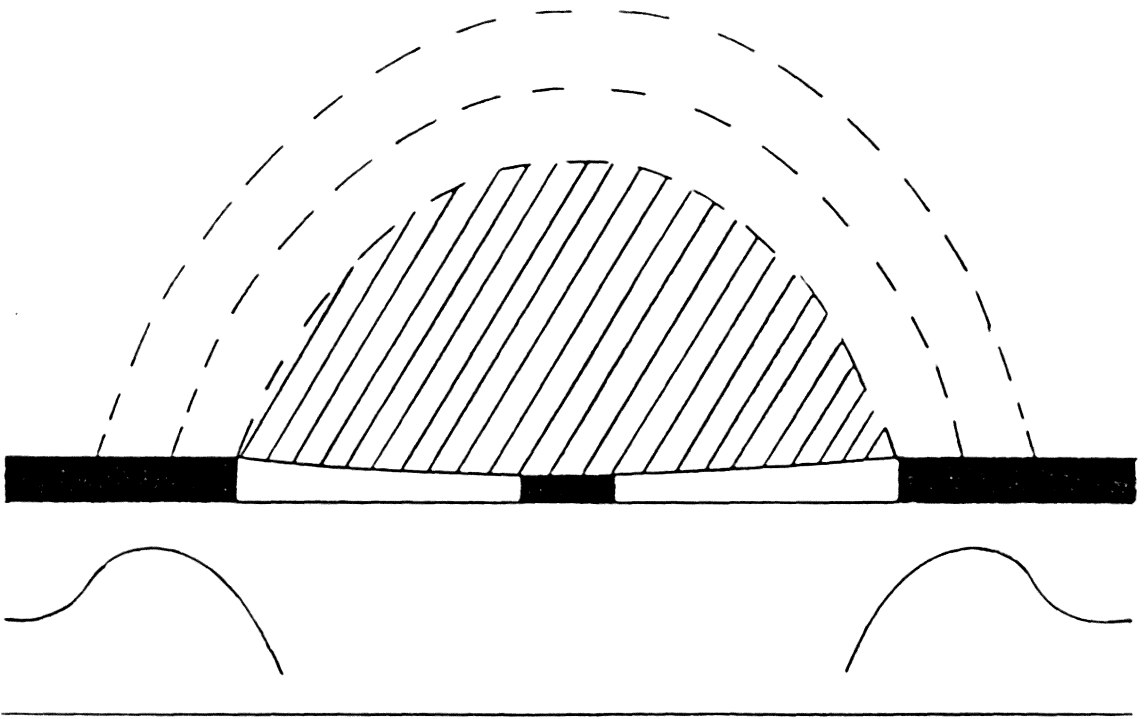


Figure 4. Major Pressure Arch Formed From Merger of Minor Arches (after Dinsdale, 1937).

The rigid dome theory is the simplest of these theories since it is based on the equilibrium of forces at the boundary of the dome. This theory does not take deformation into account, however, it does consider failure which occurs when the load reaches a critical value called the failure load. In order to simplify the theory, a dome which is normally three dimensional is reduced to a two dimensional problem, as in the case of a longwall panel where the length of the panel is of sufficient length to eliminate it from the calculations. Also, a distinction must be made between sufficiently cohesive rock and insufficiently cohesive rock.

In the case of sufficiently cohesive rock, the core of the dome or the intradosal ground will not separate from the dome boundary. For this reason the rock along the dome boundary must carry the weight of the core of the dome. If the span of the dome becomes too large, the weight of the core will exceed the cohesive resistance of the rock and a sudden collapse of the core or a major portion of it may occur. Any support which is under the dome would have to take a large amount of weight suddenly.

If the rock is insufficiently cohesive, portions of the core will separate from the dome boundary either gradually or at short intervals as the span of the dome increases. Of the two conditions, this is the more favorable with respect to ground control considerations. As the span of the dome

increases, the core may form smaller domes within the main dome in order to support itself.

Denkhaus then presented the following formulas to determine the span at any depth, the maximum height for a stable dome and the corresponding maximum span. In the case of insufficiently cohesive rock, the formula for span is:

$$s = \sqrt{\frac{8\sigma_c d}{w} (1-h/d) \log(1-h/d)} \quad (\text{Eq. 2.1})$$

where s is the span, h is the height of the dome, d is the depth of the opening below the surface, w is the specific weight of the material, and σ_c is the uniaxial compressive strength of the rock. The formulas for the maximum height for a stable dome and its corresponding span are:

$$H_{\max} = 0.63d \quad (\text{Eq. 2.2})$$

$$S_{\max} = \sqrt{\frac{2.96\sigma_c d}{w}} \quad (\text{Eq. 2.3})$$

For sufficiently cohesive rock, the formulas change to the following:

$$s = \sqrt{\frac{8\sigma_c h}{w} (1-h/d)} \quad (\text{Eq. 2.4})$$

$$H_{\max} = 0.5d \quad (\text{Eq. 2.5})$$

$$S_{\max} = \sqrt{\frac{2\sigma_c d}{w}} \quad (\text{Eq. 2.6})$$

Note: when the rock is sufficiently cohesive the core of the dome remains in situ and the shape of the dome is parabolic. The above formulas are based on the assumption that the rock is both homogeneous and isotropic as well as other assumptions which are presented in the original and not discussed in this report.

As the height and the span of the dome increase, the probability that non-homogeneities and anisotropics exist in the rock increases. Their presence would weaken the actual strength of the rock medium.

The rigid dome theory does not give any information about the stress or movement ahead of the face nor around or within the dome. It does, however, set limits to a zone of movement; displacement does not occur outside the dome but it may occur within the dome. This, of course, is because the rigid dome theory does not account for deformation of the rock, as it is considered a rigid medium. *

The second theory that Denkhaus discusses is that of the fracture dome in elastic rock. In this theory the rock is considered to be a homogeneous isotropic elastic body. According to Denkhaus, "If a failure criterion for rock, that is the condition under which rock fails for a given state of stress, is applied to the stress distribution around an excavation, it is possible to predict the shape and size of the fracture zone that may surround the

excavation." In this theory, it is assumed that a fracture zone will assume a shape and size so that at the dome boundary neither the tensile stress exceeds the uniaxial tensile strength nor the compressive stress exceeds the uniaxial compressive strength.

For this theory an axis ratio, $2h/s$, can be obtained from the following formulas:

$$2h/s = (1 + \sigma_t/wd)/2k - 0.5 \quad (\text{Eq. 2.7})$$

$$2h/s = 2/(k - 1 + \sigma_c/wd) \quad (\text{Eq. 2.8})$$

where k is the ratio of lateral to vertical initial rock pressure, σ_t is the uniaxial tensile strength and the other symbols are the same as those used previously. The fracture dome will take the shape of an ellipse that will use the largest of the two ratios above. Note: when k equals zero, ratio $2h/s$ equals infinity.

The advantage to the fracture dome in elastic rock theory is that the ground within the ellipse or the intradosal ground is fractured and therefore cannot be taken as a homogeneous elastic medium, while the extradossal ground is still a homogeneous elastic medium whose stress and displacements may still be predicted by using the theory of elasticity. The weakness of the elastic dome theory is that it is based on an oversimplification of the way in which rock actually fails.

There are two major factors that are usually ignored in elastic dome theory that should be considered. First, whenever failure is initiated, the stress distribution around the opening changes. The new stress distribution of the changed geometry should be determined and the failure criterion reapplied and repeated until no further propagation of fracture occurs. Second, the forces exerted from the fractured rock in the intradosal zone onto the dome boundary must be taken into account. Due to its own weight, the fractured rock in the intradosal zone tends to sag, until blocks of the fractured material wedge between each other and the side of the dome boundary. Therefore, the vertical downward forces of the individual blocks may have components causing thrust between the blocks and against the dome boundary and other components tending to shear blocks out of the arch system formed by the thrust. This shear is resisted by the friction between the blocks which in turn is increased by the thrust so that the arch system remains stable. These arch systems are known as Voussoir arches. This dome shape with Voussoir arches is illustrated in Figure 5.

Another theory discussed by Denkhaus is beam and plate theory. In both the rigid dome and elastic dome theory, the rock was considered to be a homogeneous and isotropic medium. One type of non-homogeneity and anisotropy that can

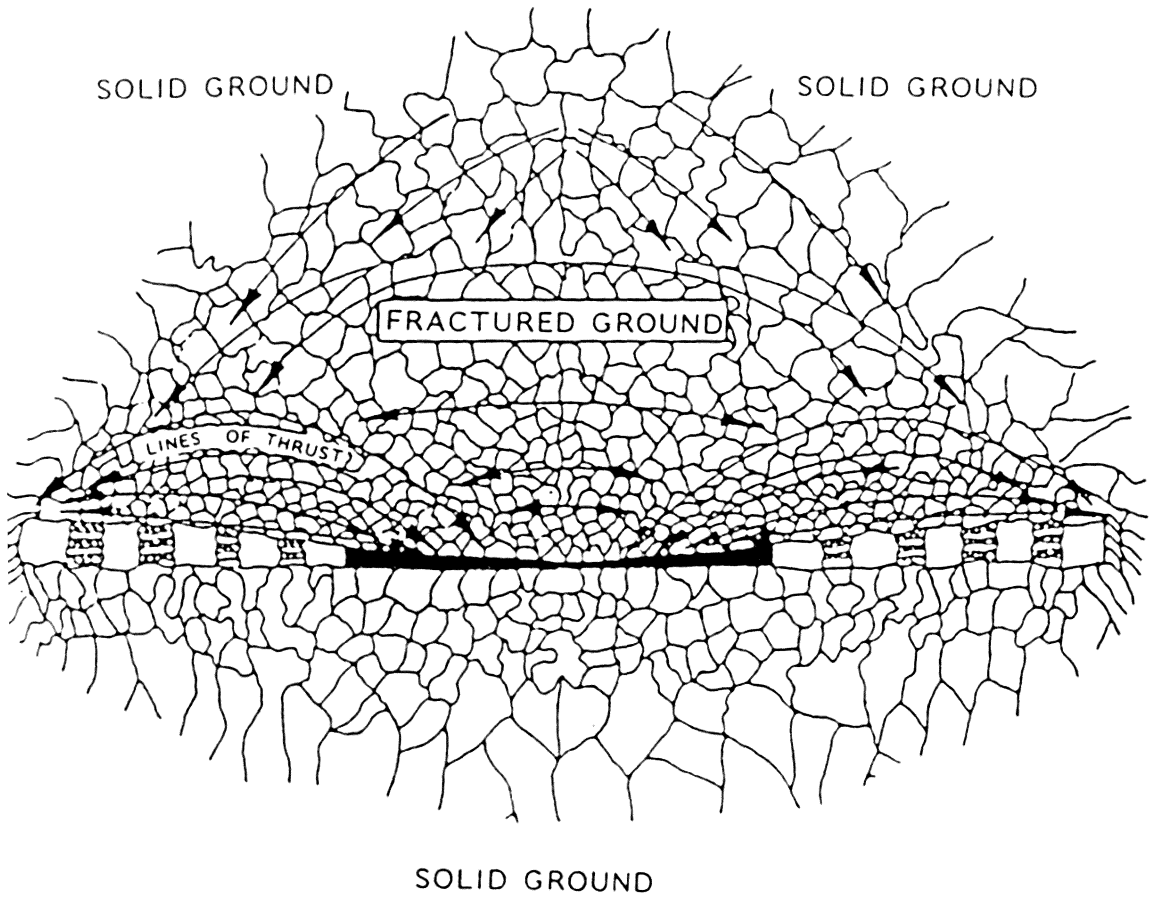


Figure 5. Hypothetical Shape of Dome with Intradossal Voussoir Systems (after Denkhaus, 1964).

more easily be dealt with theoretically is the stratification of a rock medium. This is a case of a series of plates (three dimensional) or beams (two dimensional) which overlie each other.

In beam theory, the maximum stress occurs at the face and, if the stress is greater than the strength, failure will occur there. If the beams are assumed to be clamped at both ends, failure will occur at the two ends. However, if the beams are somewhat elastic, the point of maximum stress and, therefore, failure moves toward the midpoint along the face. This process continues upwards through the strata until it stops.

The amount of deflection in each beam depends upon the thickness of the strata and its elastic deformation modulus. Therefore, it is possible for a lower strata may deflect more than the overlying beam so that a gap (called the Weber cavity) occurs between the two beams.

The dome itself is defined as the area within which the layers deflect and possibly fail and where Weber cavities may occur, while no deflection or failure occurs in the the extradossal ground outside the dome. Note that the beam theory is based on the assumption that no bond exists between the successive layers so that they may deflect freely.

2.2 - Arch Shape and Size

As already shown in this report, the shape of the pressure arch has been found to be one of three shapes: (1) elliptical, (2) parabolic or (3) a modified shape. Mohr (1956) believed in an elliptically shaped dome where the ratio of the height of the dome to the semi-width of the dome would vary with the ratio of the vertical stress to the horizontal stress. Mohr's relationship is as follows:

$$\frac{B}{L} = \frac{ZZ}{XX} = \frac{1-PR}{PR} \quad (\text{Eq. 2.9})$$

where B= the height of the dome from the central axis
 L= the semi-width of the dome
 ZZ= the vertical stress
 XX= the horizontal stress
 PR= Poisson's Ratio

This finding appears to be accurate for arches in massive and intact rock and can be determined by measuring the principal stresses present underground. According to this equation, as a hydrostatic stress field condition is reached, the ratio of the axes equals one and the shape of the dome becomes a semi-circular arc as proposed by Irving (1946).

Another important factor in the determination of the shape of the pressure arch is the nature of the strata in which the arch is formed. According to Randolph there will be a high arch in strong strata with few joints. Therefore,

under a strong sandstone bed, the fall of the arch will be so slow that it allows a large span to be excavated from the underlying seam. The arch span enlarges until the stress is so great that failure occurs either at the pillar face or back in the excavation. This continues until the resulting roof falls allow the side of the pressure arch to rest on the gob, thereby reducing the span of the pressure arch.

Another important work on the pressure arch theory was performed by the National Coal Board (1954) which found that with an increase in the width of the underground opening, the size of the pressure arch will increase until a certain width is reached at which the superincumbent pressure can no longer be supported by the abutments along the solid sides of the excavation. At this point, the excavation is spanned by a pressure arch with one abutment on the solid coal and the other resting on the gob. The National Coal Board theorized that the pressure arch extends as far below the seam as it does above the seam and when the abutment of an arch in one seam is superimposed upon an arch abutment from an adjacent seam, the stresses will be additive. The superposition of pressure arch abutments is illustrated in Figure 6. The National Coal Board also indicated that the pressure in a certain area may be below that of the superincumbent pressure. This would occur where an upper seam lies within the de-stressed zone of a pressure arch

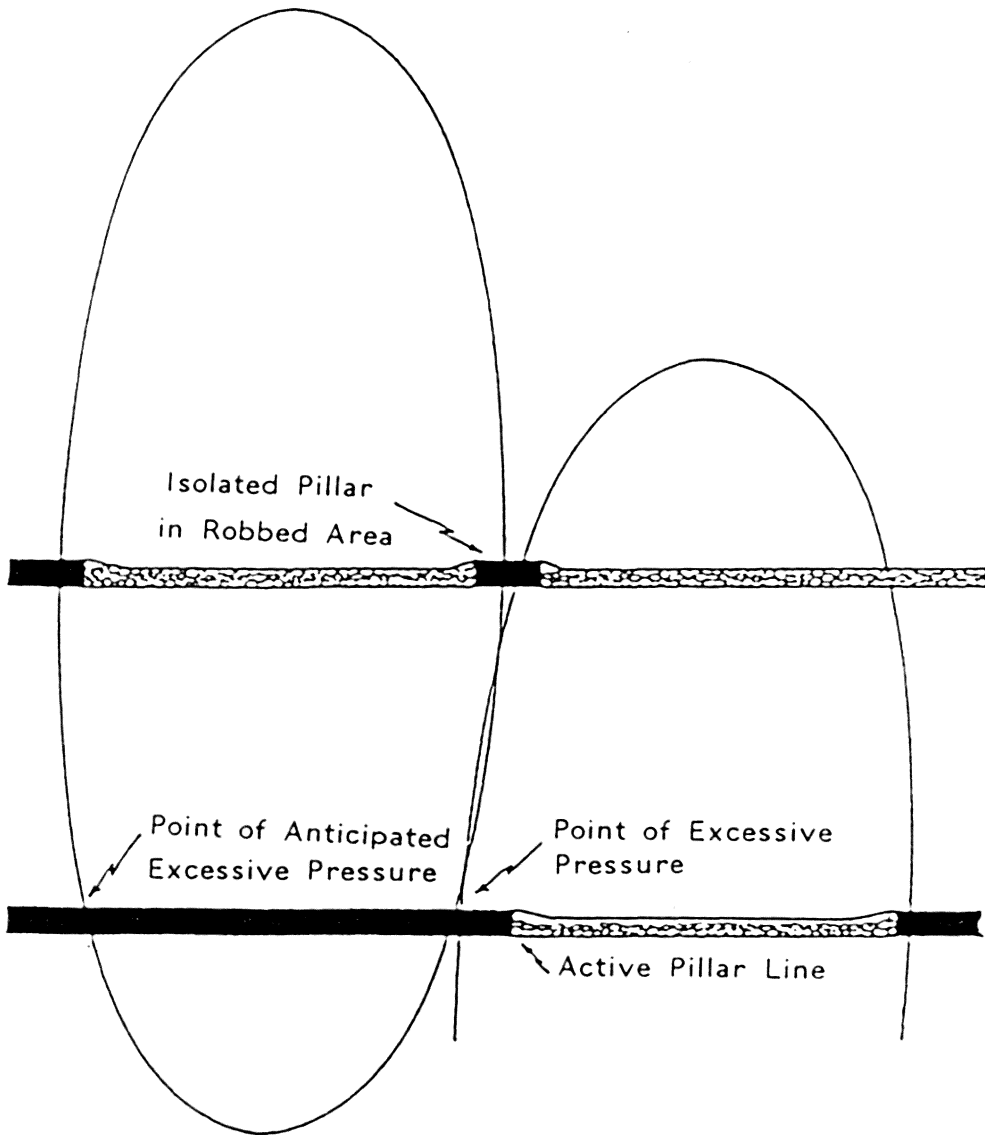


Figure 6. Superposition of Arch Stresses (after Stemple, 1956)

created by the mining of a superjacent or subjacent coal seam. The National Coal Board felt that the strata is under great pressure for about 20 to 30 yards beyond the outer edge of the de-stressed intradosal zone. However, beyond this distance, the pressure rapidly reduces to the normal superincumbent load. The height of the pressure arch was held to be about twice the width of the pressure arch. The National Coal Board created a formula to obtain the width of the maximum pressure arch for depths between 400 and 2,000 feet:

$$W = D/20 + 20 \qquad \text{(Eq. 2.10)}$$

where W = width of the maximum pressure arch in yards
and D = depth of seam below surface in feet

For example, if Seam "C" is 600 feet underground and being mined, it is possible for a pressure arch to form to a height of 300 feet above Seam "C". If Seam "B" is only 120 feet above "C" it may be affected by this maximum pressure arch of Seam "C". If Seam "A" is 350 feet above Seam "C" it will not be affected by the pressure arch, as shown in Figure 7. A comparison of the size of pressure arches according to both theory and experience is illustrated in Figure 8.

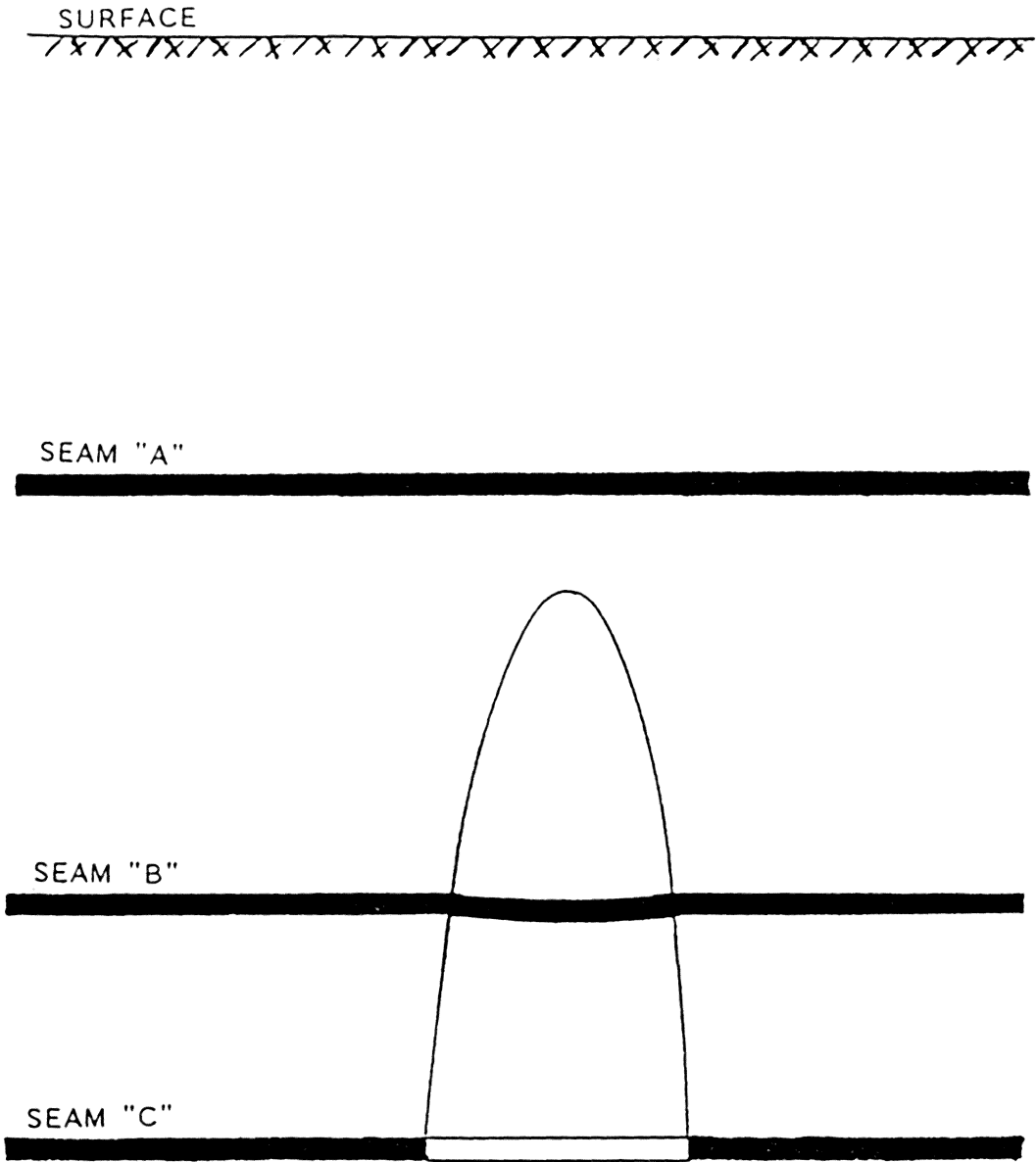


Figure 7. Extent of Major Pressure Arch

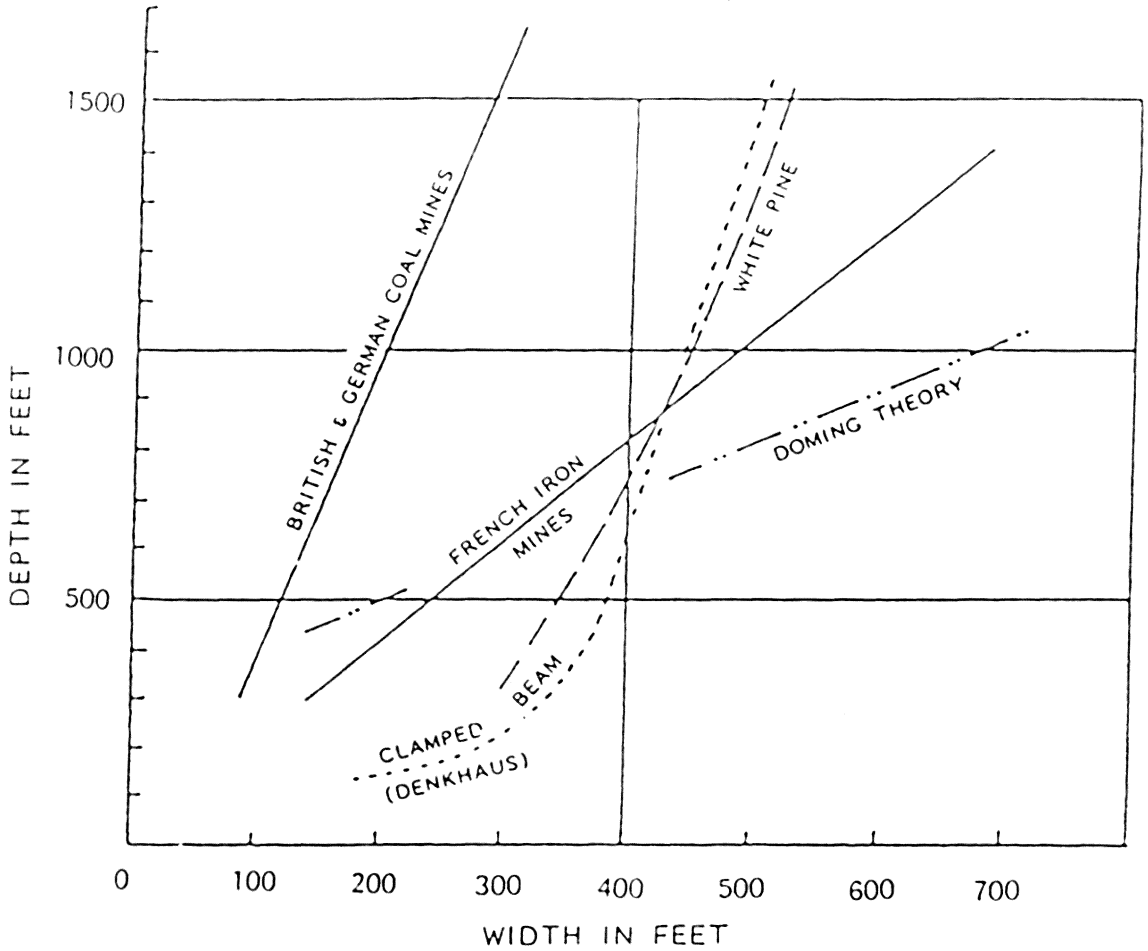


Figure 8. Comparison of Pressure Arch Size, Theory and Experience (after Barrientos and Parker, 1969).

2.3 - Finite Element Method

The finite element method is a mathematical technique in which a continuous solid is modeled by the use of a mesh containing a finite number of elements interconnected at the corner or nodal points. The nodal points and elements are then assigned numbers, and the coordinates of the nodal points are determined. Throughout experimental displacement of the model, the straight lines which form the elements are forced to remain straight. The stresses and strains that arise from forcing the elements to remain straight are evaluated according to equilibrium equations. The basic equilibrium equation used in finite element analysis is (Desai and Abel, 1972):

$$[k]\{q\} = \{Q\} \quad (\text{Eq. 2.11})$$

where $[k]$ is the element property matrix,
 $\{q\}$ is the vector of nodal displacements,
 $\{Q\}$ is the vector of element model forcing parameters.

. These equilibrium equations are then assembled in order to obtain a relationship of the following form (Desai and Abel, 1972),

$$[K]\{r\} = \{R\} \quad (\text{Eq. 2.12})$$

where $[K]$ is the assemblage property matrix,
 $\{r\}$ is the assemblage vector of nodal displacements, and
 $\{R\}$ is the assemblage vector of nodal forcing parameters.

The boundary conditions and the specific loading conditions for any particular point can be incorporated into the finite element analysis to solve for the nodal displacements. The stresses and strains can then be determined by using a transformation matrix such as the one below (Desai and Abel, 1972):

$$\{S\} = [c][B]\{q\} \quad (\text{Eq. 2.13})$$

where $\{S\}$ is the stress in any element,
 $[c]$ is the stress-strain matrix,
 $[B]$ is the transformation matrix, and
 $\{q\}$ is as above in Equation 2.11

Further discussion of the finite element method is beyond the scope of this thesis. Additional information on the finite element method may be obtained from Desai and Abel, 1972, and Zienkiewicz, 1977 as well as many other works.

The output from most finite element programs is in the form of displacement at the nodes, the vertical and horizontal stresses, the principal stresses and the angles at which they occur, and the shear stress for any given element.

2.3.1 - Advantages of the Finite Element Method

It is important to understand why the finite element method is preferred over other methods of stress analysis. Several of these advantages are listed by Wilson, 1965.

- 1) The method is completely general with respect to the geometry and material properties.

- 2) Complex bodies composed of many different materials can easily be modeled.
- 3) Anisotropic materials are automatically included in the formulation and thereby allows filament structures to be handled easily.
- 4) Displacements or stress boundary conditions may be specified for any nodal point of the finite element mesh.
- 5) Arbitrary thermal, mechanical and accelerated loads can also be included in the analysis.
- 6) In regards to the accuracy, it has been shown mathematically that the solution of a finite element analysis converges to the exact solution as the number of elements for a particular size mesh is increased. In this way the desired degree of accuracy can be obtained.
- 7) In the mechanics of the finite element method, a symmetric, positive, definite matrix which most often occurs in a banded form can be solved by using a minimum of computer storage.

2.3.2 - Modeling Criteria for the Finite Element Method

Perhaps the most important aspect of the finite element method is the discretization of the model body itself. The choice of the number, size, shape and configuration of the

elements should be made in order to simulate the original body as closely as possible and to obtain a higher degree of accuracy in the results of the finite element method.

Although a certain degree of engineering judgment is essential in the discretization of the model, there are several guidelines suggested by Desai and Abel (1972) that make this process easier.

- 1) In the location of the nodes, subdivision lines and planes are usually placed where abrupt changes in geometry, loading and material properties occur.
- 2) A finer subdivision is necessary in regions where stress concentrations may be expected.
- 3) Curved boundaries of the model can be approximated as a step-like edge formed from the sides of the elements adjacent to the boundary, if straight-sided elements are to be employed. Isoparametric elements with curved sides can be used in lieu of straight-sided elements.
- 4) To minimize the computer time and storage for the overall stiffness matrix, the band width should be as small as possible. The band width is given as,

$$B = (D + 1)f \quad (\text{Eq. 2.14})$$

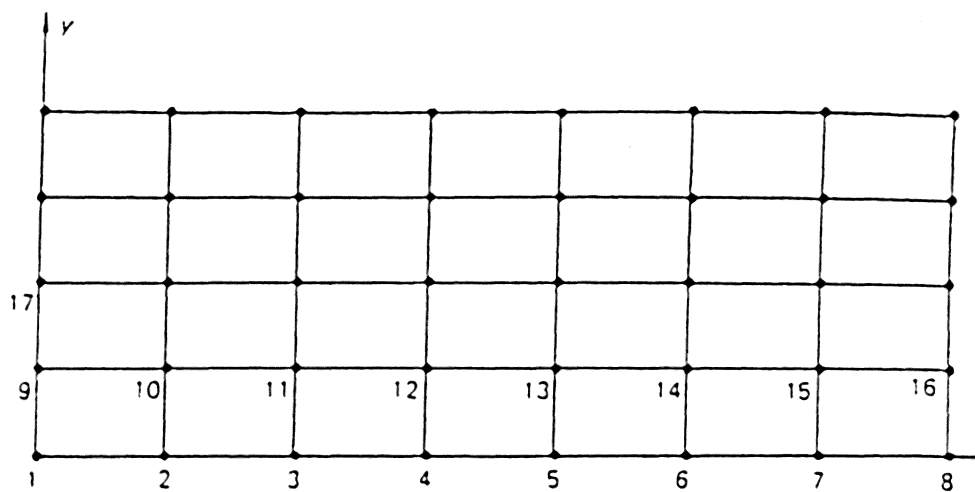
where B is the semi band width

D is the maximum difference occurring for all elements of the assemblage, and f is the number of the degrees of freedom at each node.

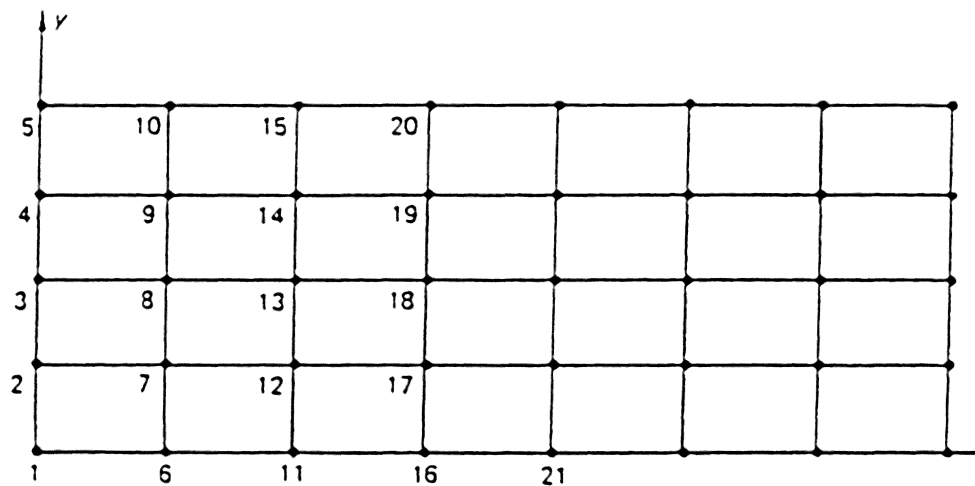
For this reason the numbering system of the nodes is very important in terms of computer time and storage. Figure 9 (b) shows the better way to number the nodes and elements for the model shown.

- 5) The aspect ratio of the elements affects the accuracy of the finite element solution. The aspect ratio is the largest dimension of the element to the smallest dimension. Long, narrow elements are usually avoided in a finite element mesh, whereas equilateral quadrangles are most often used. Figure 10 shows the inaccuracy of solutions as a function of the aspect ratio.
- 6) For a body of infinite lateral dimensions, side boundaries can be assumed and the side nodes are allowed to move only vertically, not horizontally.

Kulhawy (1974) showed that for geotechnical problems, such as those under consideration in this study, arbitrary, linear strain quadrilateral elements are the most appropriate. Kulhawy recommends a minimum of 125-150 elements for the analysis of simple structures in



(a)



(b)

Figure 9. Numbering of Nodes to Reduce Band Width
(after Desai and Abel, 1972).

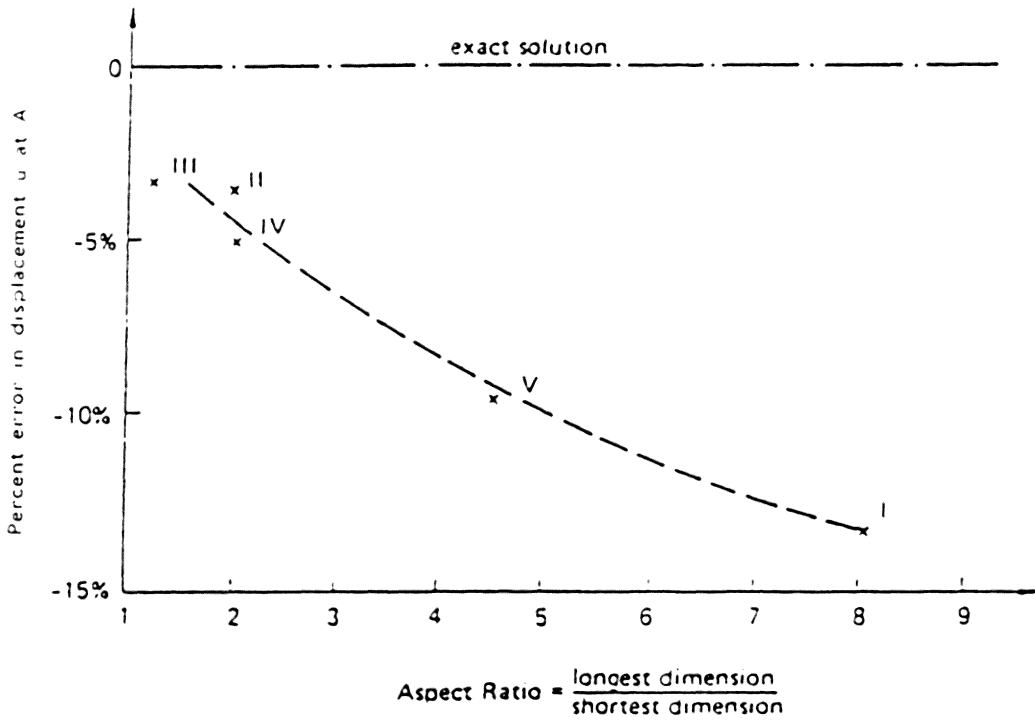


Figure 10. Inaccuracy of Solution as a Function of Aspect Ratio (after Desai and Abel, 1972).

homogeneous rock and that the boundaries of the finite element mesh should be at least six radii away from the center of the opening in order to minimize the boundary effects upon the solution as shown in Figure 11.

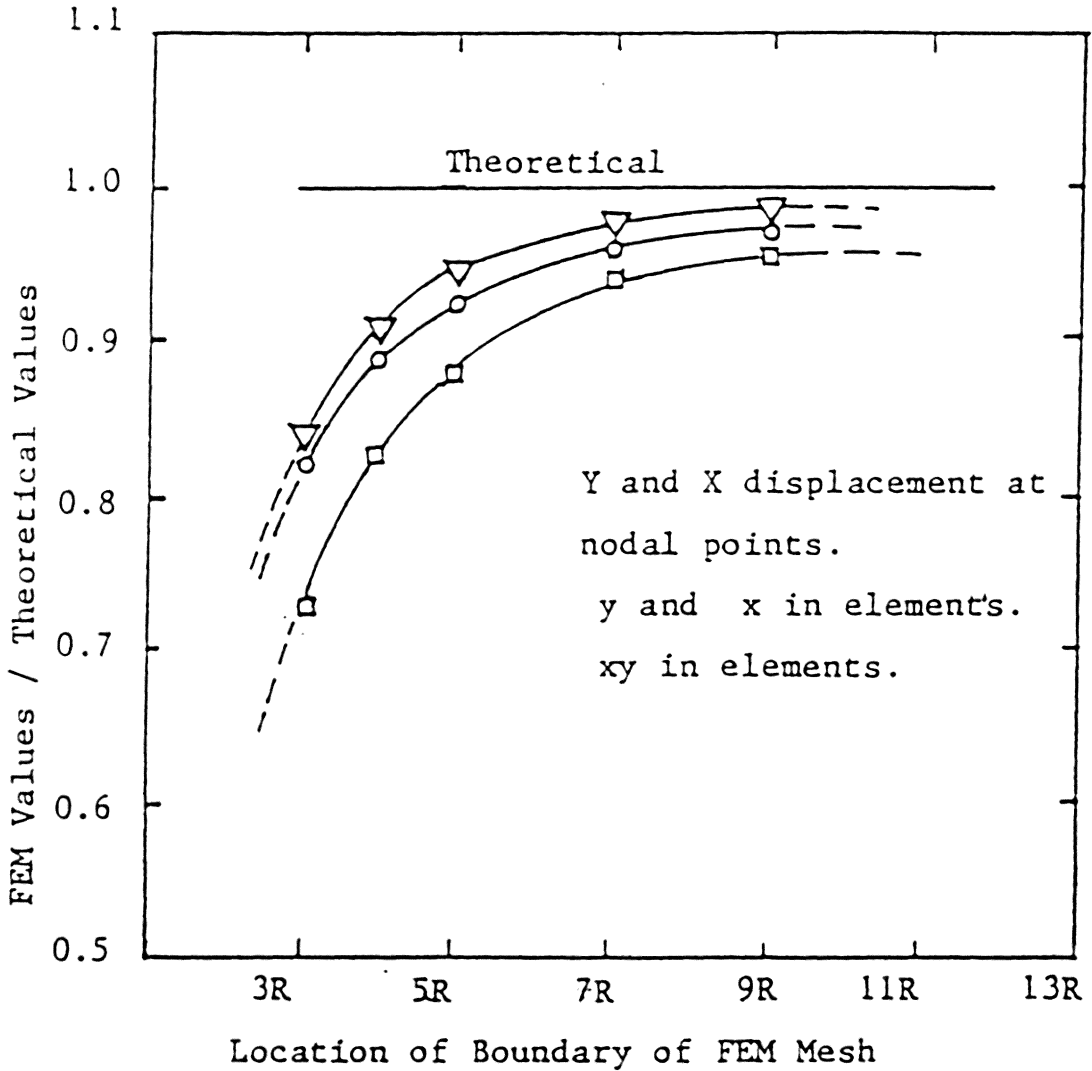


Figure 11. Effect of External Boundary Location on Accuracy of Finite Element Method Solution (after Kulhawy, 1974).

III. - CASE STUDIES

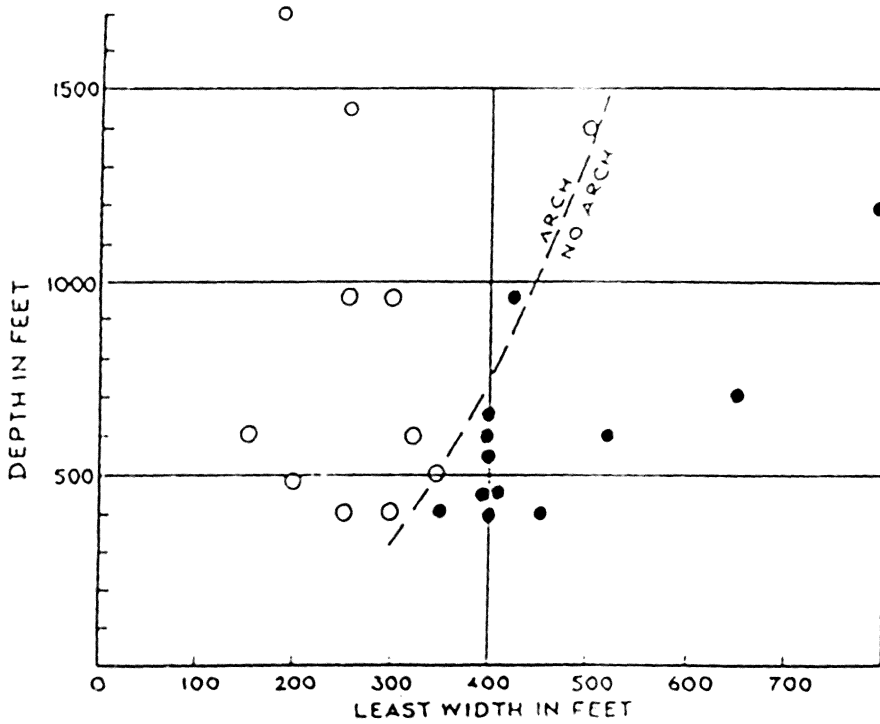
In order to analyze the effects of the pressure arch upon multiple seam mining, several case studies were collected from published literature.

3.1 - White Pine Copper Mine

The study by Barrientos and Parker (1974) was conducted at the White Pine copper mine in Michigan and relates how simple observations and measurements were used to define the limits of the pressure arch.

Mining conditions at the White Pine mine were stable until the excavation reached a critical width of approximately 300 feet. Observations were made at many underground failures, some ^{of} which were not planned but the majority of which were created by pillar robbing operations. At this point it became clear to Barrientos and Parker that, within some critical width of excavation, pillars could fail without a major collapse of the roof occurring and that this critical width of excavation increased slightly with an increase in depth. The results of these observations are shown in Figure 12.

In July 1966, full scale workings of various dimensions were developed at White Pine in order to test the pressure arch theory and to define the maximum width of the arch.



Underground collapse appeared at surface ●
 Underground collapse did not appear at surface ○

Figure 12. Critical Width versus Depth
 (after Barrientos and Parker, 1974).

Several conclusions were drawn from the information supplied by the test panels:

- 1) A pressure arch can be formed,
- 2) The maximum width of the arch at a depth of 550 feet was at least 308 feet,
- 3) Pillars within the panel must be small enough to yield or no arch would form,
- 4) Load was transferred to abutment pillars,
- 5) Distribution of load could be arranged through design of pillar stiffness,
- 6) High extraction (in this case 92%) can be attained within the narrow panel,
- 7) Effective modulus of deformation of small pillars was less than half of the laboratory value (Barrientos and Parker, 1974).

The extent of the pressure arch which formed as a result of the mining conducted at White Pine is shown in Figure 13. Barrientos and Parker believed that the rock mass could not exert any significant resistance to tensile stress. However, due to many measurements and observations they felt that it was the lateral compressive forces which held the jointed rock mass in place in the roof. They used these findings to further explain the pressure arch theory. According to Barrientos and Parker the weight of the overburden above a cave or yielding pillars can be supported

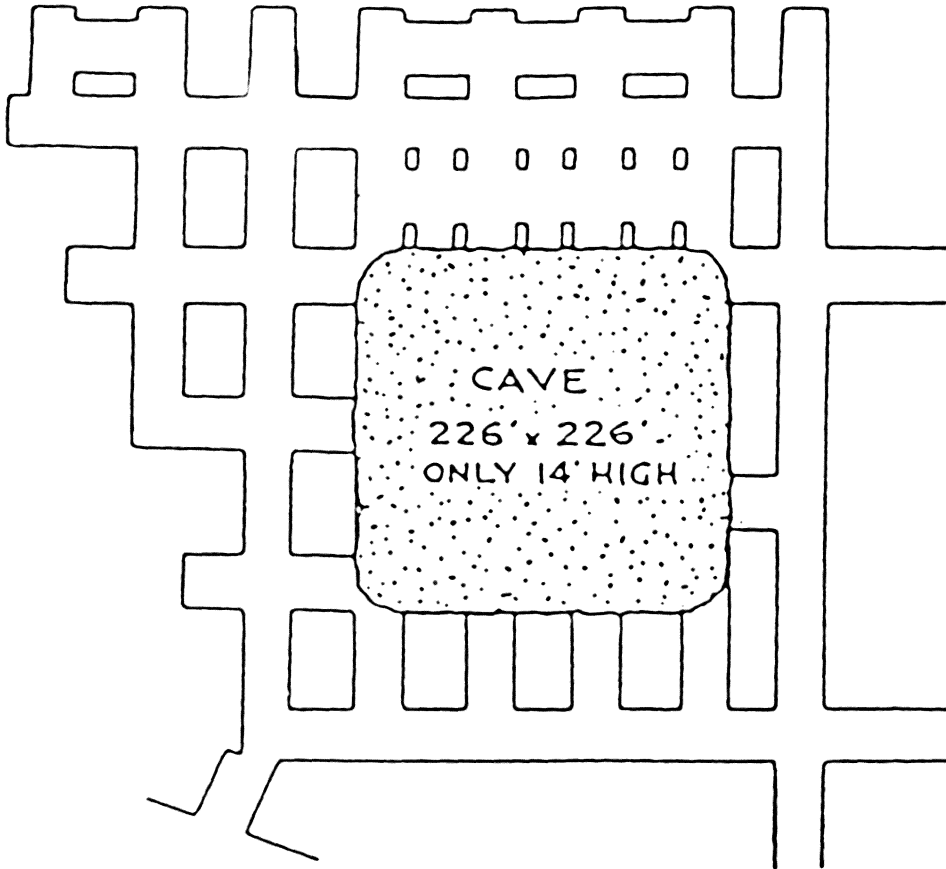


Figure 13. Extent of Pressure Arch Formed as Result of Mining at White Pine (after Barrientos and Parker, 1974).

from the sides if the lateral stress is great enough and the weight of the rock is not too great. Since the weight of the rock mass within the pressure arch, per square inch of side support area, depends upon the unsupported span, for each different lateral stress condition there will be a different critical width of excavation. Since the lateral stress is comprised of two parts, a primitive stress that exists near the surface and changes little with depth and the Poisson component of vertical stress that does change with depth, the width of the pressure arch can be expected to increase as depth increases. The two components of lateral stress are illustrated in Figure 14.

3.2 - Cadley Hill Colliery

This case study was conducted at the Cadley Hill Colliery of the Main Coal District. The Main Coal seam lies at a depth of approximately 1600 feet and averages 14 feet 6 inches thick. Approximately 190 feet below the Main Coal lies the four foot thick Woodfield seam, 60 feet below that is the 5 foot 8 inch Stockings seam and about 50 feet below that is the 4 foot Eureka seam.

The roadways of the Main Coal workings crossed over areas that were worked in the lower Stockings seam and the following observations were made:

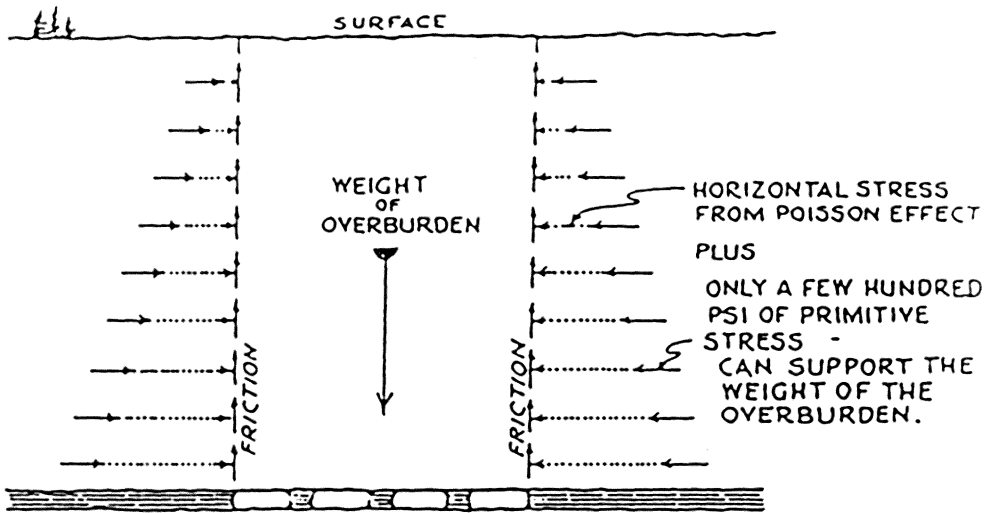


Figure 14. Two Components of Lateral Stress
(after Barrientos and Parker, 1974).

1) The ground immediately above the worked panel of the lower Stockings seam was de-stressed and the roadways in the Main Coal seam were in excellent shape.

2) The ground immediately above or to one side of the edge of the gob in the Stockings seam was highly stressed and the roadways driven in the Main Coal seam deteriorated badly.

Specific examples of the effect of areas of high stress and low stress upon an upper seam include a return gate which was driven in the Main Coal seam directly above a pillar edge in the Eureka seam experienced over five feet of floor heave before the face retreated. A Main Coal main gate that was above the Stockings gob stood in good shape until the entries passed the edge of the gob and began to deteriorate. A cross-section of the Main Coal seam and the Woodfield workings is shown in Figure 15. These examples of the effect of the stresses around a pre-existing lower mining opening upon an upper seam should be noted in the future in the mine design of an upper seam working over a previously mined lower seam.

3.3 - Monongalia County, West Virginia

This case study is one of many documented by Stemple (1956). In this instance the lower seam is the Pittsburgh

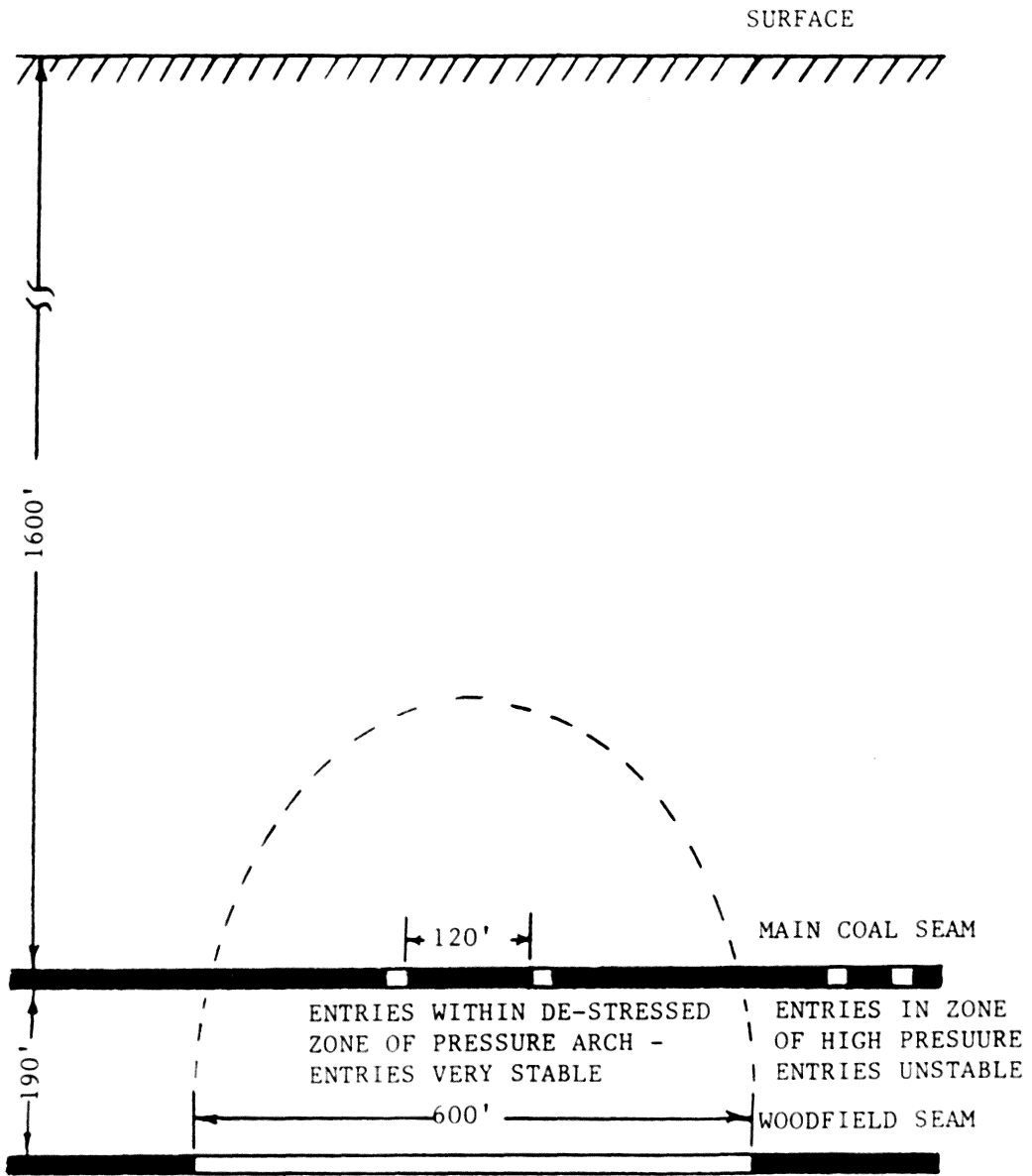


Figure 15. Cross-section of the Main Coal and Woodfield Workings.

seam which averages 96 inches in thickness. The upper seam is the Sewickley seam which is about 66 inches thick. The Pittsburgh seam is mined by driving twenty foot rooms on ninety foot centers with an overall extraction ratio of 60% and up to 85% where pillaring has occurred. The Sewickley seam is mined with twenty foot rooms on seventy foot centers with a resulting extraction ratio of approximately 75 percent. The innerburden between the two seams is about ninety feet thick and is comprised of mostly shales and limestone. The overburden is approximately 400 feet thick and is comprised of shales, fireclays, limestones and sandstones.

This case study is an example of the disturbance that may occur in an upper seam over a line between the solid coal and the gob in the lower seam. However, the greatest damage is not directly over the edge of the remaining coal in the lower seam. Instead, the most damage occurred in an area out over the gob away from the solid coal, usually at a distance of 100 to 300 feet from the edge of the solid coal. A cross-section view of the case study is shown in Figure 16.

The location of the damage is due to the fact that the overlying strata above the gob fail successively further out over the gob. This results in an arch shape which carries the damage out to a point away from the edge of the solid coal in the lower seam.

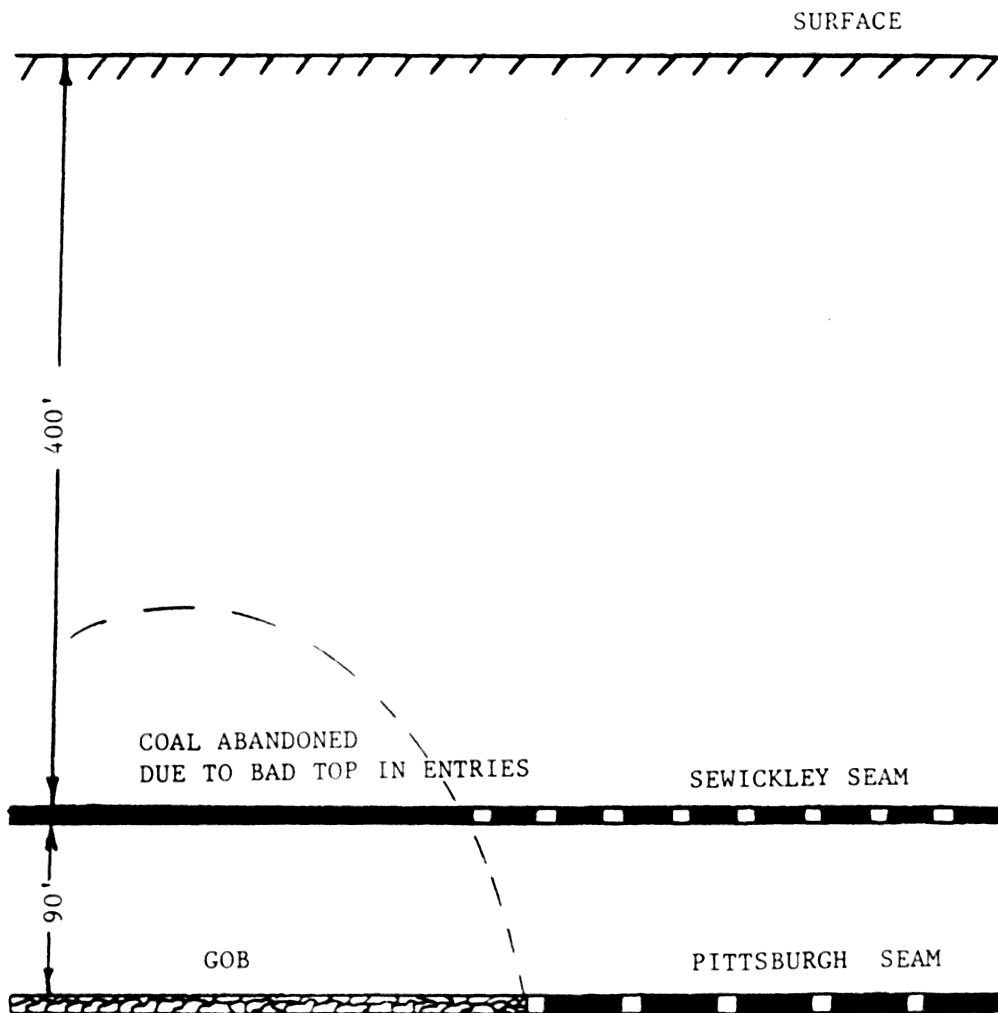


Figure 16. Cross-section of Sewickley and Pittsburgh Seams Showing Line of Damage Above Gob of the Lower Seam.

IV. - FINITE ELEMENT MODEL DEVELOPMENT

4.1 - The Finite Element Computer Program

In an effort to evaluate the effect of the pressure arch upon multiple seam mining, finite element computer modelling was used to simulate certain mining conditions. In this way, with proper input, the program accurately yields the principal stresses and their directions across the model.

The computer program used in this study was developed and published by Desai and Abel (1972). This program was selected for both its simplicity and generality. The program can be used for the linear, elastic, plane strain, or plane stress analysis of isotropic bodies. The finite element program was written in FORTRAN IV and can be used with both quadrilateral and triangular element shapes.

Most of the calculations are performed in the various subroutines within the computer program. The main program itself reads the title of the problem, computes the semi-band width (as explained in Section 2.3.2 of this text), solves the overall equilibrium equations, and prints the displacements. Following is a list of the subroutines within this finite element program with an explanation of their functions.

- 1) DATAIN: Reads and prints the input data.
Performs error checks on the input.

- 2) ASSEMBL: Initializes and assembles the overall stiffness matrix, and the load vector. Temporarily stores information needed for later calculations. Introduces geometric boundary conditions on the model.
- 3) QUAD: Computes the stress-strain matrix, stiffness matrix, strain-displacement matrix and body force vector of either a quadrilateral or triangular matrix.
- 4) CST: Compute the strain-displacement matrix, body force vector, and stiffness matrix for a constant strain triangle element.
- 5) GEOMBC: Applies the prescribed boundary conditions for each individual node.
- 6) BANSOL: Triangularizes the overall stiffness matrix by symmetric Gauss-Doolittle decomposition or solves for the displacement vector corresponding to a particular load vector.
- 7) STRESS: Computes the strains, stresses and the principal stresses. Prints the stresses at the centroid of the elements.

More information concerning this program is available in Desai and Abel (1972) and in Appendix C-1.

4.1.1 - Preparation of Finite Element Model

The first step in preparing a finite element model is to sketch what the model is supposed to represent. In this case, eighteen different models were prepared. In each case the height of the mining opening was set at five feet. The width of the opening was set at a minimum of 100 feet and was increased by multiples of 100 feet to a maximum of 600 feet. The depth of the mine opening below the surface was set at 500 feet, 750 feet and 1000 feet. The lateral extent of the model was limited to a maximum of 2000 feet, that is, 1000 feet from the centerline of the mine opening.

In order to make the results of the finite element program as accurate as possible, the values used to define the material properties of the model itself must also be as accurate as possible. In this study, three different materials were used, a sandstone, a shale and a coal. The material properties for these different strata are shown in Table 1.

The finite element program is then run using the necessary input as described in Appendix C-1. The program will produce values for the horizontal stress, vertical stress, shear stress, principal stresses and their directions for each element of the model.

Table 1

Material Properties Used in the Analysis

<u>Rock Type</u>	<u>Modulus of Elasticity</u>	<u>Poisson Ratio</u>	<u>Density</u>
Shale	1.61 x 10 ⁸ psi	0.10	158.0 pcf
Coal	0.72 x 10 ⁸ psi	0.25	125.0 pcf
Sandstone	3.00 x 10 ⁸ psi	0.15	144.0 pcf

4.2 - The Mesh-Plot Program

The finite element program requires large amounts of input in order to make the required calculations. If, however, an error occurs in the input, the finite element program will run until the error is detected thereby incurring a loss of by time and computer funds. For this reason, an auxiliary program was created (Bhattacharya, 1980) to detect any errors in the input of the nodal points and elements themselves. This mesh-plot program generates a plot of the finite element mesh.

The mesh-plot program was written in FORTRAN and is tailored for use at the facilities of the Virginia Tech Computing Center. The mesh-plot program is capable of plotting the finite element mesh on either a Versatec 1200 electrostatic plotter or a CALCOMP 1051 drum plotter.

The formatting of the input is identical for both the finite element program and the mesh-plot program. In this way the element and nodal point data for the finite element program can be checked in the mesh-plot program before the finite element program is run.

The mesh-plot program checks for negative element areas and missing element or nodal numbers. Further information on the mesh-plot program is furnished in Appendix C-2. An example of the output from the mesh-plot program is shown in Figure 17.

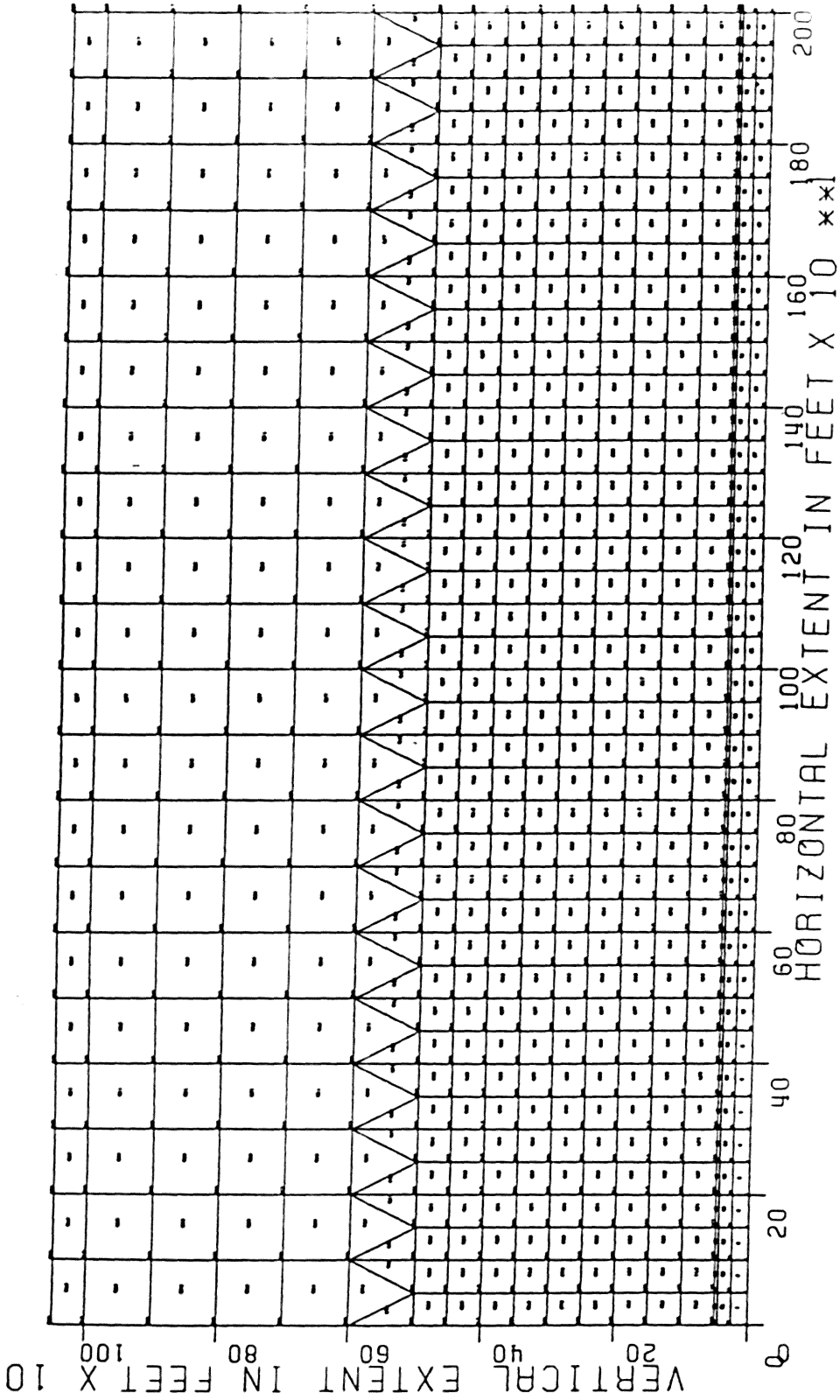


Figure 17. Example of Mesh-Plot Output

4.3 - The Stress-Plot Program

As part of the output of the finite element program, principal stresses at each element and their directions are produced. The stress-plot program plots the scaled magnitudes of the principal stresses and directions of these stresses at their proper relative positions (Bhattacharya, 1980). This program has been modified to read as input the output from the finite element program. This eliminates any errors which may occur in the transfer of data from one format to another caused by operator error.

The stress-plot program plots the principal stresses by calculating the coordinates of the ends of the stress vector as shown in Figure 18. The sign convention for the stresses is identical to that used in the finite element program, that is, tensile stress is positive and compressive stress is negative. An example of a stress vector diagram is shown in Figure 19. Additional information on the stress-plot program is given in Appendix C-3.

4.4 - The General Purpose Contouring Program

Another method of showing the stresses caused by an underground opening is through the use of contours. This is accomplished with the help of the General Purpose Contouring

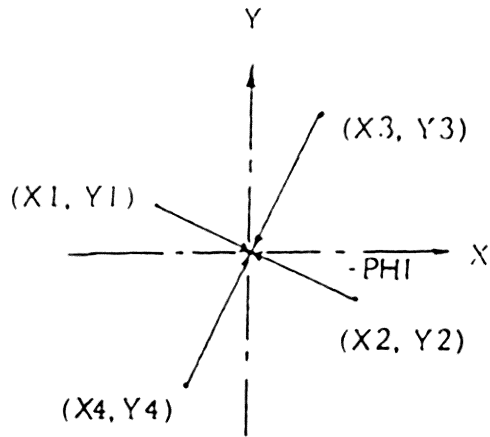
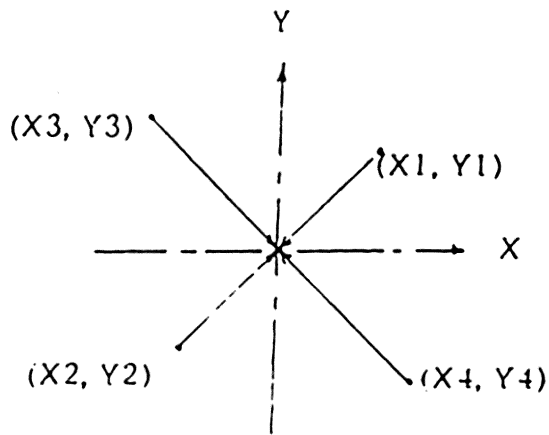
a) $\text{PHI} = -ve$ b) $\text{PHI} = +ve$

Figure 18. Sign Convention for Plotting Stress Vectors (after Coates, 1969).

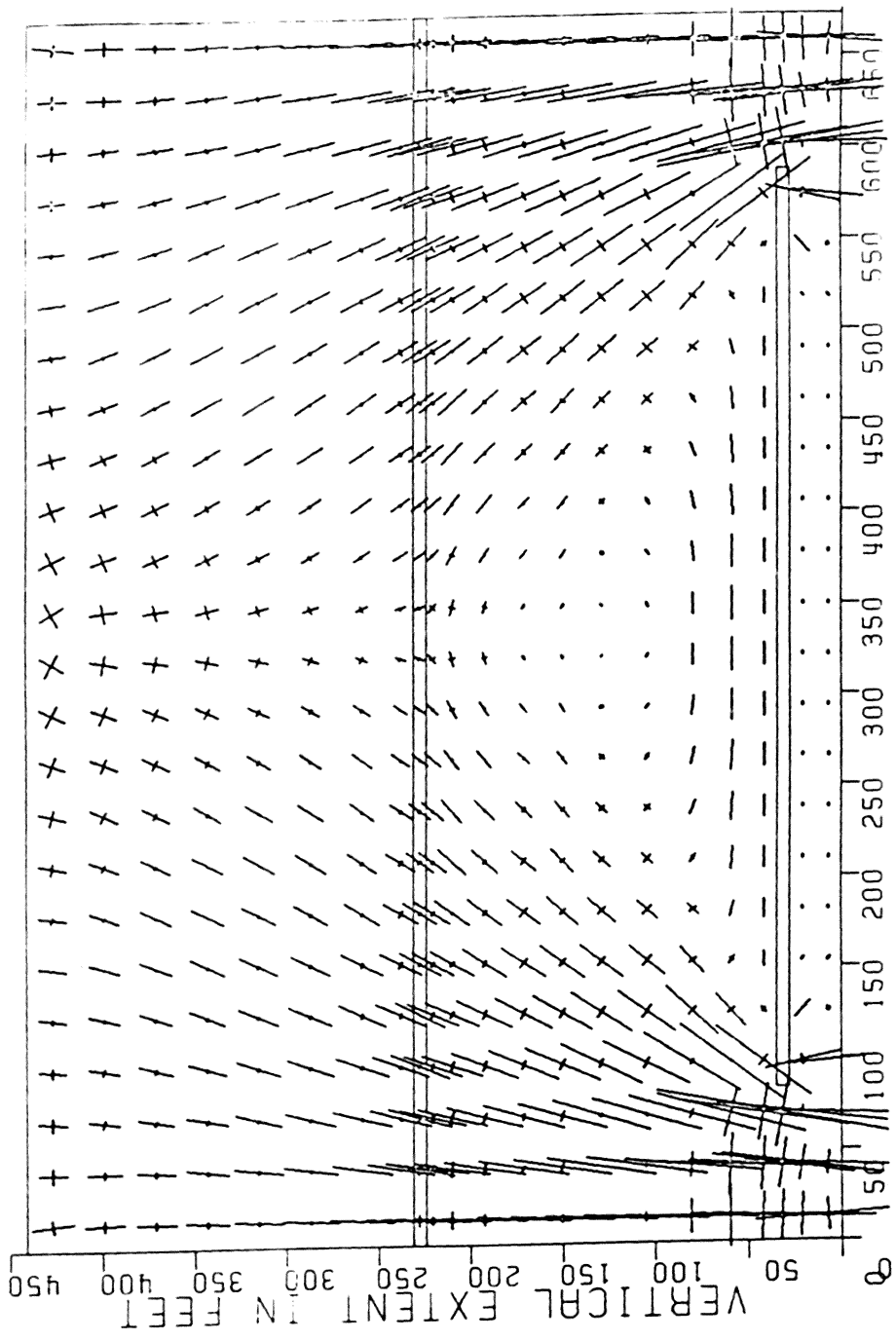


Figure 19. Example of Stress Vector Diagram

Program (GPCP) developed by Batten and available through the California Computer Products, Inc. (1971).

The program graphically displays the functions of two variables as contour maps. GPCP is a very flexible program that allows the user to: specify a function at random points or at an array; delete the contour plotting in specific areas; plot bold index contour lines with or without labels; suppress contour lines in areas of high contour density; and make notations on the plot.

The General Purpose Contouring Program is written in FORTRAN and uses either a Versatec or CALCOMP plotter. Since the GPCP package is made available from California Computer Products, Inc. directly to the Virginia Tech Computing Center, a listing of the program is not available to the public. A sample of GPCP input is included in Appendix C-4. An example of the output from GPCP is shown in Figure 20.

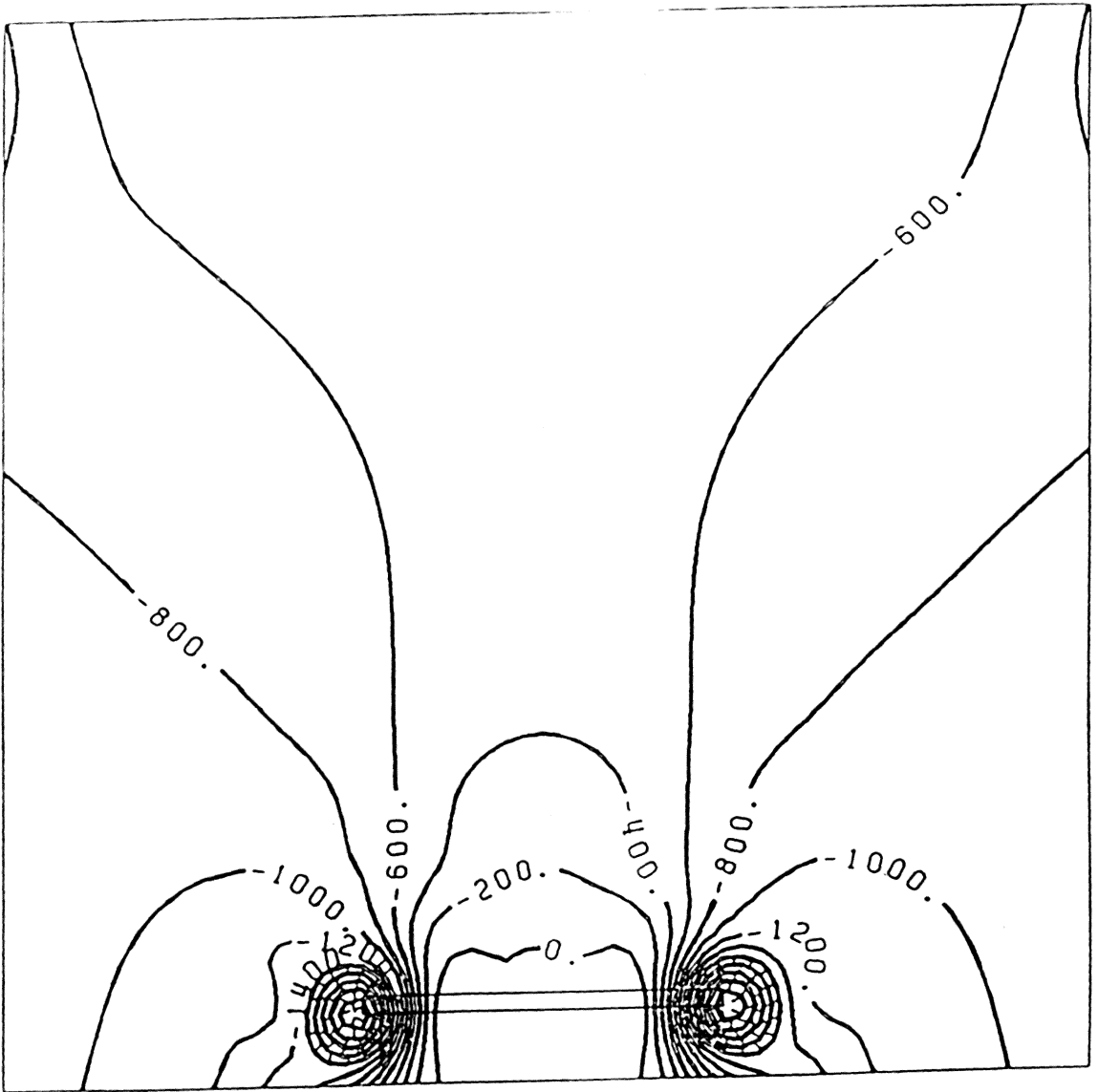


Figure 20. Example of GPCP Output

V. - PHOTOELASTIC MODEL DEVELOPMENT

The basis of photoelasticity is that when a birefringent material is loaded and viewed through the plates of a polariscope, fringes appear which are directly proportional to the resulting shear stresses in the material. To elaborate, after a photoelastic model is loaded, the material is viewed with the light from a dark field circular polariscope. Alternating light and dark patterns can be seen across the stressed areas of the model. The dark bands on the model represent patterns of light interference and are known as fringes. These fringes are assigned an order, or number, depending upon the boundary conditions of the model. The value of the fringe order is directly proportional to the maximum shear stress at any point or the difference between principal stresses at that point, as shown in the following equation.

$$\tau_{\max} = \frac{S_1 - S_2}{2} = \frac{n f}{t} \quad (\text{Eq. 5.1})$$

where τ_{\max} = maximum shear stress

S_1 = major principal stress

S_2 = minor principal stress

n = fringe order

f = material fringe factor

t = material thickness

By using photoelastic methods it is also possible to determine the principal stresses across the model. By adjusting the polariscope a plane polarized light field gives the inclination of the principal stresses to the vertical for any point on the model. The shear stress along the x-y plane is defined in terms of the following variables:

$$\tau_{xy} = \frac{nf}{t} \sin 2\theta \quad (\text{Eq. 5.2})$$

where τ_{xy} = shear stress in x-y plane

θ = principal stress inclination

and other variables as in Eq. 5.1.

In this study, the photoelastic modelling was limited to two dimensional analysis. According to Coates (1965), two dimensional approximations are adequate for any engineering purpose when the length of the opening is greater than twice the opening width. This finding was substantiated by Heuze (1970) who found only minor changes in the stresses along a line of pillars in a room and pillar mines. An additional constraint of plane stress analysis was also placed on the model. Plane stress theory will give accurate results when, as noted by Frocht (1948), the lateral dimensions of the photoelastic model are at least four times the thickness.

In an effort to obtain a more accurate stress pattern in the photoelastic model, two horizontal slots were machined into each edge of the photoelastic material pillar in order

to model the yield zone which lies along the perimeter of coal pillars. This had the effect of reducing the normally high stresses that are found at the edge of the opening. The photoelastic material, polyurethane rubber (PSM-4) was machined according to the techniques outlined by Neall and Haycocks (1974) and Neall (1975).

In order to model the stresses surrounding an underground opening, several photoelastic models were used. A crossed circular polariscope was used to eliminate the isoclinic lines from the fringe pattern since the directions of the principal stresses were not desired from this model. The principal stress difference, however was desired as this would show the areas of high and low stress across the model. The fringe pattern is known as an isochromatic fringe pattern. When the model is viewed with white light, where all the wavelengths of the visible spectrum are present, the isochromatic fringe pattern will appear as a series of colored bands. A black fringe will appear only when the principal stress difference is zero and a zero order of extinction occurs for all wavelengths of light. This black area correlates with the de-stressed region within a pressure arch. Examples of isochromatic fringe patterns which show the de-stressed zone above the model openings are shown in Figures 21 and 22.

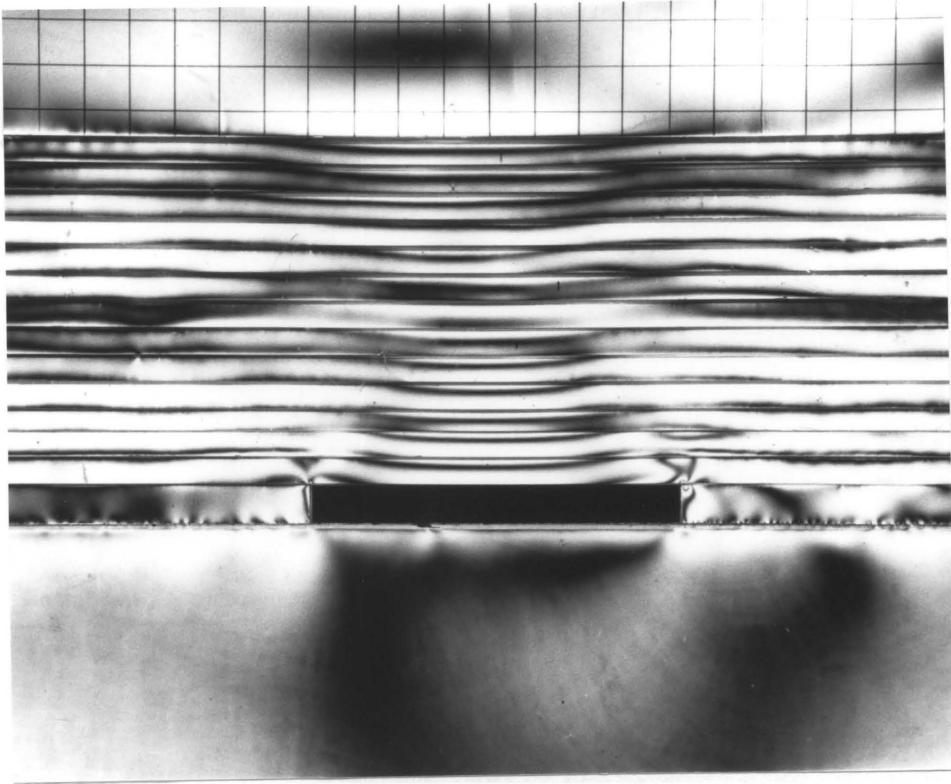


Figure 21. Example No. 1 of Isochromatic Fringe Pattern

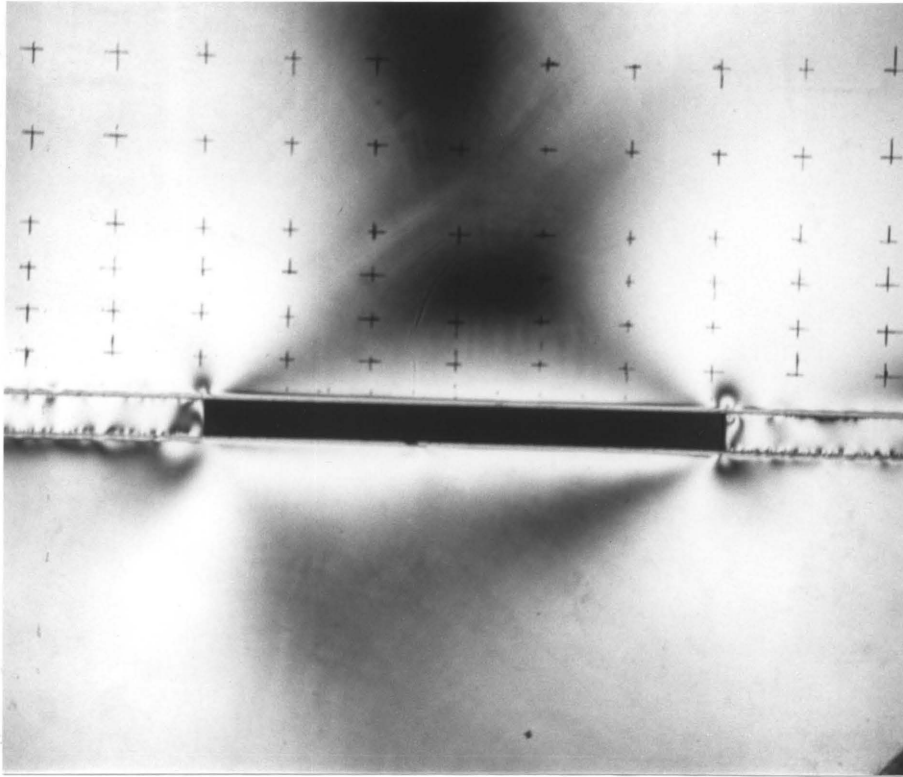


Figure 22. Example No. 2 of Isochromatic Fringe Pattern

VI. - CASE STUDY CORRELATION

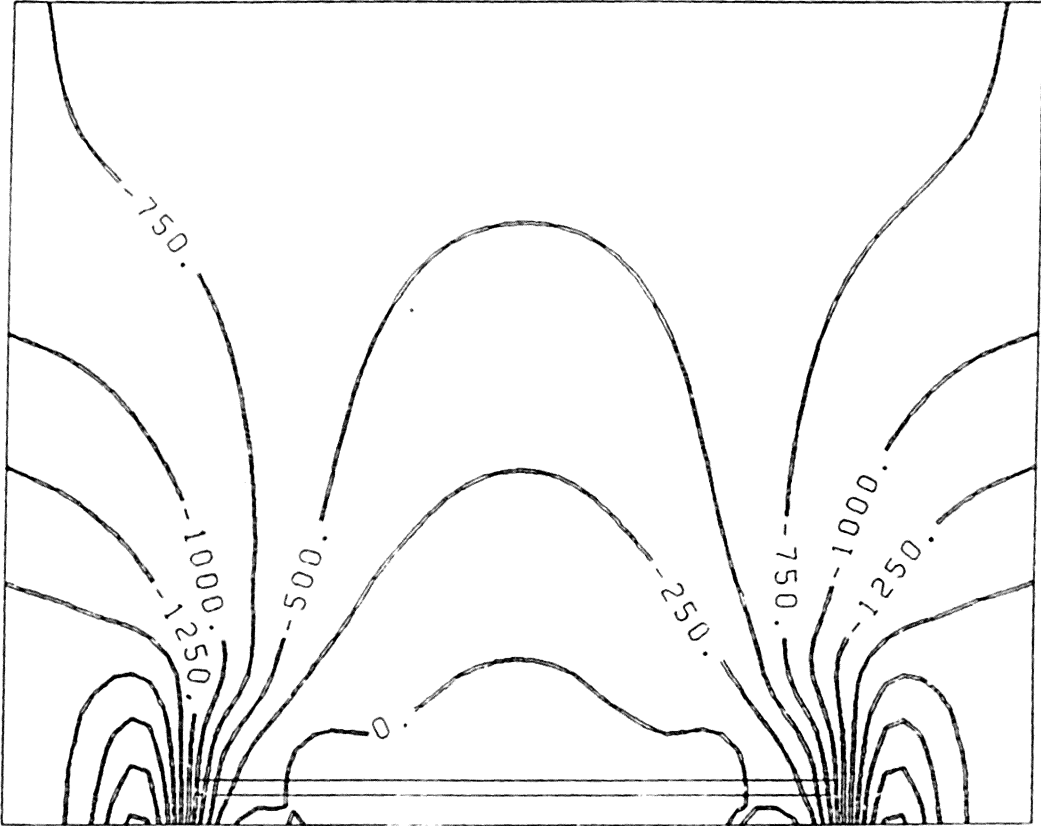
In order to check the accuracy of the finite element computer method, it was necessary to run the program with input derived from a documented case study and to check the results obtained from the finite element analysis against those noted in the case study.

For this purpose a case study was selected that measured the stresses around an underground opening. Howell et al (1976) documented the stresses around a shortwall mining area comprised of six adjacent panels at the Hendrix No. 22 Mine in Kentucky. Each of the faces were 170 feet wide on 270 foot centers, with an extracted seam height of four feet. The depth of cover over the shortwall area ranged from 770 feet above panel 1 to a depth of 170 feet over panel 5. The overburden consisted of 115 feet of shale and coal strata directly above the mined seam, a hundred foot thick sandstone layer above that and layers of shale and sandstone reaching to the surface. The results were obtained from a borehole, drilled from the surface, above the centerline of panel 1, which was the first panel to be mined.

According to Howell, the first 33 feet above the shortwall face consisted of a large tensile zone, which was due to caving of material into the excavation. Between 33

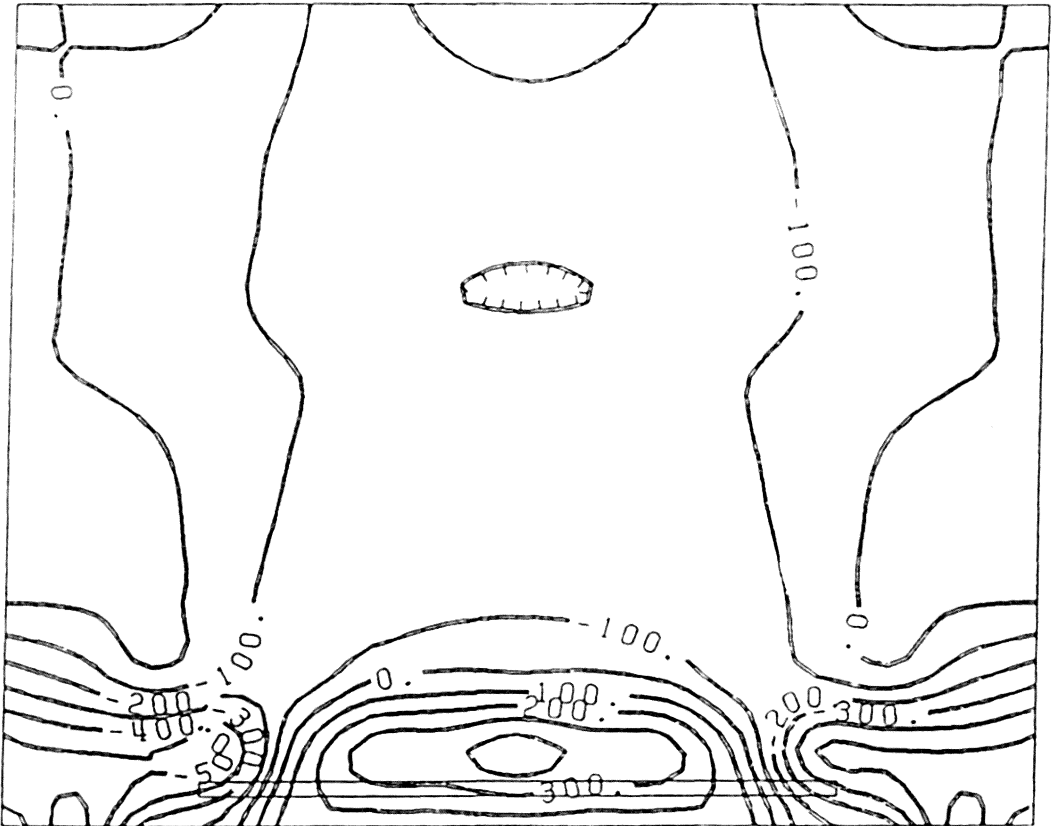
and 49 feet above the opening the strains were compressive, perhaps due to the rotation of blocks as they caved. The strata fell in large blocks due to the sandy nature of the shale. Above this compression zone the strains again became tensile, perhaps due to bed separation at the base of the thick sandstone layer. This indicates that the sandstone bed may have bridged over the excavation, acting as a beam.

The conditions described in the case study were duplicated as closely as possible in the input of the finite element program. A mine opening of 170 feet wide by 4 feet in height was modeled and the model duplicated the geologic column of the Hendrix mine as closely as possible. The results from the finite element program and subsequent contouring of the output show that a tension zone extends approximately 30 feet above the mine opening. This could be seen in Figures 23 and 24 which are contours of the vertical and horizontal stresses respectively. However, the finite element program used in this research could not duplicate the bed separation which may have occurred between the different materials in the overburden. From this correlation it was decided that the finite element program was sufficiently accurate.



SCALE: 1 INCH = 50 FEET

Figure 23. Contour of Vertical Stresses, Hendrix Mine Case Study.



SCALE: 1 INCH = 50 FEET

Figure 24. Contour of Horizontal Stresses, Hendrix Mine Case Study.

VII. - FINITE ELEMENT RESULTS

The finite element program was run for varying widths of mine opening, depths of cover and overburden material. The output from the finite element program for each of these different mining conditions is summarized in Appendices A and B. The width of opening ranged from 100 to 600 feet in increments of 100 feet. The depth of overburden was set at 500, 750 and 1000 feet. It is believed that the range of these values would cover the majority of mining conditions in the Appalachian region. As an additional variable to be considered, the overburden was selected as either completely sandstone or completely shale as these would be the two extremes to be encountered in the mining of coal seams.

From the various output it was determined that a de-stressed zone lies above each opening. In this region the reported stresses in the overburden are actually less than the stresses that would be present if no mine opening was present. The vertical stresses and horizontal stresses both exhibit this trend. The extent and magnitude of this de-stressed zone is dependent upon both the width of opening and depth below the surface. For example, for an opening 200 feet wide under 500 feet of overburden, a tension zone exists to a height of approximately 50 feet above the opening along the centerline of the mine opening. At a

distance of 70 feet above the opening the vertical stresses are just ten percent of the superincumbent pressure. At 175 feet above the opening the vertical stresses are only 55 percent of the superincumbent pressure. This trend holds for all the models, where a region of reduced stress overlies the mine opening.

For a given depth below the surface, the tension zone increases in both width and height as the width of the mine opening increases. For an opening 300 feet wide under 500 feet of overburden, a tension zone extends 90 feet above the opening; for a 400 foot opening, 125 feet above the opening; for a 500 foot opening, 175 feet; and, for a 600 foot wide opening, the tension zone extends 225 feet above the opening.

For a given width of opening, the height of tensile zone decreases as the depth of overburden increases. For a 300 foot opening under 500 feet of overburden, a tension zone reaches approximately 90 feet above the mine opening. For an opening of the same width under 750 feet of overburden, the tensile zone is about 30 feet high. Under 100 feet of cover the tensile zone is approximately 20 feet in height.

For points within the intradosal ground or pressure arch, research shows that the stresses decrease as the the width of opening increases for any given depth. In other words, as the width of opening increases the zone above the opening is subject to decreasing stresses creating an envelope above

the opening where the vertical stresses within the overlying rock are minimal.

However, just as the intradosal stresses decrease with an increase in opening size, so do the abutment pressures increase around the intradosal zone. For a 100 foot opening under 500 feet of overburden, the abutment pressures around the opening are just 10 percent more than the superincumbent pressure. The abutment pressures around a 600 foot opening under the same depth of cover can approach and surpass twice the superincumbent pressure. As the depth of cover for a given opening width increases, the abutment pressures get closer to the superincumbent pressures.

The different materials of the overburden did not have a major effect upon the finite element output for the different opening widths and depth of overburden. The results obtained using a completely shale overburden are within ten percent of those obtained using a sandstone overburden. Therefore, the values cited above are average values for a given mining condition.

The de-stressed zone above the mine openings as shown in the finite element analysis correlates to that exhibited in the photoelstic models. This correlation can also be seen in the stress trajectories drawn for both the finite element model and for the photoelastic model as shown in Figures 25 and 26. This zone of decreased stress should be important in the mine design of future operations in an upper seam.

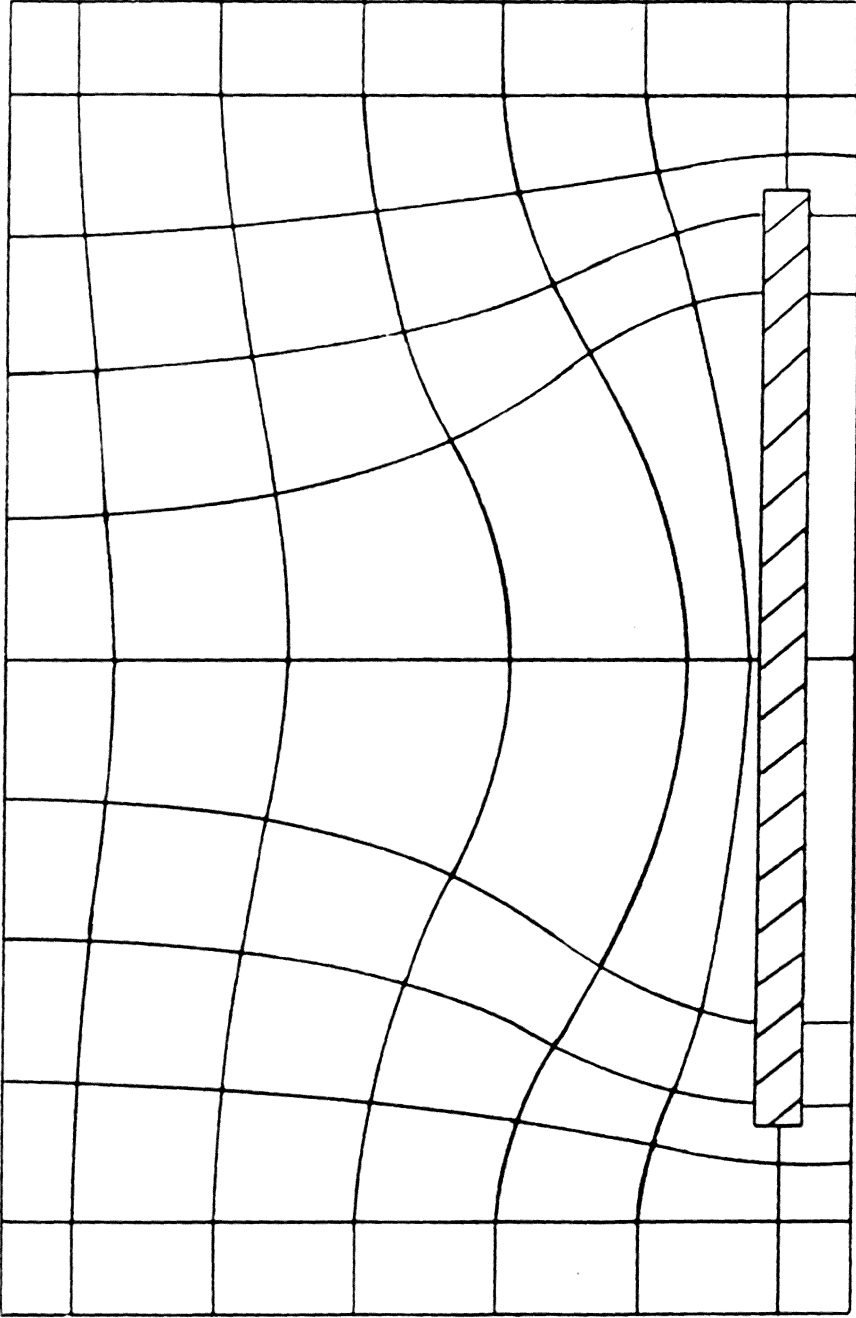


Figure 25. Stress Trajectories from a Finite Element Model.

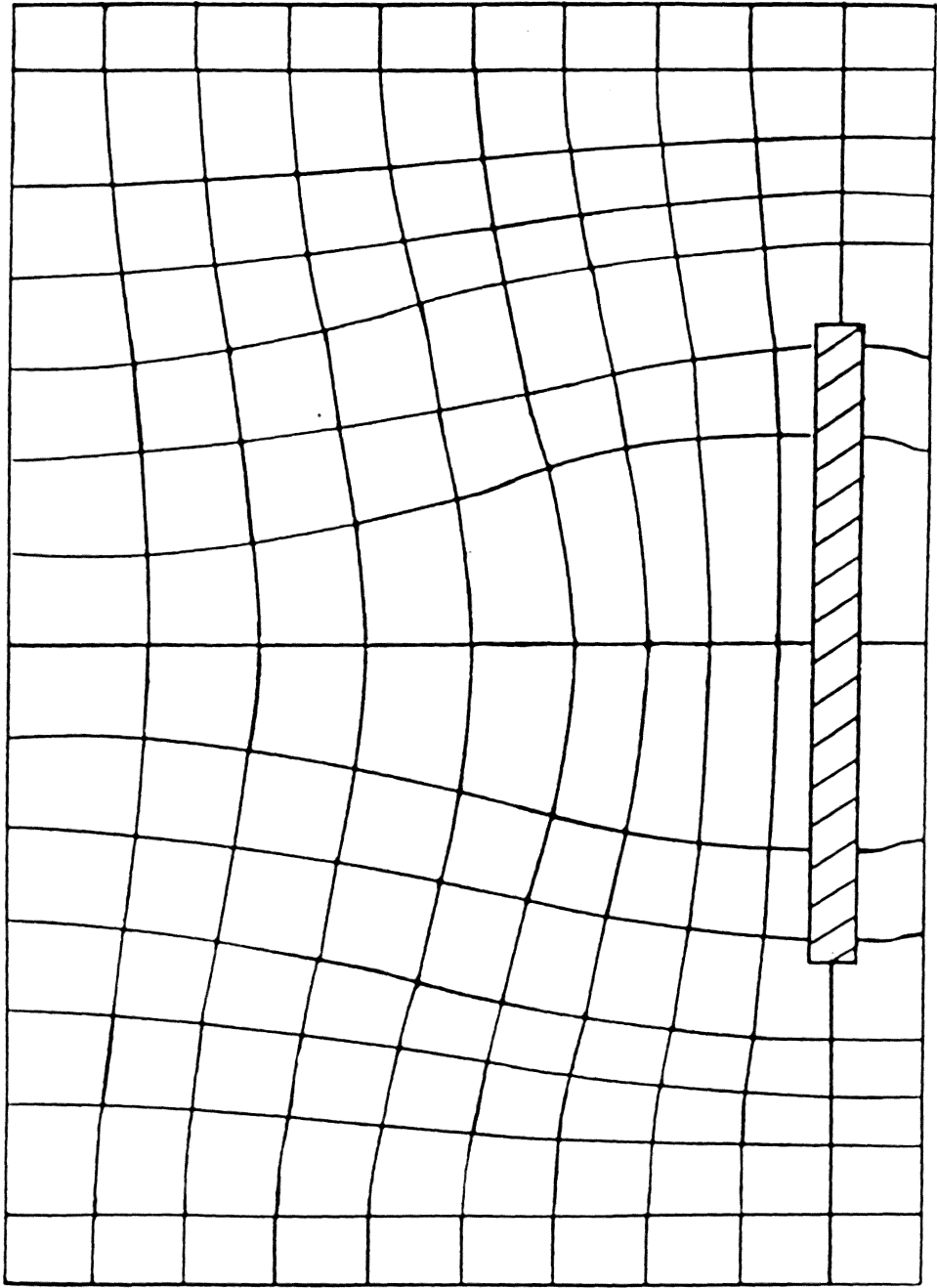


Figure 26. Stress Trajectories from a Photoelastic Model.

By using the tables in Appendices A and B, it is also possible to correlate information obtained from the case studies with experimental values. The case study shown in section 3.4 of this report had a lower seam opening width of 500 feet, a depth of overburden of approximately 1000 feet and an interseam thickness of about 200 feet. The case study reported that the upper seam entries experienced no roof control problems as they were in a de-stressed zone above the lower panel. The tables of Appendix A show that the vertical stress at that point is only about forty percent of the superincumbent pressure that may be expected if there were no opening below.

VIII. - SUMMARY

In order to ascertain the effects that a pressure arch has upon the mining of an upper seam, it is necessary, first, to evaluate the stresses created by an underlying mine opening.

The excavation of an opening underground disturbs the pre-existing stress field within the rock. These changes in the stress field result in both the deformation and displacement of the strata above the mine opening. The extent and degree of these changes in the stress field affects the possible future mining conditions in an overlying seam. If an excavation is formed in an upper seam at a later date, the location of the opening with respect to the pressure arch formed by a previous lower opening is very important.

For this reason research was conducted in an attempt to evaluate the extent and degree of the change of the stress field due to an underground opening. Case studies were collected and analyzed to determine those changes in the stress field that have been documented by previous authors. After this, the finite element program was utilized to find trends in the changes of the stress field due to various widths of mine opening, depths of cover and overburden materials. These findings are summarized in Appendices A

and B. These tables are to be used as a design tool for future mining operations in a previously mined area. These tables must be used as approximations as each different mine will have different geologic conditions between the two seams.

Although the tables obtained in this research are approximations, it is felt that the finite element method which is presented can be applied with confidence anywhere if the input to the program is as accurate as possible in regards to the material properties, geologic column and size of the mine openings.

The results of the finite element analysis was checked qualitatively by using photoelastic modelling. Photoelastic modelling produced a similar de-stressed zone above the mine opening that was found in the finite element analysis. It is also possible to use the photoelastic modelling method to obtain the principal stresses and their inclinations for points across the model. This would give further information with which to check the finite element analysis method. However, this option was beyond the scope of this project and its timetable.

IX. - CONCLUSIONS AND RECOMMENDATIONS

9.1 - Conclusions

Based on the findings of this research the following conclusions can be made:

1) The underground mining of a seam alters the native stress field within the rock.

2) This altered stress field is in the form of a pressure arch which forms above the opening and is divided into two distinct zones.

a) The first of these zones is the de-stressed intradosal zone above the opening where the stresses are now below the superincumbent pressures present before mining.

b) The second zone is the pressure ring which surrounds the de-stressed zone. In this pressure ring the pressures are higher than the native stresses.

3) If in the future an upper seam is to be extracted, the position of the new mine opening in relation to the pressure arch around the lower opening is of importance.

a) If the upper opening is driven in the intradosal zone, lower pressures can be expected than in the surrounding rock and, possibly, fewer roof control

problems will be encountered.

b) If the upper opening is driven through the pressure ring of an existing arch, higher pressures will be encountered along with a probable increase in roof control problems.

9.2 - Recommendations

In areas where multiple seam mining is to take place, the determination of the stress field that may be encountered should be an important factor in the design of the mine layout. An accurate account of these stresses would enable the mine engineers to avoid areas of high stress or at least to be prepared for them when they are encountered. In order to obtain results that are as accurate as possible, the input into the program should also be accurate. This would be the result of actual core information as well as accurate values for the modulus of elasticity, Poisson's ratio and the weight density of each material in the overburden.

Any theoretical approach to a rock mechanics problem is an accurate approximation only if the theoretical approach can be applied to a known situation and give an accurate representation of the actual values. In order^{to} ensure that this finite element approach is accurate, case studies which evaluate the present stress fields should be collected from literature or, more importantly, from actual field data.

The photoelastic modelling method also requires more work. In order to more fully understand how the stresses in

a photoelastic model correlate to those obtained in the finite element analysis, information about the values of the principal stresses as obtained from a photoelastic model must be compared to those of an equivalent finite element model. This technique exists and should be further investigated in future research.

Another aspect that must be considered in this area is the variable of time. It must be accurately determined if the period of time between mining the lower seam and mining the upper seam will alter the stress field in magnitude and extent.

REFERENCES

- Barrientos, G. and Parker, J., "Use of the Pressure Arch in Mine Design at White Pine," Transactions, SME-AIME, Volume 255, March 1974, pp. 75-82.
- Bhattacharya, S., Finite Element Analysis of Coal Mine Entries in Tectonic Stress Fields, M. S. Thesis, Virginia Polytechnic Institute and State University, October, 1980.
- California Computer Products, Inc., "A General Purpose Contouring Program," User's Manual, April, 1971.
- Coates, D. F., "Pillar Loading," Research Report, Department of Mines and Technical Surveys, Ottawa, Canada, 1965.
- Denkhaus, H. G., "Critical Review of Strata Movement Theories and Their Application to Practical Problems," Journal of the South African Institute of Mining and Metallurgy, Volume 64, 1964, pp. 310-332.
- Desai, C. S. and Abel, J. F., Introduction to the Finite Element Method, Von Nostrand Reinhold Co., New York, 1972.
- Dinsdale, J. R., "Ground Failure around Excavations," Transactions of the Institution of Mining and Metallurgy, London, Volume XLVI, 1937.
- Fayol, M., Revue de l'Industrie Minerale, Volume xiv, 1885.
- Fayol, M., see above, "Effect of Coal Mining on the Surface," translated by H. F. Bulman, The Colliery Engineer, Volume 33, 1913, pp. 548-52, 617-22.
- Frocht, M. M., Photoelasticity, John Wiley and Sons, Inc., New York, Volume 2, 1948.
- Haycocks, C. and Karmis, M., "Ground Control Mechanisms in Multi-Seam Mining," Research Performance Report, Office of Surface Mining, June, 1981.
- Heuze, F. E., "The Design of Room and Pillar Structures in Competent Jointed Rock," Doctor of Engineering Dissertation, University of California, Berkeley, 1970.

- Howell, R. C., Wright, F. D. and Dearing, J. A., "Ground Movements and Pressure Changes Associated with Shortwall Mining," Proceedings, 17th United States Symposium on Rock Mechanics, Snowbird, Utah, 1976.
- Irving, C. J., "Some Aspects of Ground Movement (The Witwatersrand Goldfield)," Journal of the Chemical, Metallurgical and Mining Society of South Africa, Volume 46, 1946, pp. 278-312.
- Kulhawy, F. H., "Finite Element Modeling Criteria for Underground Openings in Rock," International Journal of Rock Mechanics and Mining Science and Geomechanics Abstracts, Volume 11, No. 12, 1974, pp. 465-472.
- Mohr, F., "Influence of Mining on Strata," Mine and Quarry Engineering, Volume 22, 1956.
- National Coal Board, "Divisional Stress Control Research Committee N.C.B., Durham and Northern Divisions Report of the Effects of Working in Adjacent Seams upon New Developments," Transactions of the Institution of Mining Engineers, Volume 113, 1954, p. 398.
- National Coal Board, "Design of Mine Layouts," Working Party Report, 1972.
- Neall, G. M., "A Photoelastic Study of Roof-Truss Interactions in a Multilayered Mine Model," Master of Science Thesis in Mining Engineering, Virginia Polytechnic Institute and State University, August, 1975.
- Neall, G. M. and Haycocks, C., "Design in Underground Coal Systems," R & D Report 91, Interim Report No. 1, Prepared for the Office of Coal Research, 1974.
- Randolph, B. S., "The Theory of the Arch in Mining," The Colliery Engineer, Volume 35, 1915, pp. 427-29.
- Stemple, D. T., "A study of the Problems Encountered in Multiple-Seam Coal Mining in the Eastern United States," Bulletin of Virginia Polytechnic Institute, Volume XLIX, No. 5, 1956, p. 65.
- Wilson, E. L., "Structural Analysis of Axisymmetric Solids," AIAA Journal, No.12, Sec. 1965, pp. 2269-2274.
- Zienkiewicz, O. C., The Finite Element Method, 3rd edition, McGraw-Hill Book Company, London, 1977.

BIBLIOGRAPHY

- Barko, E. N., Mechanics of Interseam Failure in Multiple Horizon Mining, M. S. Thesis, Virginia Polytechnic Institute and State University, 1982.
- Britton, S. G., "Mining Multiple Seams," Coal Mining and Processing, December 1980, pp. 64-70.
- Coates, D. F., and Y. S. Yu, "Development and Use of Computer Programs for Finite Element Analysis," Department of Energy, Mines, and Resources Research Report R198, Mines Branch, Ottawa, Canada, July 1969.
- Denkhaus, H. G., "The Application of the Mathematical Theory of Elasticity to Problems of Stress in Hard Rock at Great Depth," Association of Mine Managers of South Africa, Papers and Discussions, 1958, pp. 271-309.
- Dunham, R. K. and Stace, R. L., "Interaction Problems in Multi-Seam Mining," Proceedings, 19th United States Symposium on Rock Mechanics, Mackay School of Mines, Volume 1, 1978, pp. 174-179.
- Ehgartner, B. L., Pillar Load Transfer Mechanisms in Multi-Seam Mining, M. S. Thesis, Virginia Polytechnic Institute and State University, 1982, pp. 165.
- Evans, W. H., "The Strength of Undermined Strata," Transactions of the Institute of Mining and Metallurgy, Volume 50, 1941, pp. 475-532.
- Fenner, F., "Untersuchungen zur Erkenntniss des Gebirgdrucks, Gluckauf, No. 32, pp. 681-95, No. 33, 1938, pp. 705-15.
- Hasler, H. H., "Simultaneous vs Consecutive Working of Coal Beds," Mining Engineering, May 1951, pp. 436-440.
- Jones, D. C., "Morris Creek is now a 3-Seam Producer," Coal Mining and Processing, March, 1969, pp. 32-36.
- Peng, S. S. and Chandra, U., "Aspects of Ground Control Consideration in Multiple-Seam Mining," Coal Mining and Processing, December, 1980.
- Spedding, M., "Multiple Seam Mining," Chapter 4, Proceedings, 17th United States Symposium on Rock Mechanics, Snowbird, Utah, 1976, pp. 22-27.

- Styler, A. N. and Dunham, R. K., "Strata Deformation Above Longwall Faces," Proceedings, 21st United States Symposium on Rock Mechanics, Rolla, Missouri, 1980, pp. 308-318.
- Wardell, K. and Eynon, P., "Structural Concept of Strata Control and Mine Design," The Mining Engineer, August, 1968, pp. 633-656.
- Whittaker, B. N. and Pye, J. H., "Design and Layout Aspects of Longwall Methods of Coal Mining," 16th Symposium on Rock Mechanics, 1975, pp. 303-328.
- Wilson, J. W., Singh, B. D. and Nakajima, S., "Design Considerations for Mining Thick Seams and Seams Lying in Close Proximity to One Another," 17th Symposium on Rock Mechanics, Snowbird, Utah, 1976, pp. 3-13.

APPENDIX A

VALUES OF SIGMA (γ) FOR VARIOUS DEPTHS AND WIDTHS

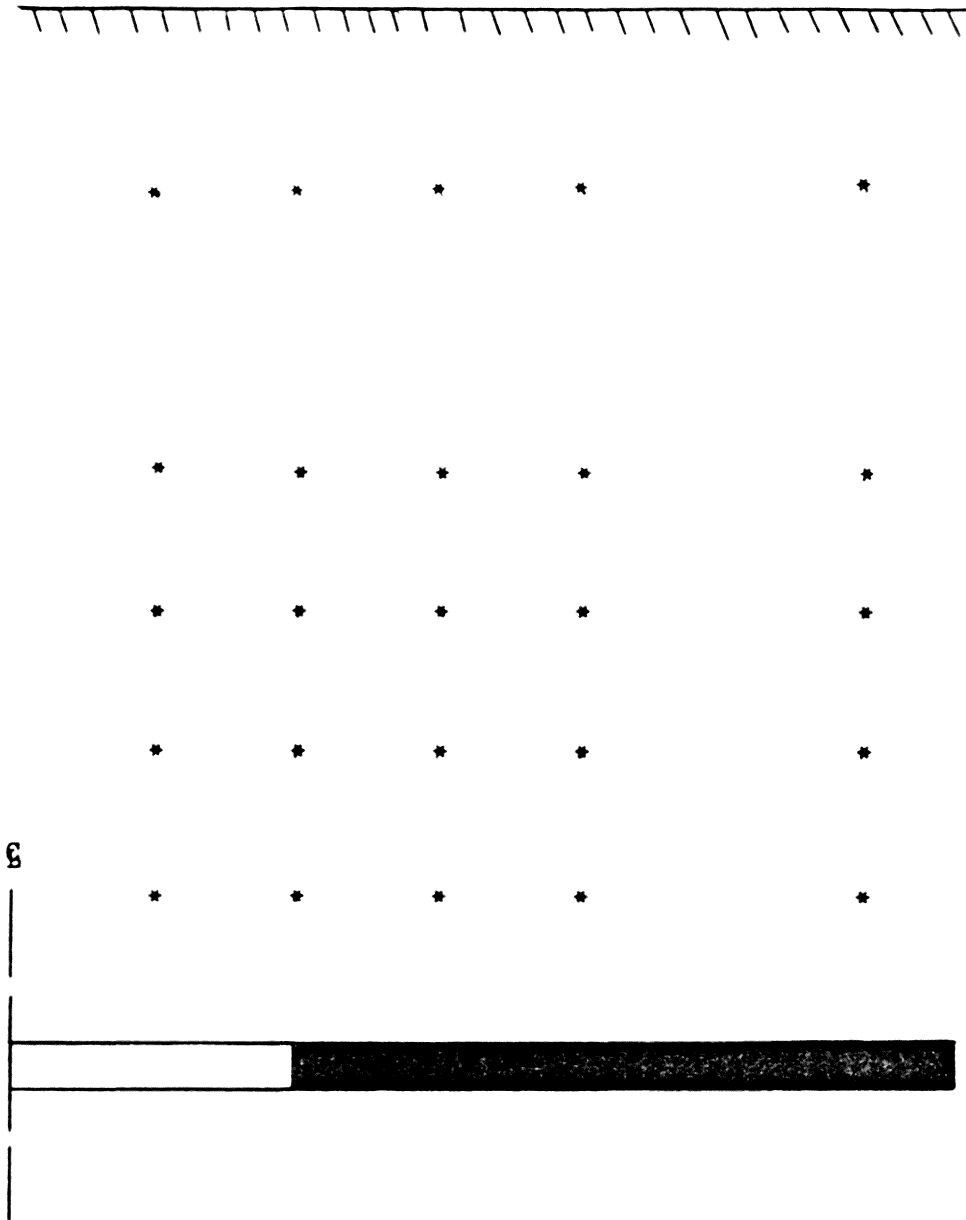


Figure 27. Example Grid of Location of Values from Tables of Appendices A and B.

Table A-1

Sigma (Y) for Opening 100' by 5', 500' Sandstone Overburden

Height Above Seam		Sigma (Y) as a Percentage of the Overburden Pressure at set Distances from Centerline of Mine Opening				
H/W	feet	25'	50'	75'	100'	150'
4 1/2	450'	97.94	98.17	98.40	98.73	99.53
4	400'	96.74	97.07	97.40	98.03	99.33
3 1/2	350'	95.43	95.92	96.40	97.37	99.17
3	300'	94.10	94.94	95.78	97.02	99.24
2 1/2	250'	92.30	93.68	95.06	96.72	99.66
2	200'	89.79	91.92	94.04	96.50	99.84
1 1/2	150'	85.69	89.56	93.44	97.10	101.64
1	100'	78.12	86.57	95.02	99.98	105.44
3/4	75'	73.18	84.94	96.71	102.24	107.29
1/2	50'	64.48	84.31	104.14	107.02	108.33
1/4	25'	55.79	83.68	111.58	111.79	109.37

H/W = Height above seam divided by width of opening

Table A-2

Sigma (Y) for Opening 200' by 5', 500' Sandstone Overburden

Height Above Seam		Sigma (Y) as a Percentage of the Overburden Pressure at set Distances from Centerline of Mine Opening				
H/W	feet	50'	100'	150'	200'	300'
2	400'	87.46	91.43	96.23	100.70	105.80
1 1/2	300'	78.43	86.28	95.42	103.00	109.62
1	200'	66.72	83.06	99.48	109.62	113.12
3/4	150'	56.20	84.24	107.70	117.11	114.80
1/2	100'	45.39	88.82	117.72	121.67	113.36
1/4	50'	23.61	103.94	138.66	127.16	112.33

Table A-3

Sigma (Y) for Opening 300' by 5', 500' Sandstone Overburden

Height Above Seam		Sigma (Y) as a Percentage of the Overburden Pressure at set Distances from Centerline of Mine Opening				
H/W	feet	75'	150'	225'	300'	450'
1 1/2	450'	85.54	94.16	102.60	107.35	108.94
1	300'	63.94	87.54	109.16	118.76	119.73
3/4	225'	53.09	88.09	116.55	124.90	121.27
1/2	150'	36.16	95.94	133.41	131.78	120.66
1/4	75'	16.61	114.90	149.72	131.71	116.83

Table A-4

Sigma (Y) for Opening 400' by 5', 500' Sandstone Overburden

Height Above Seam		Sigma (Y) as a Percentage of the Overburden Pressure at set Distances from Centerline of Mine Opening				
H/W	feet	100'	200'	300'	400'	600'
1	400'	75.28	97.93	114.57	117.14	105.48
3/4	300'	59.31	98.53	124.89	126.98	108.34
1/2	200'	43.95	105.42	138.41	133.33	108.86
1/4	100'	22.81	124.71	155.08	133.38	107.40

Table A-5

Sigma (Y) for Opening 500' by 5', 500' Sandstone Overburden

Height Above Seam		Sigma (Y) as a Percentage of the Overburden Pressure at set Distances from Centerline of Mine Opening				
H/W	feet	125'	250'	375'	500'	750'
3/4	375'	65.52	106.80	128.80	122.80	100.40
1/2	250'	43.06	115.64	148.40	132.60	100.76
1/4	125'	16.32	137.06	165.87	132.53	100.00

Table A-6

Sigma (Y) for Opening 600' by 5', 500' Sandstone Overburden

Height Above Seam		Sigma (Y) as a Percentage of the Overburden Pressure at set Distances from Centerline of Mine Opening				
H/W	feet	150'	300'	450'	600'	900'
3/4	450'	78.73	109.80	121.43	111.25	96.76
1/2	300'	47.28	124.89	151.40	125.95	92.86
1/4	150'	16.17	157.86	173.07	126.00	92.00

Table A-7

Sigma (Y) for Opening 100' by 5', 750' Sandstone Overburden

Height Above Seam		Sigma (Y) as a Percentage of the Overburden Pressure at set Distances from Centerline of Mine Opening				
H/W	feet	25'	50'	75'	100'	150'
7	700'	**.**	99.00	99.08	99.17	99.34
6 1/2	650'	**.**	98.66	98.83	99.00	99.34
6	600'	**.**	98.33	98.58	98.83	99.33
5 1/2	550'	**.**	98.50	98.78	99.06	99.64
5	500'	**.**	97.72	97.95	98.12	98.73
4 1/2	450'	96.65	96.89	97.12	97.32	98.01
4	400'	96.31	96.66	97.02	97.44	98.36
3 1/2	350'	95.53	95.96	96.40	97.08	98.38
3	300'	94.48	95.08	95.68	96.62	98.44
2 1/2	250'	92.94	93.94	94.92	96.26	98.78
2	200'	90.52	92.27	94.02	96.14	99.65
1 1/2	150'	86.52	89.97	93.42	96.73	101.45
1	100'	79.04	86.88	94.72	99.34	104.47
3/4	75'	74.07	85.11	96.15	101.41	106.30
1/2	50'	65.04	84.18	103.32	106.12	107.46
1/4	25'	56.00	83.24	110.48	110.82	108.62

. = Percentage undeterminable from model used

Table A-8

Sigma (Y) for Opening 200' by 5', 750' Sandstone Overburden

Height Above Seam		Sigma (Y) as a Percentage of the Overburden Pressure at set Distances from Centerline of Mine Opening				
H/W	feet	50'	100'	150'	200'	300'
3 1/2	700'	96.00	96.75	97.50	98.55	100.30
3	600'	94.00	95.00	96.00	97.66	100.66
2 1/2	500'	91.38	92.92	95.12	97.54	101.68
2	400'	87.36	90.06	93.59	97.28	102.75
1 1/2	300'	82.09	87.21	93.49	99.13	105.34
1	200'	72.64	84.38	96.52	104.54	108.83
3/4	150'	65.10	84.36	101.32	109.58	110.27
1/2	100'	54.84	87.55	110.28	115.76	111.00
1/4	50'	42.52	96.08	123.45	120.52	110.86

Table A-9

Sigma (Y) for Opening 300' by 5', 750' Sandstone Overburden

Height Above Seam		Sigma (Y) as a Percentage of the Overburden Pressure at set Distances from Centerline of Mine Opening				
H/W	feet	75'	150'	225'	300'	450'
2	600'	88.50	92.00	96.50	100.66	105.33
1 1/2	450'	79.16	86.06	93.88	100.89	105.73
1	300'	67.91	84.66	100.80	109.69	112.04
3/4	225'	59.43	85.34	107.24	115.24	113.05
1/2	150'	46.88	90.92	119.54	121.54	112.88
1/4	75'	27.11	104.60	136.74	125.26	111.78

Table A-10

Sigma (Y) for Opening 400' by 5', 750' Sandstone Overburden

Height Above Seam		Sigma (Y) as a Percentage of the Overburden Pressure at set Distances from Centerline of Mine Opening				
H/W	feet	100'	200'	300'	400'	600'
1 1/2	600'	82.66	91.34	100.67	106.67	107.67
1	400'	66.44	86.94	105.70	114.98	112.76
3/4	300'	56.92	88.24	112.76	120.70	113.56
1/2	200'	44.40	94.84	125.30	126.40	112.92
1/4	100'	24.24	112.93	142.65	128.28	111.10

Table A-11

Sigma (Y) for Opening 500' by 5', 750' Sandstone Overburden

Height Above Seam		Sigma (Y) as a Percentage of the Overburden Pressure at set Distances from Centerline of Mine Opening				
H/W	feet	125'	250'	375'	500'	750'
1	500'	66.63	91.20	111.41	118.00	110.44
3/4	375'	54.93	92.14	119.47	124.67	111.87
1/2	250'	40.86	99.58	130.19	128.96	111.37
1/4	125'	18.16	119.44	150.56	130.48	109.20

Table A-12

Sigma (Y) for Opening 600' by 5', 750' Sandstone Overburden

Height Above Seam		Sigma (Y) as a Percentage of the Overburden Pressure at set Distances from Centerline of Mine Opening				
H/W	feet	150'	300'	450'	600'	900'
1	600'	72.67	96.67	114.67	116.33	106.66
3/4	450'	56.71	94.81	119.29	121.12	105.68
1/2	300'	40.00	104.94	138.73	131.81	110.02
1/4	150'	16.98	127.25	155.68	130.97	107.93

Table A-13

Sigma (Y) for Opening 100' by 5', 1000' Sandstone Overburden

Height Above Seam		Sigma (Y) as a Percentage of the Overburden Pressure at set Distances from Centerline of Mine Opening				
H/W	feet	25'	50'	75'	100'	150'
9 1/2	950'	**.**	99.53	99.54	99.55	99.57
9	900'	**.**	99.40	99.42	99.45	99.50
8 1/2	850'	**.**	99.20	99.27	99.35	99.50
8	800'	**.**	99.00	99.12	99.25	99.50
7 1/2	750'	**.**	98.84	98.94	99.04	99.25
7	700'	**.**	98.67	98.76	98.84	99.00
6 1/2	650'	**.**	98.46	98.57	98.67	98.88
6	600'	**.**	98.25	98.38	98.50	98.75
5 1/2	550'	**.**	98.16	98.36	98.58	98.97
5	500'	**.**	97.70	97.90	98.06	98.56
4 1/2	450'	96.99	97.16	97.32	97.54	98.19
4	400'	96.60	96.80	97.01	97.42	98.29
3 1/2	350'	95.86	96.21	96.55	97.12	98.27
3	300'	94.88	95.41	95.94	96.76	98.36
2 1/2	250'	93.43	94.29	95.15	96.38	98.63
2	200'	91.05	92.63	94.20	96.16	99.92
1 1/2	150'	86.84	90.16	93.48	96.60	101.11
1	100'	79.30	86.96	94.63	99.11	104.06
3/4	75'	74.49	85.24	96.00	101.14	105.89
1/2	50'	65.35	84.11	102.87	105.70	107.04
1/4	25'	56.21	82.98	109.74	110.26	108.20

Table A-14

Sigma (Y) for Opening 200' by 5', 1000' Sandstone Overburden

Height Above Seam		Sigma (Y) as a Percentage of the Overburden Pressure at set Distances from Centerline of Mine Opening				
H/W	feet	50'	100'	150'	200'	300'
4 1/2	900'	97.60	97.85	98.10	98.55	99.45
4	800'	96.00	96.50	97.00	97.75	99.25
3 1/2	700'	94.67	95.34	96.00	97.00	99.00
3	600'	93.25	94.12	95.00	97.50	99.25
2 1/2	500'	91.36	92.53	94.23	96.24	99.89
2	400'	88.00	90.19	93.22	96.37	101.19
1 1/2	300'	83.02	87.50	93.00	97.98	103.72
1	200'	73.75	84.52	95.65	103.13	107.34
3/4	150'	66.18	84.26	100.18	108.04	108.99
1/2	100'	55.78	87.04	108.93	114.38	109.98
1/4	50'	43.01	95.30	122.17	119.43	110.26

Table A-15

Sigma (Y) for Opening 300' by 5', 1000' Sandstone Overburden

Height Above Seam		Sigma (Y) as a Percentage of the Overburden Pressure at set Distances from Centerline of Mine Opening				
H/W	feet	75'	150'	225'	300'	450'
3	900'	95.19	96.05	97.40	98.78	101.00
2 1/2	750'	91.08	92.84	95.28	97.84	102.34
2	600'	86.69	89.50	93.81	97.88	104.00
1 1/2	450'	80.27	90.21	92.50	98.94	105.65
1	300'	69.44	84.00	98.16	106.47	110.09
3/4	225'	61.03	84.46	104.26	111.94	111.42
1/2	150'	48.38	89.40	116.14	118.50	111.74
1/4	75'	28.32	102.60	132.97	123.24	111.35

Table A-16

Sigma (Y) for Opening 400' by 5', 1000' Sandstone Overburden

Height Above Seam		Sigma (Y) as a Percentage of the Overburden Pressure at set Distances from Centerline of Mine Opening				
H/W	feet	100'	200'	300'	400'	600'
2	800'	88.25	91.75	96.50	101.00	105.50
1 1/2	600'	79.62	87.00	95.88	103.12	109.25
1	400'	67.24	84.34	100.83	110.28	112.74
3/4	300'	58.41	85.62	107.60	116.05	113.57
1/2	200'	46.02	91.64	119.82	122.30	113.22
1/4	100'	25.59	108.84	137.65	125.56	111.79

Table A-17

Sigma (Y) for Opening 500' by 5', 1000' Sandstone Overburden

Height Above Seam		Sigma (Y) as a Percentage of the Overburden Pressure at set Distances from Centerline of Mine Opening				
H/W	feet	125'	250'	375'	500'	750'
1 1/2	750'	80.81	89.66	99.60	106.58	110.50
1	500'	65.28	85.75	104.92	114.21	115.27
3/4	375'	55.68	87.20	112.16	120.28	115.88
1/2	250'	42.44	94.28	125.68	126.17	114.88
1/4	125'	20.00	113.14	144.00	128.00	112.69

Table A-18

Sigma (Y) for Opening 600' by 5', 1000' Sandstone Overburden

Height Above Seam		Sigma (Y) as a Percentage of the Overburden Pressure at set Distances from Centerline of Mine Opening				
H/W	feet	150'	300'	450'	600'	900'
1 1/2	900'	86.70	94.70	103.00	107.00	108.00
1	600'	65.25	88.38	109.25	118.25	118.38
3/4	450'	55.99	89.81	115.62	123.74	118.98
1/2	300'	40.92	97.39	130.36	130.12	118.23
1/4	150'	18.78	118.56	148.46	130.31	114.88

Table A-19

Sigma (Y) for Opening 100' by 5', 500' Shale Overburden

Height Above Seam		Sigma (Y) as a Percentage of the Overburden Pressure at set Distances from Centerline of Mine Opening				
H/W	feet	25'	50'	75'	100'	150'
4 1/2	450'	98.18	98.40	98.64	98.92	99.61
4	400'	97.38	97.69	98.02	98.58	99.54
3 1/2	350'	96.38	96.83	97.28	98.03	99.48
3	300'	95.10	95.77	96.44	97.43	99.46
2 1/2	250'	93.59	94.66	95.72	97.16	99.77
2	200'	91.42	93.20	94.98	97.14	100.67
1 1/2	150'	87.66	91.09	94.52	97.79	102.32
1	100'	80.72	88.50	96.27	100.52	104.99
3/4	75'	76.13	87.07	98.01	102.62	106.58
1/2	50'	67.90	86.66	105.42	107.05	107.30
1/4	25'	59.67	86.24	112.82	111.48	108.02

Table A-20

Sigma (Y) for Opening 200' by 5', 500' Shale Overburden

Height Above Seam		Sigma (Y) as a Percentage of the Overburden Pressure at set Distances from Centerline of Mine Opening				
H/W	feet	50'	100'	150'	200'	300'
2	400'	88.36	92.04	96.68	101.00	105.50
1 1/2	300'	79.80	87.22	95.96	103.10	109.14
1	200'	68.50	84.43	100.11	109.52	112.32
3/4	150'	58.39	85.88	108.20	116.64	113.86
1/2	100'	47.79	91.13	119.89	120.91	112.33
1/4	50'	26.20	108.16	138.23	125.78	111.39

Table A-21

Sigma (Y) for Opening 300' by 5', 500' Shale Overburden

Height Above Seam		Sigma (Y) as a Percentage of the Overburden Pressure at set Distances from Centerline of Mine Opening				
H/W	feet	75'	150'	225'	300'	450'
1 1/2	450'	85.96	94.48	102.74	107.34	108.60
1	300'	65.46	88.55	109.14	118.12	118.60
3/4	225'	54.86	89.32	116.67	124.13	120.15
1/2	150'	38.26	97.78	133.17	130.56	119.34
1/4	75'	18.53	118.82	148.72	130.03	115.34

Table A-22

Sigma (Y) for Opening 400' by 5', 500' Shale Overburden

Height Above Seam		Sigma (Y) as a Percentage of the Overburden Pressure at set Distances from Centerline of Mine Opening				
H/W	feet	100'	200'	300'	400'	600'
1	400'	76.24	98.58	114.44	116.72	105.38
3/4	300'	60.84	99.34	124.63	126.15	107.85
1/2	200'	45.86	106.90	137.99	132.09	108.17
1/4	100'	24.83	127.50	153.54	131.92	106.76

Table A-23

Sigma (Y) for Opening 500' by 5', 500' Shale Overburden

Height Above Seam		Sigma (Y) as a Percentage of the Overburden Pressure at set Distances from Centerline of Mine Opening				
H/W	feet	125'	250'	375'	500'	750'
3/4	375'	66.62	107.87	129.01	122.08	100.22
1/2	250'	57.88	116.84	147.83	131.42	100.44
1/4	125'	18.20	139.86	164.03	131.10	99.64

Table A-24

Sigma (Y) for Opening 600' by 5', 500' Shale Overburden

Height Above Seam		Sigma (Y) as a Percentage of the Overburden Pressure at set Distances from Centerline of Mine Opening				
H/W	feet	150'	300'	450'	600'	900'
3/4	450'	79.12	110.48	121.66	111.12	96.66
1/2	300'	48.82	126.06	150.67	124.86	93.96
1/4	150'	17.97	154.02	169.37	125.57	91.99

Table A-25

Sigma (Y) for Opening 100' by 5', 750' Shale Overburden

Height Above Seam		Sigma (Y) as a Percentage of the Overburden Pressure at set Distances from Centerline of Mine Opening				
H/W	feet	25'	50'	75'	100'	150'
7	700'	**.**	99.07	99.14	99.20	99.34
6 1/2	650'	**.**	98.74	98.86	98.96	99.18
6	600'	**.**	98.42	98.57	98.72	99.03
5 1/2	550'	**.**	98.88	99.05	99.35	99.70
5	500'	**.**	98.09	98.32	98.46	98.92
4 1/2	450'	97.07	97.26	97.45	97.73	98.44
4	400'	97.02	97.20	97.40	97.86	98.76
3 1/2	350'	96.34	96.65	96.96	97.53	98.71
3	300'	95.47	95.94	96.42	97.22	98.83
2 1/2	250'	94.18	94.99	95.80	96.98	99.14
2	200'	92.03	93.54	95.06	96.88	99.92
1 1/2	150'	88.34	91.45	94.56	97.44	101.48
1	100'	81.50	88.74	95.99	99.92	104.10
3/4	75'	76.96	87.22	97.49	101.84	105.69
1/2	50'	68.46	86.60	104.75	106.30	106.56
1/4	25'	59.96	85.98	112.01	110.75	107.42

Table A-26

Sigma (Y) for Opening 200' by 5', 750' Shale Overburden

Height Above Seam		Sigma (Y) as a Percentage of the Overburden Pressure at set Distances from Centerline of Mine Opening				
H/W	feet	50'	100'	150'	200'	300'
3 1/2	700'	96.17	96.90	97.63	98.54	100.18
3	600'	94.17	95.38	96.60	98.12	100.55
2 1/2	500'	92.06	93.52	95.48	97.78	101.62
2	400'	88.34	90.85	94.20	97.64	102.76
1 1/2	300'	83.42	88.24	94.17	99.46	105.15
1	200'	74.50	85.77	97.20	104.66	108.38
3/4	150'	67.23	85.93	101.92	109.40	109.70
1/2	100'	57.33	89.58	110.75	115.10	110.26
1/4	50'	45.35	99.08	123.72	119.26	110.12

Table A-27

Sigma (Y) for Opening 300' by 5', 750' Shale Overburden

Height Above Seam		Sigma (Y) as a Percentage of the Overburden Pressure at set Distances from Centerline of Mine Opening				
H/W	feet	75'	150'	225'	300'	450'
2	600'	89.92	92.35	96.90	100.46	105.10
1 1/2	450'	80.14	86.76	94.22	100.98	105.55
1	300'	69.54	85.87	101.34	109.70	111.58
3/4	225'	61.28	86.68	107.64	114.93	112.50
1/2	150'	49.02	92.66	119.69	120.79	112.24
1/4	75'	29.42	107.42	136.30	14.09	111.07

Table A-28

Sigma (Y) for Opening 400' by 5', 750' Shale Overburden

Height Above Seam		Sigma (Y) as a Percentage of the Overburden Pressure at set Distances from Centerline of Mine Opening				
H/W	feet	100'	200'	300'	400'	600'
1 1/2	600'	83.24	91.74	100.55	106.62	107.84
1	400'	67.65	87.78	105.95	114.80	112.34
3/4	300'	58.50	89.42	113.02	120.33	113.05
1/2	200'	46.22	98.90	125.26	125.67	111.96
1/4	100'	26.16	115.87	141.53	127.20	110.53

Table A-29

Sigma (Y) for Opening 500' by 5', 750' Shale Overburden

Height Above Seam		Sigma (Y) as a Percentage of the Overburden Pressure at set Distances from Centerline of Mine Opening				
H/W	feet	125'	250'	375'	500'	750'
1	500'	67.58	91.88	111.58	117.58	107.52
3/4	375'	56.38	93.20	119.56	124.18	111.30
1/2	250'	42.55	100.95	132.90	130.40	113.80
1/4	125'	19.83	122.19	150.19	129.48	108.70

Table A-30

Sigma (Y) for Opening 600' by 5', 750' Shale Overburden

Height Above Seam		Sigma (Y) as a Percentage of the Overburden Pressure at set Distances from Centerline of Mine Opening				
H/W	feet	150'	300'	450'	600'	900'
1	600'	72.90	97.20	114.82	116.34	106.32
3/4	450'	57.79	95.51	119.34	120.49	105.05
1/2	300'	41.63	106.26	138.53	130.99	109.38
1/4	150'	18.53	130.07	154.74	129.87	107.37

Table A-31

Sigma (Y) for Opening 100' by 5', 1000' Shale Overburden

Height Above Seam		Sigma (Y) as a Percentage of the Overburden Pressure at set Distances from Centerline of Mine Opening				
H/W	feet	25'	50'	75'	100'	150'
9 1/2	950'	**.**	99.79	99.79	99.79	99.79
9	900'	**.**	99.36	99.36	99.36	99.36
8 1/2	850'	**.**	99.36	99.36	99.36	99.36
8	800'	**.**	99.36	99.36	99.36	99.36
7 1/2	750'	**.**	99.20	99.23	99.27	99.34
7	700'	**.**	99.03	99.10	99.18	99.33
6 1/2	650'	**.**	98.84	98.94	99.03	99.22
6	600'	**.**	98.66	98.77	98.88	99.11
5 1/2	550'	**.**	98.64	98.79	98.94	99.25
5	500'	**.**	98.16	98.32	98.44	98.84
4 1/2	450'	97.52	97.67	97.82	98.02	98.57
4	400'	97.22	97.41	97.60	97.98	98.73
3 1/2	350'	96.62	96.90	97.18	97.70	98.71
3	300'	95.78	96.24	96.68	97.40	98.75
2 1/2	250'	94.51	95.26	96.02	97.07	99.00
2	200'	92.44	93.82	95.20	96.89	99.70
1 1/2	150'	88.84	91.76	94.68	97.37	101.19
1	100'	82.00	89.00	96.01	99.65	103.56
3/4	75'	77.45	87.45	97.45	101.44	104.94
1/2	50'	68.82	86.82	104.81	106.10	106.22
1/4	25'	60.20	86.18	112.17	110.77	107.50

Table A-32

Sigma (Y) for Opening 200' by 5', 1000' Shale Overburden

Height Above Seam		Sigma (Y) as a Percentage of the Overburden Pressure at set Distances from Centerline of Mine Opening				
H/W	feet	50'	100'	150'	200'	300'
4 1/2	900'	97.27	97.72	98.18	98.64	99.54
4	800'	96.80	97.26	97.72	98.40	99.78
3 1/2	700'	95.44	96.05	96.66	97.57	99.39
3	600'	93.62	94.53	95.44	96.81	99.32
2 1/2	500'	92.10	93.22	94.84	96.69	100.04
2	400'	89.03	91.06	93.88	96.82	101.28
1 1/2	300'	84.37	88.57	93.74	98.42	103.65
1	200'	75.62	85.97	96.48	103.38	107.10
3/4	150'	68.33	85.91	100.82	107.86	108.67
1/2	100'	58.24	89.24	109.51	113.58	109.37
1/4	50'	45.78	98.32	122.58	118.18	109.12

Table A-33

Sigma (Y) for Opening 300' by 5', 1000' Shale Overburden

Height Above Seam		Sigma (Y) as a Percentage of the Overburden Pressure at set Distances from Centerline of Mine Opening				
H/W	feet	75'	150'	225'	300'	450'
3	900'	95.68	96.36	97.72	99.09	100.91
2 1/2	750'	91.75	93.46	95.86	98.32	102.51
2	600'	87.47	90.21	94.30	98.18	103.87
1 1/2	450'	81.16	86.72	93.07	99.17	104.84
1	300'	71.02	85.10	97.74	106.48	109.71
3/4	225'	62.94	85.82	104.82	111.88	111.03
1/2	150'	50.54	91.07	116.74	118.17	111.50
1/4	75'	30.54	105.32	133.00	122.16	109.85

Table A-34

Sigma (Y) for Opening 400' by 5', 1000' Shale Overburden

Height Above Seam		Sigma (Y) as a Percentage of the Overburden Pressure at set Distances from Centerline of Mine Opening				
H/W	feet	100'	200'	300'	400'	600'
2	800'	89.04	92.70	97.26	101.37	105.71
1 1/2	600'	80.41	87.70	96.24	103.19	108.88
1	400'	68.47	85.27	101.17	110.24	112.27
3/4	300'	59.96	86.70	107.96	115.79	113.03
1/2	200'	47.90	93.26	120.16	121.90	112.85
1/4	100'	27.48	111.74	137.10	124.31	111.15

Table A-35

Sigma (Y) for Opening 500' by 5', 1000' Shale Overburden

Height Above Seam		Sigma (Y) as a Percentage of the Overburden Pressure at set Distances from Centerline of Mine Opening				
H/W	feet	125'	250'	375'	500'	750'
1 1/2	750'	81.57	90.30	99.88	106.53	110.20
1	500'	66.41	86.54	105.13	114.05	114.80
3/4	375'	57.01	88.22	112.42	120.00	115.38
1/2	250'	44.10	95.71	125.90	125.56	114.30
1/4	125'	21.66	115.72	142.69	127.59	111.97

Table A-36

Sigma (Y) for Opening 600' by 5', 1000' Shale Overburden

Height Above Seam		Sigma (Y) as a Percentage of the Overburden Pressure at set Distances from Centerline of Mine Opening				
H/W	feet	150'	300'	450'	600'	900'
1 1/2	900'	87.06	94.80	103.01	106.88	108.02
1	600'	66.08	89.08	109.37	118.02	117.91
3/4	450'	57.08	90.70	115.75	123.37	118.26
1/2	300'	42.40	98.71	130.42	129.46	117.52
1/4	150'	20.22	121.32	147.62	129.50	114.47

APPENDIX B

VALUES FOR SIGMA (X) FOR VARIOUS DEPTHS AND WIDTHS

Table B-1

Sigma (X) for Opening 100' by 5', 500' Sandstone Overburden

Height Above Seam		Sigma (X) in Pounds per Square Inch at set Distances from the Centerline of Mine Opening				
H/W	feet	25'	50'	75'	100'	150'
4 1/2	450'	-21.35	-20.65	-19.95	-18.70	-15.95
4	400'	-25.50	-24.90	-24.30	-23.25	-21.00
3 1/2	350'	-31.40	-30.68	-29.95	-28.78	-26.40
3	300'	-38.60	-37.50	-36.40	-34.80	-31.80
2 1/2	250'	-47.00	-45.08	-43.15	-40.72	-36.65
2	200'	-56.70	-53.00	-49.30	-45.58	-40.30
1 1/2	150'	-67.85	-60.25	-52.65	-47.45	-42.42
1	100'	-79.25	-61.90	-44.55	-43.75	-46.95
3/4	75'	-84.70	-60.30	-35.90	-40.20	-50.80
1/2	50'	-44.46	-48.50	-52.55	-57.52	-64.42
1/4	25'	-4.21	-36.70	-69.20	-74.85	-78.05

H/W = Height above seam divided by width of opening

Negative values are compressive

Positive values are tensile

Table B-2

Sigma (X) for Opening 200' by 5', 500' Sandstone Overburden

Height Above Seam		Sigma (X) in Pounds per Square Inch at set Distances from the Centerline of Mine Opening				
H/W	feet	50'	100'	150'	200'	300'
2	400'	-46.20	-39.38	-29.92	-19.78	-2.76
1 1/2	300'	-55.80	-45.75	-34.28	-25.35	-23.45
1	200'	-74.48	-49.95	-30.22	-24.52	-35.92
3/4	150'	-74.22	-35.70	-17.88	-28.20	-53.56
1/2	100'	-73.95	-21.44	-5.54	-31.88	-71.21
1/4	50'	-27.05	+0.75	-28.95	-78.35	-97.90

Table B-3

Sigma (X) for Opening 300' by 5', 500' Sandstone Overburden

Height Above Seam		Sigma (X) in Pounds per Square Inch at set Distances from the Centerline of Mine Opening				
H/W	feet	75'	150'	225'	300'	450'
1 1/2	450'	-86.95	-53.60	-12.90	-24.18	+66.02
1	300'	-71.95	-43.02	-17.90	-8.02	-8.44
3/4	225'	-79.60	-38.35	-12.50	-17.85	-39.65
1/2	150'	-78.86	-27.37	-10.14	-38.72	-75.10
1/4	75'	-26.88	+3.04	-41.81	-99.29	-125.25

Table B-4

Sigma (X) for Opening 400' by 5', 500' Sandstone Overburden

Height Above Seam		Sigma (X) in Pounds per Square Inch at set Distances from the Centerline of Mine Opening				
H/W	feet	100'	200'	300'	400'	600'
1	400'	-132.25	-78.85	-24.38	+11.74	+32.42
3/4	300'	-95.92	-46.32	-12.08	-5.26	-13.40
1/2	200'	-70.9	-10.42	+3.97	-24.75	-55.50
1/4	100'	-7.85	+17.30	-32.00	-80.10	-97.45

Table B-5

Sigma (X) for Opening 500' by 5', 500' Sandstone Overburden

Height Above Seam		Sigma (X) in Pounds per Square Inch at set Distances from the Centerline of Mine Opening				
H/W	feet	125'	250'	375'	500'	750'
3/4	375'	-157.00	-69.80	+4.25	+36.20	+39.55
1/2	250'	-103.50	-16.83	+7.62	-16.80	-36.82
1/4	125'	-15.80	+28.30	-32.60	-92.35	-104.00

Table B-6

Sigma (X) for Opening 600' by 5', 500' Sandstone Overburden

Height Above Seam		Sigma (X) in Pounds per Square Inch at set Distances from the Centerline of Mine Opening				
H/W	feet	150'	300'	450'	600'	900'
3/4	450'	-295.00	-81.00	+89.35	+148.50	+123.50
1/2	300'	-131.75	-28.10	+22.28	+14.29	+2.65
1/4	150'	-20.19	+26.82	-43.67	-104.05	-107.92

Table B-7

Sigma (X) for Opening 100' by 5', 750' Sandstone Overburden

Height Above Seam		Sigma (X) in Pounds per Square Inch at set Distances from the Centerline of Mine Opening				
H/W	feet	25'	50'	75'	100'	150'
7	700'	**.**	-17.80	-17.30	-16.80	-15.80
6 1/2	650'	**.**	-23.65	-23.20	-22.75	-21.85
6	600'	**.**	-29.50	-29.10	-28.70	-27.90
5 1/2	550'	**.**	-38.78	-38.30	-37.83	-36.88
5	500'	**.**	-48.05	-47.50	-46.96	-45.86
4 1/2	450'		-50.26	-51.20	-50.56	-49.92
4	400'		-59.10	-58.48	-57.85	-56.90
3 1/2	350'		-67.80	-66.85	-65.90	-64.38
3	300'		-77.15	-75.52	-73.90	-71.60
2 1/2	250'		-87.45	-84.58	-81.70	-78.08
2	200'		-99.45	-93.82	-88.20	-82.58
1 1/2	150'		-113.00	-101.58	-90.15	-82.30
1	100'		-126.50	-100.65	-74.80	-73.52
3/4	75'		-133.00	-96.60	-60.20	-66.55
1/2	50'		-71.38	-77.24	-83.10	-90.52
1/4	25'		-9.75	-57.88	-106.00	-114.50

. = Percentage undeterminable from model used

Table B-8

Sigma (X) for Opening 200' by 5', 750' Sandstone Overburden

Height Above Seam		Sigma (X) in Pounds per Square Inch at set Distances from the Centerline of Mine Opening				
H/W	feet	50'	100'	150'	200'	300'
3 1/2	700'	-46.40	-42.75	-39.10	-33.10	-20.65
3	600'	-48.90	-45.90	-42.90	-38.45	-29.80
2 1/2	500'	-60.41	-57.35	-53.96	-49.67	-42.14
2	400'	-74.32	-68.90	-61.68	-54.70	-45.92
1 1/2	300'	-95.32	-82.75	-68.30	-57.22	-50.58
1	200'	-117.75	-86.30	-59.35	-48.62	-59.08
3/4	150'	-122.88	-74.65	-44.10	-43.78	-71.15
1/2	100'	-104.35	-46.48	-31.20	-56.08	-92.40
1/4	50'	+1.00	-58.48	-89.70	-106.32	-119.75

Table B-9

Sigma (X) for Opening 300' by 5', 750' Sandstone Overburden

Height Above Seam		Sigma (X) in Pounds per Square Inch at set Distances from the Centerline of Mine Opening				
H/W	feet	75'	150'	225'	300'	450'
2	600'	-75.02	-66.10	-48.26	-38.80	-15.60
1 1/2	450'	-84.63	-71.15	-55.91	-43.12	-33.22
1	300'	-110.50	-73.52	-43.10	-34.40	-48.98
3/4	225'	-121.00	-63.00	-26.10	-30.20	-65.35
1/2	150'	-110.00	-31.28	-7.68	-45.55	-98.52
1/4	75'	-56.80	+2.70	-50.40	-105.05	-130.00

Table B-10

Sigma (X) for Opening 400' by 5', 750' Sandstone Overburden

Height Above Seam		Sigma (X) in Pounds per Square Inch at set Distances from the Centerline of Mine Opening				
H/W	feet	100'	200'	300'	400'	600'
1 1/2	600'	-106.50	-82.20	-52.20	-24.55	+11.34
1	400'	-105.92	-68.25	-36.98	-25.62	-35.82
3/4	300'	-113.95	-53.98	-19.10	-24.62	-63.10
1/2	200'	-105.08	-20.98	-0.96	-43.40	-100.00
1/4	100'	-28.78	+10.70	-51.35	-114.92	-145.25

Table B-11

Sigma (X) for Opening 500' by 5', 750' Sandstone Overburden

Height Above Seam		Sigma (X) in Pounds per Square Inch at set Distances from the Centerline of Mine Opening				
H/W	feet	125'	250'	375'	500'	750'
1	500'	-126.98	-83.47	-28.71	-27.26	+7.21
3/4	375'	-117.00	-53.25	-14.50	-18.40	-50.05
1/2	250'	-106.50	-15.60	+4.27	-46.20	-106.70
1/4	125'	-38.70	+26.55	-47.40	-130.00	-166.50

Table B-12

Sigma (X) for Opening 600' by 5', 750' Sandstone Overburden

Height Above Seam		Sigma (X) in Pounds per Square Inch at set Distances from the Centerline of Mine Opening				
H/W	feet	150'	300'	450'	600'	900'
1	600'	-179.00	-95.10	-8.80	+48.10	+93.30
3/4	450'	-120.09	-62.62	-11.08	+0.66	-6.58
1/2	300'	-108.40	-15.02	+3.13	-48.92	-104.22
1/4	150'	-25.80	+28.48	-60.65	153.00	-192.75

Table B-13

Sigma (X) for Opening 100' by 5', 1000' Sandstone Overburden

Height Above Seam		Sigma (X) in Pounds per Square Inch at set Distances from the Centerline of Mine Opening				
H/W	feet	25'	50'	75'	100'	150'
9 1/2	950'	**.**	-14.93	-14.69	-14.45	-13.97
9	900'	**.**	-21.20	-20.98	-20.75	-20.30
8 1/2	850'	**.**	-27.95	-27.74	-27.52	-27.10
8	800'	**.**	-34.70	-34.50	-34.30	-33.90
7 1/2	750'	**.**	-42.00	-41.78	-41.55	-41.10
7	700'	**.**	-49.30	-49.05	-48.80	-48.30
6 1/2	650'	**.**	-57.00	-56.68	-56.35	-55.70
6	600'	**.**	-64.70	-64.30	-63.90	-63.10
5 1/2	550'	**.**	-73.18	-72.75	-72.30	-71.34
5	500'	**.**	-81.67	-81.20	-80.70	-79.59
4 1/2	450'	-88.16	-89.09	-88.47	-87.73	-85.86
4	400'	-98.25	-97.40	-96.55	-95.28	-92.48
3 1/2	350'	-108.00	-106.50	-105.00	-103.15	-99.22
3	300'	-118.00	-115.75	-113.50	-110.50	-104.75
2 1/2	250'	-129.50	125.75	-122.00	-117.00	-108.75
2	200'	-143.00	-135.75	-128.50	-120.75	-110.00
1 1/2	150'	-158.50	-143.50	-128.50	-117.75	-107.50
1	100'	-174.50	-140.00	-105.50	-103.75	-109.75
3/4	75'	-182.00	-133.50	-85.00	-93.50	-114.00
1/2	50'	-98.75	-106.62	-114.50	-124.25	-137.50
1/4	25'	-15.50	-79.75	-144.00	-155.00	-161.00

Table B-14

Sigma (X) for Opening 200' by 5', 1000' Sandstone Overburden

Height Above Seam		Sigma (X) in Pounds per Square Inch at set Distances from the Centerline of Mine Opening				
H/W	feet	50'	100'	150'	200'	300'
4 1/2	900'	-38.20	-36.60	-35.00	-32.25	-26.05
4	800'	-47.50	-46.15	-44.80	-42.45	-37.40
3 1/2	700'	-60.90	-59.15	-57.40	-54.75	-49.45
3	600'	-77.30	-74.50	-71.70	-67.90	-61.10
2 1/2	500'	-94.85	-91.37	-87.39	-82.58	-74.84
2	400'	-116.00	-109.00	-99.60	-90.40	-79.10
1 1/2	300'	-142.00	-125.25	-105.95	-91.25	-82.18
1	200'	-168.50	-126.65	-90.92	-76.58	-89.72
3/4	150'	-173.25	-109.28	-68.95	-68.25	-103.45
1/2	100'	-147.15	-70.25	-49.88	-82.52	-129.25
1/4	50'	-5.65	-84.12	-125.22	-147.00	-163.50

Table B-15

Sigma (X) for Opening 300' by 5', 1000' Sandstone Overburden

Height Above Seam		Sigma (X) in Pounds per Square Inch at set Distances from the Centerline of Mine Opening				
H/W	feet	75'	150'	225'	300'	450'
3	900'	-62.35	-57.40	-48.70	-38.60	-16.60
2 1/2	750'	-70.92	-66.20	-58.48	-50.25	-34.85
2	600'	-92.78	-84.60	-73.20	-63.15	-49.80
1 1/2	450'	-123.64	-105.36	-87.05	-71.92	-64.28
1	300'	-161.50	-113.08	-72.60	-60.85	-79.45
3/4	225'	-174.00	-98.30	-49.30	-53.75	-97.90
1/2	150'	-159.00	-55.16	-23.30	-71.62	-132.00
1/4	75'	-87.00	-8.35	-76.60	-146.50	-176.00

Table B-16

Sigma (X) for Opening 400' by 5', 1000' Sandstone Overburden

Height Above Seam		Sigma (X) in Pounds per Square Inch at set Distances from the Centerline of Mine Opening				
H/W	feet	100'	200'	300'	400'	600'
2	800'	-87.45	-74.80	-57.30	-38.60	-7.72
1 1/2	600'	-109.00	-89.30	-67.15	-50.30	-38.80
1	400'	-149.25	-100.90	-62.12	-49.92	-70.90
3/4	300'	-165.50	-87.02	-41.10	-47.60	-98.15
1/2	200'	-155.00	-45.44	-17.28	-69.72	-140.00
1/4	100'	-56.08	-3.10	-80.22	-159.00	-192.50

Table B-17

Sigma (X) for Opening 500' by 5', 1000' Sandstone Overburden

Height Above Seam		Sigma (X) in Pounds per Square Inch at set Distances from the Centerline of Mine Opening				
H/W	feet	125'	250'	375'	500'	750'
1 1/2	750'	-112.88	-85.90	-52.29	-23.25	-0.56
1	500'	-138.59	-94.72	-57.99	-44.97	-56.01
3/4	375'	-161.00	-80.55	-33.70	-43.00	-95.45
1/2	250'	-157.5	-39.69	-11.32	-73.38	-150.50
1/4	125'	-74.60	-3.82	-75.40	-174.50	-215.00

Table B-18

Sigma (X) for Opening 600' by 5', 1000' Sandstone Overburden

Height Above Seam		Sigma (X) in Pounds per Square Inch at set Distances from the Centerline of Mine Opening				
H/W	feet	150'	300'	450'	600'	900'
1 1/2	900'	-164.00	-101.65	-25.30	+44.00	+122.00
1	600'	-142.00	-84.10	-34.90	-17.25	-20.15
3/4	450'	-154.91	-76.60	-31.30	-38.68	-79.77
1/2	300'	-155.50	-37.14	-13.20	-79.95	-156.75
1/4	150'	-63.10	+11.88	-90.15	-199.00	-243.25

Table B-19

Sigma (X) for Opening 100' by 5', 500' Shale Overburden

Height Above Seam		Sigma (X) in Pounds per Square Inch at set Distances from the Centerline of Mine Opening				
H/W	feet	25'	50'	75'	100'	150'
4 1/2	450'	-18.35	-17.68	-17.00	-15.85	-13.30
4	400'	-20.75	-20.18	-19.60	-18.62	-16.52
3 1/2	350'	-24.75	-24.08	-23.40	-22.30	-20.08
3	300'	-28.70	-28.95	-27.90	-26.40	-23.58
2 1/2	250'	-36.40	-34.55	-32.70	-30.40	-26.55
2	200'	-44.15	-40.55	-36.95	-33.38	-28.38
1 1/2	150'	-53.55	-45.98	-38.40	-33.42	-28.72
1	100'	-64.05	-46.00	-27.95	-27.88	-31.52
3/4	75'	-69.40	-43.65	-17.90	-23.35	-34.50
1/2	50'	-29.77	-32.46	-35.15	-39.60	-45.90
1/4	25'	+9.86	-21.27	-52.40	-55.85	-57.30

Table B-20

Sigma (X) for Opening 200' by 5', 500' Shale Overburden

Height Above Seam		Sigma (X) in Pounds per Square Inch at set Distances from the Centerline of Mine Opening				
H/W	feet	50'	100'	150'	200'	300'
2	400'	-42.92	-35.88	-26.10	-15.67	+1.62
1 1/2	300'	-48.65	-38.08	-26.08	-16.88	-10.42
1	200'	-63.98	-37.62	-16.95	-11.30	-23.68
3/4	150'	-62.28	-19.30	-1.39	-13.19	-39.84
1/2	100'	-60.57	-0.97	+14.17	-15.08	-56.01
1/4	50'	-12.68	+26.90	-9.00	-60.75	-80.90

Table B-21

Sigma (X) for Opening 300' by 5', 500' Shale Overburden

Height Above Seam		Sigma (X) in Pounds per Square Inch at set Distances from the Centerline of Mine Opening				
H/W	feet	75'	150'	225'	300'	450'
1 1/2	450'	-88.75	-53.58	-10.86	+27.88	+71.22
1	300'	-66.35	-35.18	-8.55	+1.35	+0.36
3/4	225'	-71.20	-26.10	+1.15	-5.34	-28.85
1/2	150'	-68.64	-7.00	+8.70	-23.28	-62.01
1/4	75'	-12.42	+29.70	-23.32	-84.60	-110.88

Table B-22

Sigma (X) for Opening 400' by 5', 500' Shale Overburden

Height Above Seam		Sigma (X) in Pounds per Square Inch at set Distances from the Centerline of Mine Opening				
H/W	feet	100'	200'	300'	400'	600'
1	400'	-133.50	-76.75	-19.53	+17.95	+38.50
3/4	300'	-91.55	-37.90	-1.96	+4.45	-4.76
1/2	200'	-61.58	+5.74	+19.68	-11.67	-44.08
1/4	100'	+6.46	+41.50	-14.44	-65.02	-83.18

Table B-23

Sigma (X) for Opening 500' by 5', 500' Shale Overburden

Height Above Seam		Sigma (X) in Pounds per Square Inch at set Distances from the Centerline of Mine Opening				
H/W	feet	125'	250'	375'	500'	750'
3/4	375'	-160.00	-65.95	+12.20	+44.85	+46.95
1/2	250'	-85.20	-3.10	+21.35	-5.61	-26.98
1/4	125'	-2.74	+53.00	-16.70	-79.60	-91.25

Table B-24

Sigma (X) for Opening 600' by 5', 500' Shale Overburden

Height Above Seam		Sigma (X) in Pounds per Square Inch at set Distances from the Centerline of Mine Opening				
H/W	feet	150'	300'	450'	600'	900'
3/4	450'	-310.25	-80.15	+100.08	+160.00	+130.50
1/2	300'	-130.50	-17.22	+34.72	+24.86	+11.89
1/4	150'	+1.48	+50.72	-29.35	-93.22	-96.38

Table B-25

Sigma (X) for Opening 100' by 5', 750' Shale Overburden

Height Above Seam		Sigma (X) in Pounds per Square Inch at set Distances from the Centerline of Mine Opening				
H/W	feet	25'	50'	75'	100'	150'
7	700'	**.**	-15.00	-14.55	-14.10	-13.20
6 1/2	650'	**.**	-19.00	-18.58	-18.15	-17.30
6	600'	**.**	-23.00	-22.60	-22.20	-21.40
5 1/2	550'	**.**	-28.52	-28.11	-27.70	-26.90
5	500'	**.**	-34.03	-33.62	-33.21	-32.39
4 1/2	450'	-39.19	-38.61	-38.02	-37.44	-36.26
4	400'	-44.60	-44.00	-43.40	-42.52	-40.58
3 1/2	350'	-51.25	-50.32	-49.40	-47.98	-45.18
3	300'	-58.55	-56.98	-55.40	-53.22	-49.20
2 1/2	250'	-66.80	-64.00	-61.20	-57.75	-52.00
2	200'	-76.55	-71.15	-65.75	-60.35	-52.75
1 1/2	150'	-88.50	-77.12	-65.75	-58.25	-51.08
1	100'	-102.05	-74.95	-47.85	-47.65	-52.92
3/4	75'	-109.00	-70.35	-31.70	-39.75	-56.20
1/2	50'	-48.45	-52.30	-56.15	-62.70	-71.92
1/4	25'	+12.1	-34.25	-80.65	-85.65	-87.65

Table B-26

Sigma (X) for Opening 200' by 5', 750' Shale Overburden

Height Above Seam		Sigma (X) in Pounds per Square Inch at set Distances from the Centerline of Mine Opening				
H/W	feet	50'	100'	150'	200'	300'
3 1/2	700'	-44.60	-40.90	-37.20	-31.15	-18.60
3	600'	-43.00	-39.95	-36.90	-32.45	-23.75
2 1/2	500'	-50.51	-47.13	-43.75	-39.26	-31.49
2	400'	-62.02	-55.12	-47.68	-40.50	-31.52
1 1/2	300'	-78.28	-65.00	-50.00	-38.60	-32.00
1	200'	-97.98	-64.15	-35.90	-25.18	-36.45
3/4	150'	-101.98	-49.15	-17.28	-17.96	-46.62
1/2	100'	-82.20	-16.27	-16.73	-28.68	-65.88
1/4	50'	+26.00	-32.05	-58.40	-75.90	-91.70

Table B-27

Sigma (X) for Opening 300' by 5', 750' Shale Overburden

Height Above Seam		Sigma (X) in Pounds per Square Inch at set Distances from the Centerline of Mine Opening				
H/W	feet	75'	150'	225'	300'	450'
2	600'	-70.70	-61.40	-47.15	-33.10	-9.22
1 1/2	450'	-74.48	-60.01	-43.73	-30.34	-20.20
1	300'	-95.05	-55.32	-23.05	-14.36	-30.08
3/4	225'	-103.00	-40.15	-1.20	-6.45	-43.80
1/2	150'	-90.05	-1.42	+21.75	-19.37	-69.95
1/4	75'	-35.80	+40.35	-22.20	-77.50	-104.00

Table B-28

Sigma (X) for Opening 400' by 5', 750' Shale Overburden

Height Above Seam		Sigma (X) in Pounds per Square Inch at set Distances from the Centerline of Mine Opening				
H/W	feet	100'	200'	300'	400'	600'
1 1/2	600'	-104.20	-78.80	-47.20	-18.22	+19.00
1	400'	-95.28	-54.45	-21.18	-9.48	-20.92
3/4	300'	-99.80	-33.98	+2.91	-3.73	-44.90
1/2	200'	-86.35	+7.60	+27.18	-19.16	-79.08
1/4	100'	-4.60	+48.80	-22.55	-89.90	-121.50

Table B-29

Sigma (X) for Opening 500' by 5', 750' Shale Overburden

Height Above Seam		Sigma (X) in Pounds per Square Inch at set Distances from the Centerline of Mine Opening				
H/W	feet	125'	250'	375'	500'	750'
1	500'	-123.48	-75.36	-28.82	-0.34	+20.63
3/4	375'	-107.0	-36.75	+4.54	-0.55	-34.85
1/2	250'	-89.85	+11.21	+30.65	-24.37	88.70
1/4	125'	-15.80	+65.70	-20.00	-107.30	-145.00

Table B-30

Sigma (X) for Opening 600' by 5', 750' Shale Overburden

Height Above Seam		Sigma (X) in Pounds per Square Inch at set Distances from the Centerline of Mine Opening				
H/W	feet	150'	300'	450'	600'	900'
1	600'	-183.00	-93.00	-1.11	+58.90	+106.00
3/4	450'	-130.82	-50.28	+4.909	+16.45	+7.63
1/2	300'	-94.35	+9.54	+27.25	-29.70	-88.68
1/4	150'	-2.02	+67.05	-34.80	-133.32	-174.25

Table B-31

Sigma (X) for Opening 100' by 5', 1000' Shale Overburden

Height Above Seam		Sigma (X) in Pounds per Square Inch at set Distances from the Centerline of Mine Opening				
H/W	feet	25'	50'	75'	100'	150'
9 1/2	950'	**.**	-12.43	-12.19	-11.95	-11.47
9	900'	**.**	-16.70	-16.50	-16.30	-15.90
8 1/2	850'	**.**	-21.50	-21.31	-21.12	-20.75
8	800'	**.**	-26.30	-26.12	-25.95	-25.60
7 1/2	750'	**.**	-31.60	-31.40	-31.20	-30.80
7	700'	**.**	-36.90	-36.68	-36.45	-36.00
6 1/2	650'	**.**	-42.60	-42.30	-42.00	-41.40
6	600'	**.**	-48.30	-47.92	-47.55	-46.80
5 1/2	550'	**.**	-54.62	-54.19	-53.75	-52.82
5	500'	**.**	-60.95	-60.46	-59.95	-58.83
4 1/2	450'		-67.46	-66.52	-65.89	-65.18
4	400'		-73.55	-72.72	-71.90	-70.75
3 1/2	350'		-80.95	-79.72	-78.50	-76.58
3	300'		-89.15	-87.08	-85.00	-82.02
2 1/2	250'		-98.75	-94.92	-91.10	-86.45
2	200'		-110.00	-102.72	-95.45	-88.25
1 1/2	150'		-124.00	-108.90	-93.80	-83.78
1	100'		-140.00	-104.12	-68.25	-67.92
3/4	75'		-148.00	-96.90	-45.80	-56.50
1/2	50'		-66.90	-72.15	-77.40	-86.25
1/4	25'		+14.20	-47.40	-109.00	-116.00

Table B-32

Sigma (X) for Opening 200' by 5', 1000' Shale Overburden

Height Above Seam		Sigma (X) in Pounds per Square Inch at set Distances from the Centerline of Mine Opening				
H/W	feet	50'	100'	150'	200'	300'
4 1/2	900'	-34.30	-32.70	-31.10	-28.30	-22.05
4	800'	-39.60	-38.20	-36.80	-34.45	-29.35
3 1/2	700'	-49.00	-47.25	-45.50	-42.75	-37.35
3	600'	-61.40	-58.55	-55.70	-51.85	-45.00
2 1/2	500'	-75.14	-71.37	-67.15	-62.16	-54.08
2	400'	-92.62	-85.35	-75.50	-66.10	-54.52
1 1/2	300'	-115.50	-97.82	-77.70	-62.48	-53.42
1	200'	-139.25	-94.68	-57.02	-42.52	-56.85
3/4	150'	-143.22	-73.62	-31.12	-31.70	-68.88
1/2	100'	-115.88	-28.62	-8.62	-44.48	-92.85
1/4	50'	+28.40	-48.00	-82.45	-105.28	-125.50

Table B-33

Sigma (X) for Opening 300' by 5', 1000' Shale Overburden

Height Above Seam		Sigma (X) in Pounds per Square Inch at set Distances from the Centerline of Mine Opening				
H/W	feet	75'	150'	225'	300'	450'
3	900'	-59.90	-54.80	-45.72	-35.25	-12.50
2 1/2	750'	-62.09	-57.10	-49.04	-40.55	-24.60
2	600'	-77.95	-69.40	-57.55	-47.05	-33.20
1 1/2	450'	-101.93	-84.10	-65.30	-48.71	-37.24
1	300'	-137.00	-84.55	-41.90	-30.00	-50.20
3/4	225'	-148.00	-64.95	-13.20	-19.10	-66.25
1/2	150'	-130.00	-13.45	+17.95	-34.63	-98.48
1/4	75'	-57.80	+42.65	-37.90	-108.85	-141.00

Table B-34

Sigma (X) for Opening 400' by 5', 1000' Shale Overburden

Height Above Seam		Sigma (X) in Pounds per Square Inch at set Distances from the Centerline of Mine Opening				
H/W	feet	100'	200'	300'	400'	600'
2	800'	-82.30	-68.95	-50.50	-30.85	+1.48
1 1/2	600'	-96.15	-74.75	-51.15	-33.45	-21.60
1	400'	-129.00	-77.00	-35.42	-22.85	-45.78
3/4	300'	-142.25	-56.40	-7.70	-15.66	-69.92
1/2	200'	-127.95	-4.93	+22.75	-34.68	-109.25
1/4	100'	-22.62	+48.52	-40.48	-124.35	-159.75

Table B-35

Sigma (X) for Opening 500' by 5', 1000' Shale Overburden

Height Above Seam		Sigma (X) in Pounds per Square Inch at set Distances from the Centerline of Mine Opening				
H/W	feet	125'	250'	375'	500'	750'
1 1/2	750'	-107.75	-78.55	-42.85	-12.11	+23.95
1	500'	-124.27	-75.19	-34.98	-21.17	-33.84
3/4	375'	-141.00	-53.10	-3.07	-14.06	-70.65
1/2	250'	-132.00	-0.99	+27.10	-40.82	-122.75
1/4	125'	-42.60	+65.45	-37.30	-143.00	-185.00

Table B-36

Sigma (X) for Opening 600' by 5', 1000' Shale Overburden

Height Above Seam		Sigma (X) in Pounds per Square Inch at set Distances from the Centerline of Mine Opening				
H/W	feet	150'	300'	450'	600'	900'
1 1/2	900'	-170.00	-103.05	-21.70	+52.10	+134.50
1	600'	-131.00	-68.85	-16.50	+1.93	-1.78
3/4	450'	-83.40	-45.98	-3.67	-12.64	-57.60
1/2	300'	-132.50	-0.57	+22.90	-50.32	-132.25
1/4	150'	-29.98	+63.98	-53.68	-170.00	-216.00

APPENDIX C

USER'S MANUAL FOR COMPUTER PROGRAMS

Appendix C-1

The Finite Element Program

1. Definition of Variables

AK	Assemblage stiffness matrix.
AREA	Area of triangular element.
B	Matrix [B], for quadrilateral.
BODYF	Nodal load contribution from TBODY.
BT	Matrix [B], for triangle.
C	Stress-strain matrix, [C].
CB	Matrix product [C] [B].
CF	Common factor in the computation of stress-strain matrix, C.
E	Modulus of elasticity, E. In STRESS, the strains are at the centroid of the element.
EL	Length of element side where surface traction is prescribed.
FAC	Factor for averaging element strains.
IBAND	Semi-band width of assemblage equations, IBAND < MAXBW.
IE(M,I)	Element identification array, M is element number, I < M < NEL. I = 1,2,3,4 denote corner nodes of element, and I = 5 denotes MTYP for the element.
ISC,JSC	Nodal numbers of i and j for side on which surface traction is prescribed.
ISTOP	Index used to count data errors.
I,J,K,L	Indices of the four nodes of quadrilateral in QUAD.

I,J,K Indices of the three nodes of triangular element in CST.

KODE(I) Index of displacement and concentrated load conditions at node I.

KKK In BANSOL, index designating function to be used.
KKK = 1 for triangularization of stiffness.
KKK = 2 for backward solution using triangularized stiffness.

MAXBW Maximum semi-band width allowed.

MAXDOF Maximum degrees of freedom, $\text{MAXDOF} = 2 \times \text{MAXNP}$.

MAXEL Maximum number of elements allowed.

MAXMAT Maximum number of materials allowed.

MAXNP Maximum number of nodes allowed.

MAXSLC Maximum number of surface traction cards allowed.

MDIM Maximum band width, $\text{MDIM} = \text{MAXBW}$.

MTYP Material type number, $1 < \text{MTYP} < \text{NMAT}$.

NBODY Option for body force. $\text{NBODY} = 0$ for no weight.
 $\text{NBODY} = 1$ for weight force in the negative Y direction.

NDIM Maximum degrees of freedom, $\text{NDIM} = \text{MAXDOF}$.

NEL Number of elements, $\text{NEL} < \text{MAXEL}$.

NEQ Total number of equations, $\text{NEQ} = 2 \times \text{NNP} < \text{MAXDOF}$.

NMAT Number of different materials, $1 < \text{NMAT} < \text{MAXMAT}$.

NNP Number of nodal points, $\text{NNP} < \text{MAXNP}$.

NOLINE In STRESS, index to limit output to fifty lines per page.

NOPT Option for plane strain/stress. NOPT = 1 for plane strain, NOPT = 2 for plane stress.

NPROB Problem number.

NSLC Number of surface traction cards, NSLC < MAXSLC.

PR Poison's Ratio.

PXI,PXJ Nodal contributions of surface tractions in the X direction.

PYI,PYJ Nodal contributions of surface tractions in the Y direction.

Q Load vector of quadrilateral element. In STRESS, the element displacement vector.

QK Stiffness matrix of the quadrilateral element.

R Assemblage load vector. Also computed displacements for the assemblage in MAIN, BANSOL and STRESS.

RO Weight density of the material.

SIG Array for stresses.

SURTRX X and Y components of prescribed distributed tractions.

SURTRY tractions.

TBODY Total weight of triangular element.

TH Thickness, h.

TITLE Array for title of the problem (72 alphanumeric characters).

TK Stiffness matrix of the triangular element.

TOTALA Total area of quadrilateral element.

U Prescribed displacement in the X or Y direction in GEOMBC.

ULX(I) Concentrated load or displacement in the X and Y
VLY(I) directions at node I.
X(I),Y(I) X and Y coordinates of node I.
XQ,YQ Coordinates of the nodes of a quadrilateral or
triangular element. (XQ(5) and YQ(5) are
coordinates of the centroid.)

2. Input Data

The input data are called for exclusively in the SUBROUTINE DATAIN. This information is divided into the title card, the basic parameters, material properties, nodal point data, surface traction cards and an exit card.

a) Title card:

FORMAT (I5,1X,18A4) - 1 card per problem

<u>Col.</u>	<u>Symbol</u>	<u>Definition</u>
1-5	NPROB	Problem number
6		Blank
7-78	TITLE	Title of Problem

b) Basic parameters:

FORMAT (6I5) - 1 card per problem

<u>Col.</u>	<u>Symbol</u>	<u>Definition</u>
1-5	NNP	Number of nodal points
6-10	NEL	Number of elements
11-15	NMAT	Number of different materials
16-20	NSLC	Number of surface traction cards
21-25	NOPT	Option for plane strain/stress = 1 for plane strain = 2 for plane stress
26-30	NBODY	Option for body force = 0, no weight force = 1, weight force in negative Y direction

c) Material properties:

FORMAT (4E10.3) - NMAT cards per problem

<u>Col.</u>	<u>Symbol</u>	<u>Definition</u>
1-10	E	Modulus of Elasticity
11-20	PR	Poisson's Ratio
21-30	RO	Weight density of the material
31-40	TH	Thickness

d) Nodal point data:

FORMAT (2I5,4F10.1)

<u>Col.</u>	<u>Symbol</u>	<u>Definition</u>
1-5	M	Nodal point number
6-10	KODE	Option for free or fixed nodes: = 0, for fully free nodes = 1, for nodes fixed in the X-direction = 2, for nodes fixed in the Y-direction = 3, for fully fixed nodes
11-20	X	X-coordinate of node
21-30	Y	Y-coordinate of node
31-40	ULX	Prescribed load/displacement in the X direction
41-50	VLX	Prescribed load/displacement in the Y direction

e) Element data:

FORMAT (6I5)

<u>Col.</u>	<u>Symbol</u>	<u>Definition</u>
1-5	M	Element number

<u>Col.</u>	<u>Symbol</u>	<u>Definition</u>
6-10	IE(M,1)	
11-15	IE(M,2)	Corner node numbers for the
16-20	IE(M,3)	number M element
21-25	IE(M,4)	
26-30	IE(M,5)	Material type

f) Surface traction:

FORMAT (2I5,4E10.3)

<u>Col.</u>	<u>Symbol</u>	<u>Definition</u>
1-5	ISC(I)	Number i nodal point
6-10	JSC(J)	Number j nodal point
11-20	SURTRX(I)	Surface traction in the X-direction of the i node
21-30	SURTRX(J)	Surface traction in the X-direction of the j node
31-40	SURTRY(I)	Surface traction in the Y-direction of the i node
41-50	SURTRY(J)	Surface traction in the Y-direction of the j node

g) Exit card:

FORMAT (I1)

<u>Col.</u>	<u>Symbol</u>	<u>Definition</u>
1	N	Termination option = 0, for termination of program operation = 1,2,3,..., for execution of next problem

2.1 Notes on Input Data

1. Units must be consistent.

2. Usually one card is needed for each node. However, if some nodes fall on a straight line and spaced at an equal distance, data for only the first and last nodes of this group are necessary. The intermediate nodal point data are generated by linear interpolation. This applies only to the nodal point coordinates.

3. Usually one card is needed for each element. However, if some of the elements are lined up so that their corner node indices each increase by one when compared to the previous element, only the data for the first and last elements of the set are necessary.


```
8   FORMAT (/8H1PROBLEM,15,3H. . .18A4/)          MAIN 540
9   FORMAT (37H1OUTPUT TABLE 1. . . NODAL DISPLACEMENTS//13X,4HNODE,9X,11HMAIN 550
10  1HU = X-DISP.,9X,11HV = Y-DISP./ (5X,112,2E20.8)) MAIN 560
    FORMAT (///12H BANDWIDTH =,14,25H EXCEEDS MAX. ALLOWABLE =,14//30HMAIN 570
1   GO ON TO NEXT PROBLEM          )          MAIN 580
    END                                MAIN 590
```

C	FINITE ELEMENT PROGRAM - SUBROUTINE DATAIN	DATA 10
	SUBROUTINE DATAIN (MAXEL,MAXNP,MAXMAT,MAXSLC,ISTOP)	DATA 20
	COMMON NNP,NEL,NMAT,NSLC,NOPT,NBODY,MTYP,E(6),PR(6),RO(6),TH(6),IEDATA	DATA 30
	1(800,5),X(800),Y(800),ULX(800),VLY(800),KODE(800),ISC(80),JSC(80),DATA	DATA 40
	2SURTRX(80,2),SURTRY(80,2)	DATA 50
C	ISTOP=0	DATA 60
	READ 22, NNP,NEL,NMAT,NSLC,NOPT,NBODY	DATA 70
C	PRINT 23, NNP,NEL,NMAT,NSLC,NOPT,NBODY	DATA 80
		DATA 90
C	PRINT 23, NNP,NEL,NMAT,NSLC,NOPT,NBODY	DATA 100
C	CHECKS TO BE SURE INPUT DATA DOES NOT EXCEED STORAGE CAPACITY	DATA 110
	IF (NNP.LE.MAXNP) GO TO 1	DATA 120
	ISTOP=ISTOP+1	DATA 130
	PRINT 24, MAXNP	DATA 140
1	IF (NEL.LE.MAXEL) GO TO 2	DATA 150
	ISTOP=ISTOP+1	DATA 160
	PRINT 25, MAXEL	DATA 170
2	IF (NMAT.LE.MAXMAT) GO TO 3	DATA 180
	ISTOP=ISTOP+1	DATA 190
	PRINT 26, MAXMAT	DATA 200
3	IF (NSLC.LE.MAXSLC) GO TO 4	DATA 210
	ISTOP=ISTOP+1	DATA 220
	PRINT 27, MAXSLC	DATA 230
4	IF (ISTOP.EQ.0) GO TO 5	DATA 240
	PRINT 28, ISTOP	DATA 250
	STOP	DATA 260
		DATA 270
C		DATA 280
5	READ 29, (E(1),PR(1),RO(1),TH(1),I=1,NMAT)	DATA 290
	PRINT 30	DATA 300
	PRINT 31, (I,E(1),PR(1),RO(1),TH(1),I=1,NMAT)	DATA 310
		DATA 320
C	READ AND PRINT NODAL DATA (REF. 1)	DATA 330
C	PRINT 32	DATA 340
	N=1	DATA 350
6	READ 33, M,KODE(M),X(M),Y(M),ULX(M),VLY(M)	DATA 360
	IF (M-N) 7,10,8	DATA 370
7	PRINT 34, M	DATA 380
	PRINT 35, M,KODE(M),X(M),Y(M),ULX(M),VLY(M)	DATA 390
	ISTOP=ISTOP+1	DATA 400
	GO TO 6	DATA 410
8	DF=M+1-N	DATA 420
	RX=(X(M)-X(N-1))/DF	DATA 430
	RY=(Y(M)-Y(N-1))/DF	DATA 440
9	KODE(N)=KODE(N-1)	DATA 450
	X(N)=X(N-1)+RX	DATA 460
	Y(N)=Y(N-1)+RY	DATA 470
	ULX(N)=0.0	DATA 480
	VLY(N)=0.0	DATA 490
10	PRINT 35, N,KODE(N),X(N),Y(N),ULX(N),VLY(N)	DATA 500
		DATA 510
	N=N+1	DATA 520
	IF (M-N) 11,10,9	DATA 530
11	IF (N.LE.NNP) GO TO 6	

C	FINITE ELEMENT PROGRAM - SUBROUTINE ASSEMBL(ISTOP)	ASML 10
	SUBROUTINE ASEMBL (ISTOP)	ASML 20
	COMMON NNP, NEL, NMAT, NSLC, NOPT, NBODY, MTP, E(6), PR(6), RO(6), TH(6), IEASML	ASML 30
	1(800,5), X(800), Y(800), ULX(800), VLY(800), KODE(800), ISC(80), JSC(80), ASML	ASML 40
	2SURTRX(80,2), SURTRY(80,2)	ASML 50
	COMMON /ONE/ QK(10,10), Q(10), B(3,10), C(3,3), BT(3,6), XQ(5), YQ(5)	ASML 60
	COMMON /TWO/ IBAND, NEQ, R(1600), AK(1600,144)	ASML 70
	DIMENSION LP(8)	ASML 80
C		ASML 90
	REWIND 1	ASML 100
C	INITIALIZE	ASML 110
	ISTOP=0	ASML 120
C	INITIALIZE PARTS OF MATRICES C AND BT	ASML 130
	BT(1,4)=0.0	ASML 140
	BT(1,5)=0.0	ASML 150
	BT(1,6)=0.0	ASML 160
	BT(2,1)=0.0	ASML 170
	BT(2,2)=0.0	ASML 180
	BT(2,3)=0.0	ASML 190
	C(1,3)=0.0	ASML 200
	C(2,3)=0.0	ASML 210
	C(3,1)=0.0	ASML 220
	C(3,2)=0.0	ASML 230
C		ASML 240
C	INITIALIZE OVERALL STIFFNESS MATRIX AK AND OVERALL LOAD VECTOR R	ASML 250
	DO 1 I=1, NEQ	ASML 260
	R(I)=0.0	ASML 270
	DO 1 J=1, IBAND	ASML 280
1	AK(I,J)=0.0	ASML 290
C		ASML 300
C	COMPUTE ELEMENT STIFFNESSES AND LOADS ONE BY ONE	ASML 310
C		ASML 320
	DO 10 M=1, NEL	ASML 330
	IF (IE(M,5).GT.0) GO TO 2	ASML 340
	ISTOP=ISTOP+1	ASML 350
	GO TO 10	ASML 360
2	CALL QUAD (M, AREA)	ASML 370
	IF (AREA.GT.0.0) GO TO 3	ASML 380
	ISTOP=ISTOP+1	ASML 390
	PRINT 19, M	ASML 400
C		ASML 410
C	CONDENSE ELEMENT STIFF. FROM 10X10 TO 8X8, EQ.(5-64), AND ELEMENT	ASML 420
C	LOADS FROM 10X1 TO 8X1, EQ.(5-64D). (REF.2)	ASML 430
3	IF (IE(M,3).EQ.IE(M,4)) GO TO 7	ASML 440
	DO 6 J=1,2	ASML 450
	IJ=10-J	ASML 460
	IK=IJ+1	ASML 470
	PIVOT=QK(IK, IK)	ASML 480
	DO 5 K=1, IJ	ASML 490
	F=QK(IK, K)/PIVOT	ASML 500
		ASML 510
	QK(IK, K)=F	ASML 520
	DO 4 I=K, IJ	ASML 530
	QK(I, K)=QK(I, K)-F*QK(I, IK)	

4	QK(K,1)=QK(1,K)	ASML 540
5	Q(K)=Q(K)-QK(1K,K)*Q(1K)	ASML 550
6	Q(1K)=Q(1K)/PIVOT	ASML 560
C		ASML 570
C		ASML 580
C	STORE MULTIPLIERS,PIVOTS,CONDENSED LOADS, STRAIN-DISP. AND STRESS-	ASML 590
C	MATRICES ON SCRATCH TAPE NO. 1 (TO BE USED LATER TO COMPUTE STRAIN	ASML 600
C	STRESSES)	ASML 610
7	WRITE (1) ((QK(1,J),J=1,10),I=9,10),Q(9),Q(10),((B(1,J),J=1,10),I=	ASML 620
C	11,3),((C(1,J),J=1,3),I=1,3),XQ(5),YQ(5)	ASML 630
C		ASML 640
C	ASSEMBLE STIFF. AND LOADS , DIRECT STIFF. METHOD, SEC. 6-5.	ASML 650
C		ASML 660
	LIM=8	ASML 670
	IF (1E(M,3).EQ.1E(M,4)) LIM=6	ASML 680
	DO 8 I=2,LIM,2	ASML 690
	IJ=I/2	ASML 700
8	LP(I-1)=2*1E(M,IJ)-1	ASML 710
	LP(I)=2*1E(M,IJ)	ASML 720
	DO 9 LL=1,LIM	ASML 730
	I=LP(LL)	ASML 740
	R(I)=R(I)+Q(LL)	ASML 750
	DO 9 MM=1,LIM	ASML 760
	J=LP(MM)-I+1	ASML 770
	IF (J.LE.0) GO TO 9	ASML 780
	AK(I,J)=AK(I,J)+QK(LL,MM)	ASML 790
9	CONTINUE	ASML 800
10	CONTINUE	ASML 810
C		ASML 820
C	ADD EXTERNALLY APPL. CONC. NODAL LOADS TO R	ASML 830
	DO 12 N=1,NNP	ASML 840
	IF (KODE(N).EQ.3) GO TO 12	ASML 850
	K=2*N	ASML 860
	IF (KODE(N).EQ.1) GO TO 11	ASML 870
	R(K-1)=R(K-1)+ULX(N)	ASML 880
	IF (KODE(N).NE.0) GO TO 12	ASML 890
11	R(K)=R(K)+VLY(N)	ASML 900
12	CONTINUE	ASML 910
C		ASML 920
C	CONVERT LINEARLY VARYING SURFACE TRACTIONS TO STATIC EQUIVALENTS,	ASML 930
C	AND ADD TO OVERALL LOAD VECTOR R, EQ.(5-61A).	ASML 940
	IF (NSLC.EQ.0) GO TO 14	ASML 950
	DO 13 L=1,NSLC	ASML 960
	I=ISC(L)	ASML 970
	J=JSC(L)	ASML 980
	I1=2*I	ASML 990
	JJ=2*J	ASML1000
		ASML1010
	DX=X(J)-X(I)	ASML1020
	DY=Y(J)-Y(I)	ASML1030
	EL=SQRT(DX*DX+DY*DY)	ASML1040
	PXI=SURTRX(L,1)*EL	ASML1050
	PXJ=SURTRX(L,2)*EL	ASML1060
	PYI=SURTRY(L,1)*EL	ASML1070
	PYJ=SURTRY(L,2)*EL	

	R(II-1)=R(II-1)+PXI/3.0+PXJ/6.0	ASML1080
	R(JJ-1)=R(JJ-1)+PXI/6.0+PXJ/3.0	ASML1090
	R(II)=R(II)+PYI/3.0+PYJ/6.0	ASML1100
	R(JJ)=R(JJ)+PYI/6.0+PYJ/3.0	ASML1110
13	CONTINUE	ASML1120
C		ASML1130
C	INTRODUCE KINEMATIC CONSTRAINTS (GEOMETRIC BOUNDARY CONDITIONS),	ASML1140
C	EQ.(6-18). REF. 1.	ASML1150
C		ASML1160
14	DO 17 M=1,NNP	ASML1170
	IF (KODE(M).GE.0.AND.KODE(M).LE.3) GO TO 15	ASML1180
	ISTOP=ISTOP+1	ASML1190
	GO TO 17	ASML1200
15	IF (KODE(M).EQ.0) GO TO 17	ASML1210
	IF (KODE(M).EQ.2) GO TO 16	ASML1220
	CALL GEOMBC (ULX(M),2*M-1)	ASML1230
	IF (KODE(M).EQ.1) GO TO 17	ASML1240
16	CALL GEOMBC (VLY(M),2*M)	ASML1250
17	CONTINUE	ASML1260
	END FILE 1	ASML1270
	IF (ISTOP.EQ.0) GO TO 18	ASML1280
	PRINT 20, ISTOP	ASML1290
18	RETURN	ASML1300
C		ASML1310
19	FORMAT (/5X,17H AREA OF ELEMENT ,15,14H IS NEGATIVE /)	ASML1320
20	FORMAT (////42H SOLUTION WILL NOT BE PERFORMED BECAUSE OF,15,15H	ASML1330
	1 DATA ERRORS /)	ASML1340
	END	ASML1350

C	FINITE ELEMENT PROGRAM - SUBROUTINE QUAD(M,TOTALA)	QUAD 10
	SUBROUTINE QUAD (M,TOTALA)	QUAD 20
	COMMON NNP,NEL,NMAT,NSLC,NOPT,NBODY,MTYP,E(6),PR(6),RO(6),TH(6),IE	QUAD 30
	1(800,5),X(800),Y(800),ULX(800),VLY(800),KODF(800),ISC(80),JSC(80),	QUAD 40
	2SURTRX(80,2),SURTRY(80,2)	QUAD 50
	COMMON /ONE/ QK(10,10),Q(10),B(3,10),C(3,3),BT(3,6),XQ(5),YQ(5)	QUAD 60
	COMMON /TWO/ IBAND,NEQ,R(1600),AK(1600,144)	QUAD 70
C		QUAD 80
	I=IE(M,1)	QUAD 90
	J=IE(M,2)	QUAD 100
	K=IE(M,3)	QUAD 110
	L=IE(M,4)	QUAD 120
	MTYP=IE(M,5)	QUAD 130
	TOTALA=0.0	QUAD 140
C		QUAD 150
C	CONSTRUCT STRESS-STRAIN MATRIX C,EQ.(3-16C). FOR PLANE STRAIN	QUAD 160
C	NOPT=1, AND FOR PLANE STRESS NOPT=2. PRESENT CODE IS FOR	QUAD 170
C	ISOTROPIC MATERIALS	QUAD 180
	IF (NMAT.EQ.1.AND.M.GT.1) GO TO 2	QUAD 190
	IF (NOPT.EQ.2) GO TO 1	QUAD 200
	CF=E(MTYP)/((1.0+PR(MTYP))*(1.0-2.0*PR(MTYP)))	QUAD 210
	C(1,1)=CF*(1.0-PR(MTYP))	QUAD 220
	C(1,2)=CF*PR(MTYP)	QUAD 230
	C(2,1)=C(1,2)	QUAD 240
	C(2,2)=C(1,1)	QUAD 250
	C(3,3)=CF*(1.0-2.0*PR(MTYP))/2.0	QUAD 260
	GO TO 2	QUAD 270
1	CF=E(MTYP)/(1.0-PR(MTYP)*PR(MTYP))	QUAD 280
	C(1,1)=CF	QUAD 290
	C(1,2)=PR(MTYP)*CF	QUAD 300
	C(2,1)=C(1,2)	QUAD 310
	C(2,2)=CF	QUAD 320
	C(3,3)=CF*(1.0-PR(MTYP))/2.0	QUAD 330
2	LIM=4	QUAD 340
	IF (K.EQ.L) LIM=3	QUAD 350
	XQ(5)=0.0	QUAD 360
	YQ(5)=0.0	QUAD 370
	DO 3 N=1,LIM	QUAD 380
	NN=IE(M,N)	QUAD 390
	XQ(N)=X(NN)	QUAD 400
	YQ(N)=Y(NN)	QUAD 410
	XQ(5)=XQ(5)+X(NN)/FLOAT(LIM)	QUAD 420
3	YQ(5)=YQ(5)+Y(NN)/FLOAT(LIM)	QUAD 430
C		QUAD 440
C	INITIALIZE QUAD. STIFFNESS, LOAD VECTOR AND STRAIN-DISPLACEMENT VE	QUAD 450
	DO 5 II=1,10	QUAD 460
	Q(II)=0.0	QUAD 470
	DO 4 JJ=1,10	QUAD 480
4	QK(II,JJ)=0.0	QUAD 490
	DO 5 JJ=1,3	QUAD 500
5		QUAD 510
	B(JJ,II)=0.0	QUAD 520
	IF (K.NE.L) GO TO 6	QUAD 530
	CALL CST (1,2,3,TOTALA)	QUAD 540
	GO TO 7	

6	CALL CST (1,2,5,AREA)	QUAD 550
	TOTALA=TOTALA+AREA	QUAD 560
	CALL CST (2,3,5,AREA)	QUAD 570
	TOTALA=TOTALA+AREA	QUAD 580
	CALL CST (3,4,5,AREA)	QUAD 590
	TOTALA=TOTALA+AREA	QUAD 600
	CALL CST (4,1,5,AREA)	QUAD 610
	TOTALA=TOTALA+AREA	QUAD 620
7	RETURN	QUAD 630
	END	QUAD 640

C	FINITE ELEMENT PROGRAM - SUBROUTINE CST(I,J,K,AREA)	CST	10
	SUBROUTINE CST (I,J,K,AREA)	CST	20
	COMMON NNP,NEL,NMAT,NSLC,NOPT,NBODY,MTYP,E(6),PR(6),RO(6),TH(6),IECST	CST	30
	1(800,5),X(800),Y(800),ULX(800),VLY(800),KODE(800),ISC(80),JSC(80),CST	CST	40
	2SURTRX(80,2),SURTRY(80,2)	CST	50
	COMMON /ONE/ QK(10,10),Q(10),B(3,10),C(3,3),BT(3,6),XQ(5),YQ(5)	CST	60
	COMMON /TWO/ IBAND,NEQ,R(1600),AK(1600,144)	CST	70
	DIMENSION CB(3,6), LC(6), LT(3), TK(6,6)	CST	80
C		CST	90
	LT(1)=I	CST	100
	LT(2)=J	CST	110
	LT(3)=K	CST	120
C		CST	130
C	COMPUTE STRAIN-DISPLACEMENT MATRIX B FOR TRIANGLE, EQ. (5-35A)	CST	140
	BT(1,1)=YQ(J)-YQ(K)	CST	150
	BT(1,2)=YQ(K)-YQ(I)	CST	160
	BT(1,3)=YQ(I)-YQ(J)	CST	170
	BT(2,4)=XQ(K)-XQ(J)	CST	180
	BT(2,5)=XQ(I)-XQ(K)	CST	190
	BT(2,6)=XQ(J)-XQ(I)	CST	200
	BT(3,1)=BT(2,4)	CST	210
	BT(3,2)=BT(2,5)	CST	220
	BT(3,3)=BT(2,6)	CST	230
	BT(3,4)=BT(1,1)	CST	240
	BT(3,5)=BT(1,2)	CST	250
	BT(3,6)=BT(1,3)	CST	260
	AREA=(BT(2,4)*BT(1,3)-BT(2,6)*BT(1,1))/2.0	CST	270
C		CST	280
C	COMPUTE C*B	CST	290
	DO 1 II=1,3	CST	300
	DO 1 JJ=1,6	CST	310
	CB(II,JJ)=0.0	CST	320
	DO 1 KK=1,3	CST	330
1	CB(II,JJ)=CB(II,JJ)+C(II,KK)*BT(KK,JJ)	CST	340
C		CST	350
C	COMPUTE (B**T)*C*B, EQ.(5-45A)	CST	360
	DO 2 II=1,6	CST	370
	DO 2 JJ=1,6	CST	380
	TK(II,JJ)=0.0	CST	390
	DO 2 KK=1,3	CST	400
2	TK(II,JJ)=TK(II,JJ)+BT(KK,II)*CB(KK,JJ)	CST	410
C		CST	420
C	ADD TRIANGLE STIFFNESS TO QUADRILATERAL STIFFNESS, EX.(6-2).	CST	430
C	ADD TRIANGLE STRAIN-DISPLACEMENT MATRIX TO QUADRILATERAL STRAIN-	CST	440
C	DISPLACEMENT MATRIX	CST	450
	DO 3 II=1,3	CST	460
	LC(II)=2*LT(II)-1	CST	470
	LC(II+3)=2*LT(II)	CST	480
3	DO 5 II=1,6	CST	490
	LL=LC(II)	CST	500
		CST	510
	IF (AREA.EQ.0.0) GO TO 7	CST	520
	FK=1.0/(4.0*AREA)	CST	530
	FB=2.0*FK	CST	530

	DO 4 JJ=1,6	CST 540
	MM=LC(JJ)	CST 550
4	QK(LL,MM)=QK(LL,MM)+TK(II, JJ)*TH(MTYP)*FK	CST 560
	DO 5 JJ=1,3	CST 570
5	B(JJ,LL)=B(JJ,LL)+BT(JJ, II)*FB	CST 580
C		CST 590
C	DEVELOP BODY FORCE VECTOR, EQ.(5-61B)	CST 600
	IF (NBODY.EQ.0) GO TO 7	CST 610
	TBODYF=AREA*RO(MTYP)*TH(MTYP)	CST 620
	BODYF=-TBODYF/3.0	CST 630
	DO 6 II=1,3	CST 640
	JJ=2*LT(II)	CST 650
6	Q(JJ)=Q(JJ)+BODYF	CST 660
7	RETURN	CST 670
	END	CST 680

C	FINITE ELEMENT PROGRAM - SUBROUTINE STRESS	STRS 10
	SUBROUTINE STRESS	STRS 20
	COMMON NNP, NEL, NMAT, NSLC, NOPT, NBODY, MTYP, E(6), PR(6), RO(6), TH(6), IESTRS	STRS 30
	1(800,5), X(800), Y(800), ULX(800), VLY(800), KODE(800), ISC(80), JSC(80),	STRS 40
	2SURTRX(80,2), SURTRY(80,2)	STRS 50
	COMMON /ONE/ QK(10,10), Q(10), B(3,10), C(3,3), BT(3,6), XQ(5), YQ(5)	STRS 60
	COMMON /TWO/ IBAND, NEQ, R(1600), AK(1600,144)	STRS 70
	DIMENSION SIG(6), SIGI(3)	STRS 80
C	REWIND 1	STRS 90
	PRINT 10	STRS 100
	NOLINE=47	STRS 110
C		STRS 120
C	RETRIEVE MULTIPLIERS, PIVOTS, MATRICES B AND C, AND CENTROIDAL COOSTRS	STRS 130
C	FOR ELEMENT	STRS 140
C	DO 9 M=1, NEL	STRS 150
	READ (1) ((QK(I,J), J=1,10), I=1,2), Q(9), Q(10), ((B(I,J), J=1,10), I=1,	STRS 160
	13), ((C(I,J), J=1,3), I=1,3), XC, YC	STRS 170
C		STRS 180
C	SELECT NODAL DISPLACEMENTS FOR THE ELEMENT	STRS 190
	LIM=4	STRS 200
	IF (IE(M,3).EQ.IE(M,4)) LIM=3	STRS 210
	DO 1 I=1, LIM	STRS 220
	II=2*I	STRS 230
	JJ=2*IE(M, I)	STRS 240
	Q(II-1)=R(JJ-1)	STRS 250
1	Q(II)=R(JJ)	STRS 260
C		STRS 270
C	RECOVER CONDENSED DISPLACEMENTS FOR THE QUADRILATERAL, EQ. (5-64G)	STRS 280
	IF (LIM.EQ.3) GO TO 3	STRS 290
	DO 2 K=1, 2	STRS 300
	JK=K+8	STRS 310
	IK=JK-1	STRS 320
	DO 2 L=1, IK	STRS 330
2	Q(JK)=Q(JK)-QK(K,L)*Q(L)	STRS 340
C		STRS 350
C	COMPUTE ELEMENT STRAINS, EQ.(5-35A)	STRS 360
	LIM=10	STRS 370
	FAC=0.25	STRS 380
	GO TO 4	STRS 390
3	LIM=6	STRS 400
	FAC=1.0	STRS 410
4	DO 5 I=1, 3	STRS 420
	E(I)=0.0	STRS 430
	DO 5 J=1, LIM	STRS 440
5	E(I)=E(I)+B(I,J)*Q(J)*FAC	STRS 450
C		STRS 460
C	COMPUTE ELEMENT STRESSES , EQ.(5-35B)	STRS 470
	DO 6 I=1, 3	STRS 480
	SIG(I)=0.0	STRS 490
		STRS 500
		STRS 510
	DO 6 J=1, 3	STRS 520
6	SIG(I)=SIG(I)+C(I,J)*E(J)	STRS 530
C	COMPUTE PRINCIPAL STRESSES AND THE ANGLE WITH THE POSITIVE X AXIS	STRS 540
	SP=(SIG(1)+SIG(2))/2.0	

	SM=(SIG(1)-SIG(2))/2.0	STRS 550
	DS=SQRT(SM*SM+SIG(3)*SIG(3))	STRS 560
	SIG(4)=SP+DS	STRS 570
	SIG(5)=SP-DS	STRS 580
	SIG(6)=0.0	STRS 590
	IF (SIG(3).NE.0.0.AND.SM.NE.0.0) SIG(6)=28.648*ATAN2(SIG(3),SM)	STRS 600
C	PRINT STRESSES, 50 LINES PER PAGE	STRS 610
	IF (NOLINE.GT.0) GO TO 7	STRS 620
	PRINT 11	STRS 630
	NOLINE=49	STRS 640
7	NOLINE=NOLINE-1	STRS 650
C		STRS 660
C	RE-USE STORAGE SPACE IN UN-NEEDED ARRAYS FOR STRESSES & CENTROIDS	STRS 670
C		STRS 680
	DO 8 JJJ=1,5	STRS 690
	ISUB1=MOD(JJJ+1,2)*120+M	STRS 700
	ISUB2=(JJJ+1)/2	STRS 710
8	AK(ISUB1,ISUB2)=SIG(JJJ)	STRS 720
	STX=SIG(1)/144.	STRS 730
	STY=SIG(2)/144.	STRS 740
	STXY=SIG(3)/144.	STRS 750
	STMAX=SIG(4)/144.	STRS 760
	STMIN=SIG(5)/144.	STRS 770
9	WRITE (6,12) M,XC,YC,STX,STY,STXY,STMAX,STMIN,SIG(6)	STRS 780
	END FILE 1	STRS 790
	RETURN	STRS 800
C		STRS 810
10	FORMAT (47H1OUTPUT TABLE 2.. STRESSES AT ELEMENT CENTROIDS//1X,7HESTRS 820	
	1LEMENT,2X,1HX,4X,1HY,3X,8HSIGMA(X),2X,8HSIGMA(Y),2X,8HTAU(X,Y),2X,STRS 830	
	28HSIGMA(1),2X,8HSIGMA(2),2X,5HANGLE)	STRS 840
11	FORMAT (1H1,7HELEMENT,2X,1HX,4X,1HY,3X,8HSIGMA(X),2X,8HSIGMA(Y),2XSTRS 850	
	1,8HTAU(X,Y),2X,8HSIGMA(1),2X,8HSIGMA(2),2X,5HANGLE)	STRS 860
12	FORMAT (14,2F7.2,1P6E10.2)	STRS 870
	END	STRS 880

C	FINITE ELEMENT PROGRAM - SUBROUTINE GEOMBC(U,N)	GEOM 10
	SUBROUTINE GEOMBC (U,N)	GEOM 20
	COMMON /TWO/ IBAND,NEQ,R(1600),AK(1600,144)	GEOM 30
C	THIS SUBROUTINE MODIFIES THE ASSEMBLAGE STIFFNESS AND LOADS FOR TH	GEOM 40
C	PRESCRIBED DISPLACEMENT U AT DEGREE OF FREEDOM N, EQ.(6-188). (REF	GEOM 50
	DO 2 M=2,IBAND	GEOM 60
	K=N-M+1	GEOM 70
	IF (K.LE.0) GO TO 1	GEOM 80
	R(K)=R(K)-AK(K,M)*U	GEOM 90
	AK(K,M)=0.0	GEOM 100
1	K=N+M-1	GEOM 110
	IF (K.GT.NEQ) GO TO 2	GEOM 120
	R(K)=R(K)-AK(N,M)*U	GEOM 130
	AK(N,M)=0.0	GEOM 140
2	CONTINUE	GEOM 150
	AK(N,1)=1.0	GEOM 160
	R(N)=U	GEOM 170
	RETURN	GEOM 180
	END	GEOM 190

C	FINITE ELEMENT PROGRAM - SUBROUTINE BANSOL	BANS 10
	SUBROUTINE BANSOL (KKK,AK,R,NEQ,IBAND,NDIM,MDIM)	BANS 20
C	SYMMETRIC BAND MATRIX EQUATION SOLVER. (REF. 2)	BANS 30
C		BANS 40
C	KKK = 1 TRIANGULARIZES THE BAND MATRIX AK, EQ. (2-2)	BANS 50
C	KKK = 2 SOLVES FOR RIGHT HAND SIDE R, SOLUTION RETURNS IN R, EQ.(2	BANS 60
C		BANS 70
	DIMENSION AK(1600,144), R(1)	BANS 80
	NRS=NEQ-1	BANS 90
	NR=NEQ	BANS 100
	IF (KKK.EQ.2) GO TO 3	BANS 110
	DO 2 N=1,NRS	BANS 120
	M=N-1	BANS 130
	MR=MINO(IBAND, NR-M)	BANS 140
	PIVOT=AK(N, 1)	BANS 150
	DO 2 L=2,MR	BANS 160
	CP=AK(N,L)/PIVOT	BANS 170
	I=M+L	BANS 180
	J=0	BANS 190
	DO 1 K=L,MR	BANS 200
	J=J+1	BANS 210
1	AK(I,J)=AK(I,J)-CP*AK(N,K)	BANS 220
2	AK(N,L)=CP	BANS 230
	GO TO 6	BANS 240
3	DO 4 N=1,NRS	BANS 250
	M=N-1	BANS 260
	MR=MINO(IBAND, NR-M)	BANS 270
	CP=R(N)	BANS 280
	R(N)=CP/AK(N, 1)	BANS 290
	DO 4 L=2,MR	BANS 300
	I=M+L	BANS 310
4	R(I)=R(I)-AK(N,L)*CP	BANS 320
	R(NR)=R(NR)/AK(NR, 1)	BANS 330
	DO 5 I=1,NRS	BANS 340
	N=NR-1	BANS 350
	M=N-1	BANS 360
	MR=MINO(IBAND, NR-M)	BANS 370
	DO 5 K=2,MR	BANS 380
	L=M+K	BANS 390
C	STORE COMPUTED DISPLACEMENTS IN LOAD VECTOR R	BANS 400
5	R(N)=R(N)-AK(N,K)*R(L)	BANS 410
6	RETURN	BANS 420
	END	BANS 430

Appendix C-2

The Mesh-plot Program

1. Input Dataa) Option card:

FORMAT (I1)

<u>Col.</u>	<u>Symbol</u>	<u>Definition</u>
1	OPTAX	Plotting option and option for end of plot = 0, if the Y-coordinate is limited by the height of the plotter = 1, if the X-coordinate is limited by the height of the plotter = 9, to indicate the end of the plot

b) Basic parameters - card 1:

FORMAT (3F7.1,3F5.3,2I4,F10.3)

<u>Col.</u>	<u>Symbol</u>	<u>Definition</u>
1-7	XTIC	Distance between tic marks on the plot axes in inches
8-14	XLNG	Length of the X-axis in inches
15-21	YLNG	Length of the Y-axis in inches
22-26	SIZFAC	Scaling factor of the mesh
27-31	H1	Height of the element numbers to be printed in inches
32-36	H2	Height of the nodal point numbers to be printed in inches
37-40	CTR	Counter variable = 1
41-44	NTR	Second counter variable =1

<u>Col.</u>	<u>Symbol</u>	<u>Definition</u>
45-54	XMAX9	Maximum extent in X-direction - used only when OPTAX = 1

c) Basic parameters - card 2:

FORMAT (2I4,I2)

<u>Col.</u>	<u>Symbol</u>	<u>Definition</u>
1-4	NOELE	Number of elements
5-8	NOSND	Number of nodal points
9-10	NTEST	= 0, does not test safety factor

d) Nodal point data:

FORMAT (I5,5X,2F10.1)

<u>Col.</u>	<u>Symbol</u>	<u>Definition</u>
1-5	N	Nodal point number
6-10		Blank
11-20	XX(N)	X-coordinate of nodes
21-30	YY(N)	Y-coordinate of nodes

e) Element data:

FORMAT (5I5)

<u>Col.</u>	<u>Symbol</u>	<u>Definition</u>
1-5	N	Element numbers
6-10	IE(N,1)	
11-15	IE(N,2)	Node numbers of corner nodes of
16-20	IE(N,3)	the number n element
21-25	IE(N,4)	

C	MESH-PLOT PROGRAM	MSPL 10
	DIMENSION DX(4), DY(4), DXX(12), DYY(12), F(800), XX(800), YY(800)	MSPL 20
	1, IE(800,4)	MSPL 30
	COMMON XORD(800), YORD(800), NDI(800), NDJ(800), NDK(800), NTR, NDL(800)	MSPL 40
	1, XI0, YI0	MSPL 50
	COMMON /OPTA/ OPTAX	MSPL 60
	INTEGER CTR, OPTAX	MSPL 70
	CALL PLOTS (0,0,50)	MSPL 80
	CALL PLOT (5.,.5,-3)	MSPL 90
	ERROR=0.	MSPL 100
	READ (5,31) OPTAX	MSPL 110
	IF (OPTAX.EQ.0) GO TO 1	MSPL 120
	READ (5,32) XTIC, YLNG, XLNG, SIZFAC, H1, H2, CTR, NTR, XMAX9	MSPL 130
	GO TO 2	MSPL 140
1	CONTINUE	MSPL 150
	READ (5,32) XTIC, XLNG, YLNG, SIZFAC, H1, H2, CTR, NTR	MSPL 160
2	CONTINUE	MSPL 170
	IICTR=1	MSPL 180
	NTR=1	MSPL 190
	IFLAG=0	MSPL 200
	IF (CTR.EQ.0) GO TO 3	MSPL 210
	IICTR=CTR	MSPL 220
	CTR=CTR-1	MSPL 230
	IICTR=CTR	MSPL 240
	IFLAG=1	MSPL 250
3	CONTINUE	MSPL 260
	ISKP=0	MSPL 270
	IF (H1.LE.0.OR.H2.LE.0) ISKP=1	MSPL 280
C	SIZFAC IS THE SCALING FACTOR OF THE MESH	MSPL 290
C	H1 IS THE HEIGHT OF THE ELEMENT NUMBER TO BE ORINTED BEFORE FACTOM	MSPL 300
C	H2 IS THE HEIGHT OF THE NODAL POINT NUMBER OR THE SAFETY FACTOR	MSPL 310
C	NBER TO BE PRINTED BEFORE FACTORING	MSPL 320
C	IF NTEST = 0, THE NODAL POINT NUMBER WILL BE PRINTED	MSPL 330
C	IF NTEST = 1, THE SAFETY FACTOR WILL BE PRINTED	MSPL 340
C	XTIC IS THE DISTANCE BETWEEN THE TIC MARKS IN INCHES	MSPL 350
C	XLNG IS THE LENGTH OF THE X AXIS INCHES	MSPL 360
C	YXLNG IS THE LENGTH OF THE Y AXIS INCHES	MSPL 370
C	CHOOSING COORDINATES	MSPL 380
C	IF OPTAX=0 THE Y COORDINATE IS LIMITED BY THE HIGHT OF THE	MSPL 390
C	PLOTTER. IF OPTAX=1 THE X COORDINATE IS LIMTIATED.	MSPL 400
C	IF H1 OR '2 ARE 0 OR NEGATIVE THE NODAL AND ELEMENT NUMBERS WILL	MSPL 410
C	NOT BE PRINTED	MSPL 420
C	IF A BLOW UP OF A SECTION IS WANTED CTR IS THE FIRST NODE IN	MSPL 430
C	THAT SECTION. IF THE NODES ARE NOT SEQUENCED NSEQ MUST BE	MSPL 440
C	SPECIFIED AS 1.	MSPL 450
C	ONE (1) BLANK CARD IS REQUIRED AFTER THE NODAL POINT CARDS AND ALSMSPL	MSPL 460
C	AFTER THE ELEMENT CARDS....	MSPL 470
	WRITE (6,33) SIZFAC	MSPL 480
	XLNG=XLNG*SIZFAC	MSPL 490
	XLS=XTIC*SIZFAC	MSPL 500
	YLNG=YLNG*SIZFAC	MSPL 510
	READ (5,34) NOELE, NOSND, NTEST	MSPL 520
	M=1	MSPL 530
4	READ (5,35) N, XX(N), YY(N)	MSPL 540

	IF (N-M) 5,8,6	MSPL 550
5	GO TO 4	MSPL 560
6	DF=N+1-M	MSPL 570
	RX=(XX(N)-XX(M-1))/DF	MSPL 580
	RY=(YY(N)-YY(M-1))/DF	MSPL 590
7	XX(M)=XX(M-1)+RX	MSPL 600
	YY(M)=YY(M-1)+RY	MSPL 610
8	M=M+1	MSPL 620
	IF (N-M) 9,8,7	MSPL 630
9	IF (M.LE.NOSND) GO TO 4	MSPL 640
	DO 10 N=1,NOSND	MSPL 650
	XORD(N)=XX(N)	MSPL 660
	YORD(N)=YY(N)	MSPL 670
10	CONTINUE	MSPL 680
	IF (OPTAX.EQ.0) GO TO 12	MSPL 690
	DO 11 IJ=1,ICTR,NOSND	MSPL 700
	AAA=XORD(IJ)	MSPL 710
	XORD(IJ)=YORD(IJ)	MSPL 720
	YORD(IJ)=XMAX9-AAA	MSPL 730
11	CONTINUE	MSPL 740
12	CONTINUE	MSPL 750
	CTR=0	MSPL 760
	IF (IFLAG.EQ.1) CTR=ICTR	MSPL 770
	LL=0	MSPL 780
13	READ (5,36) N,(IE(N,I),I=1,4)	MSPL 790
14	LL=LL+1	MSPL 800
	IF (N-LL) 15,17,16	MSPL 810
15	GO TO 13	MSPL 820
16	IE(LL,1)=IE(LL-1,1)+1	MSPL 830
	IE(LL,2)=IE(LL-1,2)+1	MSPL 840
	IE(LL,3)=IE(LL-1,3)+1	MSPL 850
	IE(LL,4)=IE(LL-1,4)+1	MSPL 860
17	NDI(LL)=IE(LL,1)	MSPL 870
	NDJ(LL)=IE(LL,2)	MSPL 880
	NDK(LL)=IE(LL,3)	MSPL 890
	NDL(LL)=IE(LL,4)	MSPL 900
	IF (N-LL) 18,18,14	MSPL 910
18	IF (NOELE-LL) 19,19,13	MSPL 920
19	CONTINUE	MSPL 930
	CALL SAXIS (0.,0.,25HHORIZONTAL EXTENT IN FEET,-25,XLNG,0.,0.,XTIC,MSPL 940	
	1,XLS,0.)	MSPL 950
	CALL SAXIS (0.,0.,23HVERTICAL EXTENT IN FEET,23,YLNG,90.,0.,XTIC,XMSPL 960	
	1LS,0.)	MSPL 970
	CALL SYMBOL (-1.,3.,.25,12HELEMENT PLOT,90.,12)	MSPL 980
	CALL PLOT (0.,0.,-3)	MSPL 990
	DO 25 M=NTR,NOELE	MSPL1000
	I=NDI(M)	MSPL1010
	J=NDJ(M)	MSPL1020
	K=NDK(M)	MSPL1030
	L=NDL(M)	MSPL1040
	DX(1)=XORD(I)	MSPL1050
	DY(1)=YORD(I)	MSPL1060
	DX(2)=XORD(J)	MSPL1070
	DY(2)=YORD(J)	MSPL1080

	DX(3)=XORD(K)	MSPL1090
	DY(3)=YORD(K)	MSPL1100
	DX(4)=XORD(L)	MSPL1110
	DY(4)=YORD(L)	MSPL1120
	DO 20 IJ=1,4	MSPL1130
	DX(IJ)=DX(IJ)*SIZFAC	MSPL1140
	DY(IJ)=DY(IJ)*SIZFAC	MSPL1150
20	CONTINUE	MSPL1160
	CALL PLOT (DX(1),DY(1),3)	MSPL1170
	DO 21 L=1,4	MSPL1180
21	CALL PLOT (DX(L),DY(L),2)	MSPL1190
	CALL PLOT (DX(1),DY(1),2)	MSPL1200
	IF (DX(4).EQ.DX(3).AND.DY(4).EQ.DY(3)) GO TO 22	MSPL1210
	X10=(DX(2)+DX(1))/2	MSPL1220
	Y10=(DY(3)+DY(2))/2	MSPL1230
	GO TO 23	MSPL1240
22	DX(4)=DX(1)	MSPL1250
	DY(4)=DY(1)	MSPL1260
	II=I	MSPL1270
	JJ=J	MSPL1280
	KK=K	MSPL1290
	DXX(1)=XORD(II)	MSPL1300
	DYY(1)=YORD(II)	MSPL1310
	DXX(2)=XORD(JJ)	MSPL1320
	DYY(2)=YORD(JJ)	MSPL1330
	DXX(3)=XORD(KK)	MSPL1340
	DYY(3)=YORD(KK)	MSPL1350
	DXX(4)=.5*(DXX(1)+DXX(2))	MSPL1360
	DYY(4)=.5*(DYY(1)+DYY(2))	MSPL1370
	DXX(5)=.5*(DXX(2)+DXX(3))	MSPL1380
	DYY(5)=.5*(DYY(2)+DYY(3))	MSPL1390
	DXX(6)=.5*(DXX(3)+DXX(1))	MSPL1400
	DYY(6)=.5*(DYY(3)+DYY(1))	MSPL1410
	DXX(7)=.5*(DXX(4)+DXX(5))	MSPL1420
	DYY(7)=.5*(DYY(4)+DYY(5))	MSPL1430
	DXX(8)=.5*(DXX(5)+DXX(6))	MSPL1440
	DYY(8)=.5*(DYY(5)+DYY(6))	MSPL1450
	DXX(9)=.5*(DXX(6)+DXX(4))	MSPL1460
	DYY(9)=.5*(DYY(6)+DYY(4))	MSPL1470
	DXX(10)=.5*(DXX(7)+DXX(8))	MSPL1480
	DYY(10)=.5*(DYY(7)+DYY(8))	MSPL1490
	DXX(11)=.5*(DXX(8)+DXX(9))	MSPL1500
	DYY(11)=.5*(DYY(8)+DYY(9))	MSPL1510
	DXX(12)=.5*(DXX(9)+DXX(7))	MSPL1520
	DYY(12)=.5*(DYY(9)+DYY(7))	MSPL1530
	X10=DXX(10)*SIZFAC	MSPL1540
	Y10=DYY(10)*SIZFAC	MSPL1550
23	XM=M	MSPL1560
	IF (ISKP.EQ.1) GO TO 24	MSPL1570
	CALL NUMBER (X10,Y10,H1,XM,0.,-1)	MSPL1580
24	CONTINUE	MSPL1590
25	CONTINUE	MSPL1600
	IF (NTEST.EQ.0) GO TO 27	MSPL1610
	WRITE (6,37)	MSPL1620

	DO 26 I=1 ICTR,NOSND	MSPL1630
	X=XORD(I)-.5	MSPL1640
	Y=YORD(I)+.5	MSPL1650
	READ (5,38) I,F(I)	MSPL1660
	XI=F(I)	MSPL1670
	X=X*SIZFAC	MSPL1680
	Y=Y*SIZFAC	MSPL1690
	CALL NUMBER (X,Y,H2,XI,0.,1)	MSPL1700
	WRITE (6,39) I,F(I)	MSPL1710
26	CONTINUE	MSPL1720
	GO TO 30	MSPL1730
27	CONTINUE	MSPL1740
	IF (ISKP.EQ.1) GO TO 29	MSPL1750
	DO 28 I=1 ICTR,NOSND	MSPL1760
	X=XORD(I)-.25	MSPL1770
	Y=YORD(I)+.05	MSPL1780
	Z1=1	MSPL1790
	X=X*SIZFAC	MSPL1800
	Y=Y*SIZFAC	MSPL1810
	CALL NUMBER (X,Y,H2,Z1,0.,-1)	MSPL1820
28	CONTINUE	MSPL1830
29	CONTINUE	MSPL1840
C		MSPL1850
C		MSPL1860
30	CALL PLOT (XLNG+5.0,0.0,999)	MSPL1870
C		MSPL1880
C		MSPL1890
	STOP	MSPL1900
C		MSPL1910
31	FORMAT (11)	MSPL1920
32	FORMAT (3F7.1,3F5.3,2I4,F10.3)	MSPL1930
33	FORMAT (9H0 SIZFAC=,F10.4)	MSPL1940
34	FORMAT (2I4,12)	MSPL1950
35	FORMAT (15,5X,2F10.1)	MSPL1960
36	FORMAT (5I5)	MSPL1970
37	FORMAT (1H ,29H N.P. SAFETY FACTOR)	MSPL1980
38	FORMAT (1I0,F6.1)	MSPL1990
39	FORMAT (1I1,8X,F6.1)	MSPL2000
	END	MSPL2010

Appendix C-3

The Stress-Plot Program

1. Input Dataa) Title card:

FORMAT (I5,1X,18A4)

<u>Col.</u>	<u>Symbol</u>	<u>Definition</u>
1-5	NPROB	Problem number
6		Blank
7-78	TITLE	Title of plot

b) Basic parameters:

FORMAT (2I5,2F10.7)

<u>Col.</u>	<u>Symbol</u>	<u>Definition</u>
1-5	NOSEL	Number of elements
6-10	NBNDY	Number of boundary points
11-20	SC	Scaling factor for the plot
21-30	SCALE	Scaling factor for the stress vectors

c) Stress data:

FORMAT (4X,2F7.2,29X,1P3E10.2)

<u>Col.</u>	<u>Symbol</u>	<u>Definition</u>
1-4		Blank
5-11	X	X-coordinates of element centroids
12-18	Y	Y-coordinates of element centroids
19-47		Blank
48-57	STMAX(M)	Maximum principal stress of element M
58-67	STMIN(M)	Minimum principal stress of element M

<u>Col.</u>	<u>Symbol</u>	<u>Definition</u>
68-77	PHI(M)	Angle of inclination of principal stresses of element M

d) Boundary data:

FORMAT (2F10.4)

<u>Col.</u>	<u>Symbol</u>	<u>Definition</u>
1-10	XXA(N)	X-coordinate of boundary point N
11-20	YYA(N)	Y-coordinate of boundary point N

e) Exit card or title card of next plot:

FORMAT (I5,1X,18A4)

<u>Col.</u>	<u>Symbol</u>	<u>Definition</u>
1-5	NPROB	Problem number = 0, indicates end of plot = any integer, continues next plot
6		Blank
7-78		Title of next plot

Note: This program is capable of plotting four separate quadrilateral boundaries. If more boundaries are desired, they can be plotted by the additional of more logical "IF" statements in the program. It should also be noted that the first boundary point of each separate boundary should be repeated after the following three boundary points have been specified.

C	STRESS VECTOR PROGRAM	STVP 10
	DIMENSION XORD(1500), YORD(1500), STMAX(1500), STMIN(1500), PHI(1500), ANGLE(1500), XXA(1500), YYA(1500)	STVP 20
	DIMENSION TITLE(18)	STVP 30
1	READ (5,19) NPROB, (TITLE(I), I=1,18)	STVP 40
	IF (NPROB.LE.0) GO TO 18	STVP 50
	CALL PLOTS (0,0,50)	STVP 60
	CALL PLOT (5.,.25,-3)	STVP 70
	READ (5,20) NOSEL,NBNDY,SC,SCALE	STVP 80
	DO 3 M=1,NOSEL	STVP 90
	READ (5,21) X,Y,STMAX(M),STMIN(M),PHI(M)	STVP 100
	RITE=0.0	STVP 110
	IF (RITE.EQ.0.0) GO TO 2	STVP 120
	WRITE (6,21) X,Y,STMAX(M),STMIN(M),PHI(M)	STVP 130
2	XORD(M)=X*SC	STVP 140
	YORD(M)=Y*SC	STVP 150
3	CONTINUE	STVP 160
	CALL SAXIS (0.,0.,23HVERTICAL EXTENT IN FEET,23,4.5,90.,0.,25.,.25	STVP 170
	1,0.)	STVP 180
	CALL SAXIS (0.,0.,25HHORIZONTAL EXTENT IN FEET,-25,6.75,0.,0.,25.,	STVP 190
	1.250,0.)	STVP 200
	CALL SYMBOL (-.8,.5,.07,68H500 X 7 FOOT OPENING, PENG CASE STUDY	STVP 210
	1, STRESS SCALE 1 IN =10000PSI,90.,68)	STVP 220
	DO 4 N=1,NBNDY	STVP 230
	READ (5,22) XXA(N),YYA(N)	STVP 240
	XCO=XXA(N)*SC	STVP 250
	YCO=YYA(N)*SC	STVP 260
	IF (N.EQ.1) I1=3	STVP 270
	IF (N.EQ.6) I1=3	STVP 280
	IF (N.EQ.11) I1=3	STVP 290
	IF (N.EQ.16) I1=3	STVP 300
	IF (N.EQ.21) I1=3	STVP 310
	IF (N.EQ.26) I1=3	STVP 320
	IF (N.EQ.31) I1=3	STVP 330
	IF (N.EQ.36) I1=3	STVP 340
	IF (N.EQ.41) I1=3	STVP 350
	IF (N.EQ.46) I1=3	STVP 360
	IF (N.EQ.51) I1=3	STVP 370
	IF (N.EQ.56) I1=3	STVP 380
	IF (N.EQ.61) I1=3	STVP 390
	CALL PLOT (XCO,YCO,I1)	STVP 400
	I1=2	STVP 410
4	CONTINUE	STVP 420
	PI=3.14159/180.	STVP 430
	DO 17 I=1,NOSEL	STVP 440
	ANGLE(I)=ABS(PHI(I))*PI	STVP 450
	IF (PHI(I)) 5,6,6	STVP 460
5	X1=XORD(I)-ABS(STMAX(I))*COS(ANGLE(I))*SCALE	STVP 470
	Y1=YORD(I)+ABS(STMAX(I))*SIN(ANGLE(I))*SCALE	STVP 480
	X2=XORD(I)+ABS(STMAX(I))*COS(ANGLE(I))*SCALE	STVP 490
	Y2=YORD(I)-ABS(STMAX(I))*SIN(ANGLE(I))*SCALE	STVP 500
	X3=XORD(I)+ABS(STMIN(I))*SIN(ANGLE(I))*SCALE	STVP 510
	Y3=YORD(I)+ABS(STMIN(I))*COS(ANGLE(I))*SCALE	STVP 520
	X4=XORD(I)-ABS(STMIN(I))*SIN(ANGLE(I))*SCALE	STVP 530
		STVP 540

	Y4=YORD(1)-ABS(STMIN(1))*COS(ANGLE(1))*SCALE	STVP 550
	GO TO 7	STVP 560
6	X1=XORD(1)+ABS(STMAX(1))*COS(ANGLE(1))*SCALE	STVP 570
	Y1=YORD(1)+ABS(STMAX(1))*SIN(ANGLE(1))*SCALE	STVP 580
	X2=XORD(1)-ABS(STMAX(1))*COS(ANGLE(1))*SCALE	STVP 590
	Y2=YORD(1)-ABS(STMAX(1))*SIN(ANGLE(1))*SCALE	STVP 600
	X3=XORD(1)-ABS(STMIN(1))*SIN(ANGLE(1))*SCALE	STVP 610
	Y3=YORD(1)+ABS(STMIN(1))*COS(ANGLE(1))*SCALE	STVP 620
	X4=XORD(1)+ABS(STMIN(1))*SIN(ANGLE(1))*SCALE	STVP 630
	Y4=YORD(1)-ABS(STMIN(1))*COS(ANGLE(1))*SCALE	STVP 640
7	IF (STMAX(1)) 8,9,9	STVP 650
8	CALL NEWPEN (2)	STVP 660
	GO TO 10	STVP 670
9	CALL NEWPEN (3)	STVP 680
10	CALL PLOT (X1,Y1,3)	STVP 690
	CALL PLOT (X2,Y2,2)	STVP 700
	IF (STMIN(1)) 11,12,12	STVP 710
11	CALL NEWPEN (2)	STVP 720
	GO TO 13	STVP 730
12	CALL NEWPEN (3)	STVP 740
13	CALL PLOT (X3,Y3,3)	STVP 750
	CALL PLOT (X4,Y4,2)	STVP 760
	CALL NEWPEN (1)	STVP 770
	IF (PHI(1)) 14,15,15	STVP 780
14	XP=((X3+X4)/2.)-.05	STVP 790
	YP=((Y1+Y2)/2.)+.05	STVP 800
	ANGP=180.-ABS(PHI(1))	STVP 810
	XQ=((X3+X4)/2.)+.05	STVP 820
	YQ=YP	STVP 830
	ANGQ=90.-ABS(PHI(1))	STVP 840
	GO TO 16	STVP 850
15	XP=((X3+X4)/2.)-.05	STVP 860
	YP=((Y1+Y2)/2.)+.05	STVP 870
	XQ=((X3+X4)/2.)+.05	STVP 880
	YQ=YP	STVP 890
	ANGP=PHI(1)	STVP 900
	ANGQ=270.+PHI(1)	STVP 910
16	CONTINUE	STVP 920
17	CONTINUE	STVP 930
	CALL PLOT (30.,10.,999)	STVP 940
	GO TO 1	STVP 950
18	STOP	STVP 960
C		STVP 970
19	FORMAT (15,1X,18A4)	STVP 980
20	FORMAT (215,2F10.7)	STVP 990
21	FORMAT (4X,2F7.2,29X,1P3E10.2)	STVP1000
22	FORMAT (2F10.4)	STVP1010
	END	STVP1020

Appendix C-4

The General Purpose Contour Program

1. Input Dataa) Job card:

FORMAT (A4,1X,18A4,A3)

<u>Col.</u>	<u>Symbol</u>
1-4	JOB
5	Blank
6-80	Title of plot

b) Flexible mode card:

FORMAT (A4)

<u>Col.</u>	<u>Symbol</u>
1-4	FLEX
5-80	Blank

c) Refinement card:

FORMAT (A4,1X,F5.0)

<u>Col.</u>	<u>Symbol</u>
1-4	REF
5	Blank
6-10	Degree of contour smoothness
	Values: 2 through 20
	Default: 5

d) New pen assignment card:

FORMAT (A4,1X,I5)

<u>Col.</u>	<u>Symbol</u>
1-4	NWPN

<u>Col.</u>	<u>Symbol</u>
5	Blank
6-10	Pen number
	= 1, black pen; = 2 blue pen;
	= 3, red pen; = 4 green pen

e) Size card:

```
FORMAT (A4,1X,4F5.0,F10.0,F5.0,2F10.0,F5.0,F10.0)
```

<u>Col.</u>	<u>Symbol</u>
1-4	SIZE.
5	Blank
6-10	Scaling factor in X-direction (unit/inch)
11-15	Scaling factor in Y-direction (unit/inch)
16-20	X-coordinate of plotter origin (inches)
21-25	Y-coordinate of plotter origin (inches)
26-35	X-coordinate of origin of plot (units)
36-40	Increment between tic marks on X-axis (units)
41-50	Maximum extent in the X-direction (units)
51-60	Y-coordinate of the origin of plot (units)
61-65	Increment between tic marks on Y-axis (units)
66-75	Maximum extent in the Y-direction (units)
76-80	Blank

f) Control point card 1:

```
FORMAT (A4,1X,2F5.0,2I5,45X,2I5)
```

<u>Col.</u>	<u>Symbol</u>
1-4	CNTL
5	Blank

<u>Col.</u>	<u>Symbol</u>
6-20	Can be left blank if the locaton of the data points are not to be plotted
21-25	= 2 or 6, if location of data points are not to be plotted
26-70	Blank
71-75	= 8, does not plot data point centers
76-80	= 8, does not plot data point centers

g) Control point card 2:

```
FORMAT (A4,1X,13A4,A3)
```

<u>Col.</u>	<u>Symbol</u>
1-4	CNTL
5	Blank
6-80	Specify the format of the contour cards Example: (3X,2F7.2,10X,1P1E10.2,30X,13A1) Note: the format must contain exactly 16 quantities, even though they are not all used.

h) Control point card 3:

```
FORMAT (A4,1X,3I5)
```

<u>Col.</u>	<u>Symbol</u>
1-4	CNTL
5	Blank
6-10	= 1
11-15	= 2
16-20	=3
21-80	Blank

i) Contour data cards:

FORMAT as specified in Control point card 2

<u>Col.</u>	<u>Symbol</u>
see	X-coordinate of data point
above	Y-coordinate of data point
	Data value

j) Block end card:

FORMAT (A4)

<u>Col.</u>	<u>Symbol</u>
1-4	BEND

k) Blanking card:

FORMAT (A4,1X,2I5)

<u>Col.</u>	<u>Symbol</u>
1-4	BLNK
5	Blank
6-10	= 1, for beginning a blanking block
11-15	Number of blanking points

Note: A sub-region within the contouring region can be blanked, i. e. contouring can be suppressed in that area, by specifying a number of blanking points in such a manner as to traverse the region to be blanked in a clockwise direction.

1) Boundary card:

FORMAT (A4,1X,6F10.0) - number of cards as specified
in columns 11-15 of Blanking card

<u>Col.</u>	<u>Symbol</u>
1-4	BND
5	Blank
6-15	X-coordinate of first point
16-25	Y-coordinate of first point
26-35	X-coordinate of second point
36-45	Y-coordinate of second point
46-55	X-coordinate of third point
56-65	Y-coordinate of third point
66-80	Blank

m) Blanking card:

FORMAT (A4,1X,2I5)

<u>Col.</u>	<u>Symbol</u>
1-4	BLNK
5	Blank
6-10	= 0, for termination of blanking
11-15	= 0
16-80	Blank

n) Phase 4 card:

FORMAT (A4)

<u>Col.</u>	<u>Symbol</u>
1-4	PHS4
5-80	Blank

o) Bold contours card:

FORMAT (A4,1X,F5.0)

<u>Col.</u>	<u>Symbol</u>
1-4	BOLD
5	Blank
6-10	Number of levels between bold contours = 5 by default
11-80	Blank

p) Skip contours card:

FORMAT (A4,1X,F5.0)

<u>Col.</u>	<u>Symbol</u>
1-4	SKIP
5	Blank
6-10	Minimum distance between adjacent light contour lines
11-80	Blank

q) Basic contour levels card:

FORMAT (A4,1X,F5.0)

<u>Col.</u>	<u>Symbol</u>
1-4	BLEV
5	Blank
6-10	Contour interval
11-80	Blank

r) Border card:

FORMAT (A4)

Col. Symbol

1-4 BRDR

5-80 Blank

s) Pause card:

FORMAT (A4)

Col. Symbol

1-4 PAUS

5-80 Blank

t) Plot map card:

FORMAT (A4)

Col. Symbol

1-4 PLOT

5-80 Blank

u) Line card:

FORMAT (A4,1X,I5,7F5.0,I5)

Col. Symbol

1-4 LINE

5 Blank

6-10 = 0, coordinates relative to plotter origin

= 1, coordinates relative to origin of plot

11-15 X-coordinate of first point

16-20 Y-coordinate of first point

21-25 X-coordinate of second point

26-30 Y-coordinate of second point

<u>Col.</u>	<u>Symbol</u>
31-35	Distance between tic marks Blank if tic marks not required
36-40	Height of tic marks Blank if tic marks not required
41-45	Lateral displacements of line (Only required for stereoscopic maps)
46-50	Integer value that determines line type = +1, for plotting solid line
51-80	Blank

Note: Line cards are used to draw lines from one point to another. Several lines cards may be used to draw additional boundaries within the main boundary.

v) End card:

FORMAT (A4)

<u>Col.</u>	<u>Symbol</u>
1-4	END
5-80	Blank

w) Stop card:

FORMAT (A4)

<u>Col.</u>	<u>Symbol</u>
1-4	STOP
5-80	Blank

```

JOB      SIGMA (Y)
FLEX
REF      5
NWPN    1
SIZE    80.  80.  1.  1.  0.  25.  672.  0.0  25.0  441.
CNTL
CNTL    (3X,2F7.2,10X,1P1E10.2,30X,13A1)
CNTL    1  2  3  6
1  14.00  7.00 -9.14E+02 -3.95E+03  2.33E+02 -8.96E+02 -3.97E+03  4.37E+00
509 630.00 427.00  4.14E+02 -7.95E+02 -1.60E+01  4.14E+02 -7.95E+02 -7.60E-01
510 658.00 427.00  3.26E+02 -1.10E+03 -2.26E+02  3.61E+02 -1.14E+03 -8.80E+00

```

```

BEND
BLNK
PHS4
BOLD
SKIP .03
BLEV 500
BRDR
PAUS
PLOT
LINE    1  84.  28.  84.  35.  +1
LINE    1  84.  35.  588.  35.  +1
LINE    1  588.  35.  588.  28.  +1
LINE    1  588.  28.  84.  28.  +1
LINE    1  0.  0.  0.  441.  +1
LINE    1  0.  441.  672.  441.  +1
LINE    1  672.  441.  672.  0.  +1
LINE    1  672.  0.  0.  0.  +1
LINE    1  0.  224.  0.  231.  +1
LINE    1  0.  231.  672.  231.  +1
LINE    1  672.  231.  672.  224.  +1
LINE    1  672.  224.  0.  224.  +1
END
STOP

```

**The vita has been removed from
the scanned document**

THE EFFECTS OF THE PRESSURE ARCH
UPON MULTIPLE SEAM MINING

by

Stephen David Hudock

(ABSTRACT)

The coal fields of Appalachia consist of many contiguously placed, mineable coal seams. Common practice in mining multiple seams is to extract the seams in a descending order. However, the mining sequence may still be based on seam ownership, availability of the seam and the general economic situation, not on ground control considerations.

One of the major ground control mechanisms that must be considered in the design of a mine is the arching of stresses around a previously mined lower seam. This investigation deals with the extent and magnitude of the stresses above an underground opening. The finite element approach was utilized to determine the extent and magnitude of stresses for various widths of mine opening, depths of cover and overburden material. This information can then be used as an approximation of the stresses that may be encountered in an actual mining situation.